VOL. 710 NO. 2 1 SEPTEMBER 1995
THIS ISSUE COMPLETES VOL. 710

JOURNAL OF CHROMATOGRAPHY A

INCLUDING ELECTROPHORESIS AND OTHER SEPARATION METHODS

ELSEVIER

JOURNAL OF CHROMATOGRAPHY A

INCLUDING ELECTROPHORESIS AND OTHER SEPARATION METHODS

Scope. The *Journal of Chromatography A* publishes papers on all aspects of **chromatography, electrophoresis** and related methods. Contributions consist mainly of research papers dealing with chromatographic theory, instrumental developments and their applications. In the *Symposium volumes*, which are under separate editorship, proceedings of symposia on chromatography, electrophoresis and related methods are published. *Journal of Chromatography B: Biomedical Applications* —This journal, which is under separate editorship, deals with the following aspects: developments in and applications of chromatographic and electrophoretic techniques related to clinical diagnosis or alterations during medical treatment; screening and profiling of body fluids or tissues related to the analysis of active substances and to metabolic disorders; drug level monitoring and pharmacokinetic studies; clinical toxicology; forensic medicine; veterinary medicine; occupational medicine; results from basic medical research with direct consequences in clinical practice.

Submission of Papers. The preferred medium of submission is on disk with accompanying manuscript (see *Electronic manuscripts* in the Instructions to Authors, which can be obtained from the publisher, Elsevier Science B.V., P.O. Box 330, 1000 AH Amsterdam, Netherlands). Manuscripts (in English; *four* copies are required) should be submitted to: Editorial Office of *Journal of Chromatography A*, P.O. Box 681, 1000 AR Amsterdam, Netherlands, Telefax (+31-20) 485 2304, or to: The Editor of *Journal of Chromatography B: Biomedical Applications*, P.O. Box 681, 1000 AR Amsterdam, Netherlands. Review articles are invited or proposed in writing to the Editors who welcome suggestions for subjects. An outline of the proposed review should first be forwarded to the Editors for preliminary discussion prior to preparation. Submission of an article is understood to imply that the article is original and unpublished and is not being considered for publication elsewhere. For copyright regulations, see below.

Publication information. *Journal of Chromatography A* (ISSN 0021-9673): for 1995 Vols. 683–714 are scheduled for publication. *Journal of Chromatography B: Biomedical Applications* (ISSN 0378-4347): for 1995 Vols. 663–674 are scheduled for publication. Subscription prices for *Journal of Chromatography A, Journal of Chromatography B: Biomedical Applications* or a combined subscription are available upon request from the publisher. Subscriptions are accepted on a prepaid basis only and are entered on a calendar year basis. Issues are sent by surface mail except to the following countries where air delivery via SAL is ensured: Argentina, Australia, Brazil, Canada, China, Hong Kong, India, Israel, Japan, Malaysia, Mexico, New Zealand, Pakistan, Singapore, South Africa, South Korea, Taiwan, Thailand, USA. For all other countries airmail rates are available upon request. Claims for missing issues must be made within six months of our publication (mailing) date. Please address all your requests regarding orders and subscription queries to: Elsevier Science B.V., Journal Department, P.O. Box 211, 1000 AE Amsterdam, Netherlands. Tel.: (+31-20) 485 3642; Fax: (+31-20) 485 3598. Customers in the USA and Canada wishing information on this and other Elsevier journals, please contact Journal Information Center, Elsevier Science Inc., 655 Avenue of the Americas, New York, NY 10010, USA, Tel. (+1-212) 633 3750, Telefax (+1-212) 633 3764.

Abstracts/Contents Lists published in Analytical Abstracts, Biochemical Abstracts, Biological Abstracts, Chemical Abstracts, Chemical Titles, Chromatography Abstracts, Current Awareness in Biological Sciences (CABS), Current Contents/Life Sciences, Current Contents/Physical, Chemical & Earth Sciences, Deep-Sea Research/Part B: Oceanographic Literature Review, Excerpta Medica, Index Medicus, Mass Spectrometry Bulletin, PASCAL-CNRS, Referativnyi Zhurnal, Research Alert and Science Citation Index.

US Mailing Notice. *Journal of Chromatography A* (ISSN 0021-9673) is published weekly (total 52 issues) by Elsevier Science B.V., (Sara Burgerhartstraat 25, P.O. Box 211, 1000 AE Amsterdam, Netherlands). Annual subscription price in the USA US$ 5389.00 (US$ price valid in North, Central and South America only) including air speed delivery. Second class postage paid at Jamaica, NY 11431. **USA POSTMASTERS**: Send address changes to *Journal of Chromatography A*, Publications Expediting, Inc., 200 Meacham Avenue, Elmont, NY 11003. Airfreight and mailing in the USA by Publications Expediting.

See inside back cover for Publication Schedule, Information for Authors and information on Advertisements.

0021-9673/95/$09.50

Printed in the Netherlands

VOL. 710, NO. 2 JOURNAL OF CHROMATOGRAPHY A 1 SEPTEMBER 1995

CONTENTS

(Abstracts/Contents Lists published in Analytical Abstracts, Biochemical Abstracts, Biological Abstracts, Chemical Abstracts, Chemical Titles, Chromatography Abstracts, Current Awareness in Biological Sciences (CABS), Current Contents/Life Sciences, Current Contents/Physical, Chemical & Earth Sciences, Deep-Sea Research/Part B: Oceanographic Literature Review, Excerpta Medica, Index Medicus, Mass Spectrometry Bulletin, PASCAL-CNRS, Referativnyi Zhurnal, Research Alert and Science Citation Index)

REGULAR PAPERS

Column Liquid Chromatography

Gas Chromatography

Electrophoresis

SHORT COMMUNICATIONS

Column Liquid Chromatography

(Continued overleaf)

Contents (continued)

Electrophoresis

ELSEVIER

Journal of Chromatography A, 710 (1995) 259–266

JOURNAL OF CHROMATOGRAPHY A

Polymer displacement in dye-affinity chromatography

Igor Yu. Galaev, Pär Arvidsson, Bo Mattiasson*

Department of Biotechnology, Chemical Center, Lund University, P.O. Box 124, S-221 00 Lund, Sweden

Received 14 February 1995; accepted 19 April 1995

Abstract

Displacement of lactate dehydrogenase from dye-affinity matrices with poly(ethyleneimine) (PEI) was shown to be an effective elution strategy. It resulted in better recoveries and sharper elution profiles than traditional non-specific elution while the purification factors were unchanged. The elution is assumed to proceed via displacement of bound protein by PEI when the polymer binds to the dye-ligands. Complete elution of bound protein is a characteristic feature of such a mechanism. Hence displacement with PEI may be a promising strategy for eluting proteins with reported low recoveries in dye-affinity chromatography protocols.

1. Introduction

Dye-affinity chromatography has proven to be a convenient method of protein purification both in the laboratory and at a large scale [1,2]. It combines high specificity with robustness, simple coupling chemistry and cost efficiency [3–5]. Protein binding to the dye matrix is not the whole story. For a successful purification, the bound protein must be eluted with a high recovery and preferably in a small elution volume. Two strategies are traditionally used for protein elution from dye matrices. The first one is to reduce the binding efficiency of the protein to the dye ligands by eluting with a high-ionic-strength solution. This is called non-specific elution, and usually 1–2 *M* NaCl or KCl is used. The second strategy is to use a soluble ligand, which competes with the dye ligand for the same protein binding site. Usually millimolar solutions of nucleotides are used for such specific elution. Both methods are inefficient in many cases and recoveries of 40–60% are quite common in dye-affinity chromatography [6–11]. Champluvier and Kula [12] calculated an average recovery of about 60% for numerous purifications on dye-affinity matrices. Even recoveries as low as 20–30% are frequent, especially when specific elution has been used [6,13–17].

A new strategy for protein elution is to use an agent with stronger binding to the matrix than that of target protein. Binding of such an agent results in the displacement of bound protein and is therefore called displacement chromatography. Different proteins were displaced from ion-exchange matrices by polyelectrolytes, DEAE-dextran [18,19], dextran sulfate [18,19,21], poly(vinyl sulfonic acid) [22], CM-starch [23], chondroitin sulfate [20,24], low-molecular-mass compounds such as (ethyleneglycol-bis(β-amino ethylether-N,N,N′,N′-tetracetic acid) [25] or from hydrophobic matrices by poly(ethylene glycol) (PEG) [26,27]. To the best

* Corresponding author.

0021-9673/95/$09.50
SSDI 0021-9673(95)00486-6

of our knowledge displacement has not been exploited in dye-affinity chromatography.

Strong interaction of poly(ethylene imine) (PEI) with triazine dyes was found during our study of dye interaction with different polymers [28]. The idea was to try this polymer for displacement of proteins bound to dye matrices in order to improve their recovery and elution profile.

2. Materials and methods

Lactate dehydrogenase (LDH) type XXX-S from porcine muscle, β-NADH, and bicinchonic acid solution were purchased from Sigma (St. Louis, MO, USA). PEI with molecular mass 35 000 ± 5000 was purchased from Serva (Heidelberg, Germany). PEIs with molecular masses 2000 and 700 were purchased from Aldrich (Steinheim, Germany). Poly(acrylic acid) sodium salt with molecular mass 170 000 was purchased from Fluka (Buchs, Switzerland). Sepharose CL 4B and Sepharose 4 Fast Flow were purchased from Pharmacia BioProcess Technology (Uppsala, Sweden). Cibacron Blue 3GA (CB), purchased from Sigma, and Procion Red HE-3B (PR), a gift from ICI (Manchester, UK), were used as received. The heterogeneous character of commercially available dye preparations is well known [29], nevertheless it is common to use triazine dyes in spectral studies without additional purification [30–33].

Blue Sepharose and Red Sepharose were synthesised by coupling CB or PR to Sepharose CL 4B according to [34]. Scarlet Sepharose was a generous gift from Professor R.K. Scopes (Centre for Protein Research and Enzyme Technology, La Trobe, Australia) and was synthesized by coupling of Procion Scarlet HGA to Sepharose CL-4B according to [34].

The spectral titration was performed at room temperature according to [30]. Sample and reference cuvettes each containing 2 ml of a dye solution in an appropriate buffer were placed in a double beam Shimadzu UV-260 spectrophotometer. Small volumes (1–10 μl) of PEI solution were added to the sample cuvette and equal volumes of buffer were added to the reference cuvette. The contents of the cuvettes were mixed and spectra in the region of 400–650 nm were registered.

Chromatographic procedures were done at room temperature. LDH and BSA were applied to the column in equilibrating buffer (20 m*M* Tris · HCl buffer pH 7.3) and eluted with either 1% PEI, or 1.5 *M* KCl, or 1 m*M* NADH + 10 m*M* oxamate in the same buffer. The Blue Sepharose and Fast Blue Sepharose columns were regenerated after PEI elution with 0.1 *M* glycine buffer pH 12, containing 1 *M* NaCl. The Red Sepharose column was regenerated by a pulse of equilibrating buffer and then with 0.1 *M* glycine buffer pH 12, containing 1 *M* NaCl and 1% polyacrylate. The columns were reequilibrated after regeneration in 20 m*M* Tris · HCl buffer pH 7.3.

Pork was purchased in a local shop and was homogenized in ice-cold 20 m*M* Tris · HCl buffer, pH 7.3 containing 1 m*M* EDTA (3 ml of buffer per g of muscle tissue). The homogenate was centrifuged at 16 000 *g* for 15 min to remove cell debris and the supernatant was filtered through Munktell Grade 3 filter paper (Gryckssbo, Sweden) to remove traces of fat. The porcine muscle extract was kept frozen without any loss of LDH activity and was applied directly to the Red Sepharose column after thawing and filtering.

LDH activity was measured in the fractions according to a reported procedure [35]. Protein was determined according to the manufacturer's instruction for Bio-Rad protein assay (Bio-Rad Labs., Munich, Germany).

3. Results and discussion

Two triazine dyes, CB and PR were chosen for the study. PR is a bis-monochlorotriazine dye whereas CB is a monochlorotriazine dye (Fig. 1). The CB molecule contains three acidic sulfonate groups and four basic primary or secondary amino groups (ratio 3:4). The PR molecule contains six sulfonate groups and only four secondary amino groups (ratio 3:2) and bears

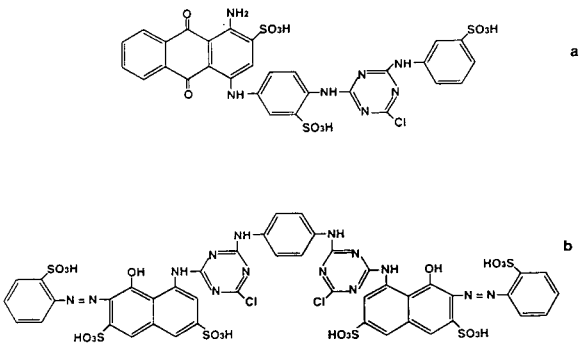

Fig. 1. Structures of Cibacron Blue 3GA (a) and Procion Red HE-3B (b).

higher total negative charge at neutral and basic conditions.

Both dyes interacted strongly with PEI at neutral conditions, resulting initially in a spectral change in the visible range and finally in precipitation of the dye–polymer complex. The difference spectra at low PEI concentration had a clear isobestic point indicating formation of soluble complexes (Fig. 2). At higher PEI concentrations this complex became insoluble and precipitated. Precipitation occurred at a polymer:CB ratio of 2:1 and a polymer:PR ratio of 6–7:1 (monomer units per dye molecule). It is reasonable that these complexes should precipitate when their total net charge is zero. Thus, the higher ratio in the case of PR is due to the more negative charge of this dye molecule, and more positive charges or more monomer units of PEI were needed to neutralize the charges.

Addition of excess polymer to the suspension of insoluble complex did not result in its dissolution. When an excess of PEI was added initially to the dye solution no precipitate formed. The difference spectrum of such soluble "PEI-saturated" complex (Fig. 2, dashed line) was quite close to that obtained just before precipitation starts and was independent of further increase in polymer concentration. The PEI–dye complex seemed to be kinetically stable. It precipitated at zero net charge and no redistribution of dye molecules between the precipitate and excessive polymer took place.

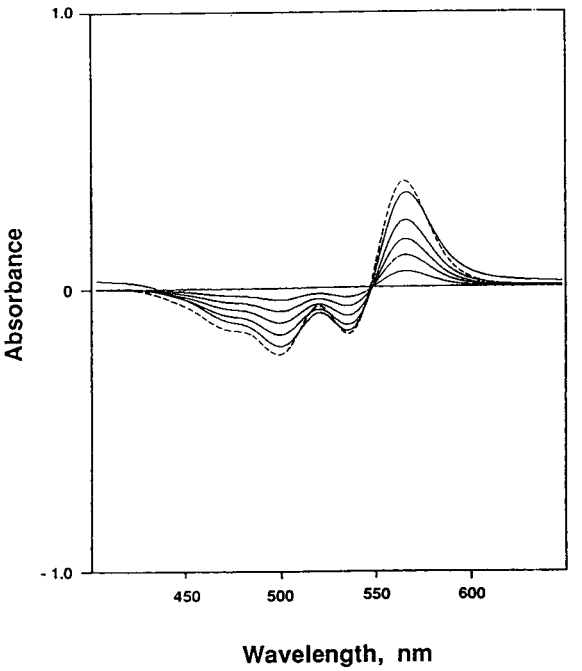

Fig. 2. Difference spectra obtained when Procion Red was titrated with increasing concentrations of PEI-35 000. Both sample and reference cuvette contained 2 ml of 0.05 mg/ml Procion Red in 20 m*M* Tris·HCl pH 7.3. Identical 1-μl portions of 0.25% PEI-35 000 solution in 20 m*M* Tris·HCl pH 7.3 and buffer were added in the reference and sample cuvette respectively. The dashed line was obtained when initially 10 μl of 10% PEI-35 000 solution in 20 m*M* Tris·HCl pH 7.3 were added to 2 ml of 0.05 mg/ml Procion Red in 20 m*M* Tris·HCl pH 7.3.

The application of the mathematical model previously developed [36] for calculation of constants for the binding of dyes with the soluble polymers, was prohibited by the precipitation of CB–PEI and PR–PEI complexes. Still some estimations of dye–PEI complex strength can be done on the basis of the amount of PEI needed for obtaining complete spectral changes. Using this scale, CB complexing with PEI at a pH around neutrality was about ten-fold more efficient than CB complexing with non-ionic polymer, poly(N-vinyl pyrrolidone). Dye interactions with PEI were also under experimental conditions used independent of the polymer molecular mass (700–35 000) resulting in nearly the

same difference spectra and the same polymer:dye ratio when precipitation took place.

The multipoint interaction of poly(N-vinyl pyrrolidone) and poly(vinyl alcohol) with dye ligands, coupled to the chromatographic matrix, was successfully exploited in polymer-shielded dye-affinity chromatography [28,36–40]. The interaction of poly(N-vinyl pyrrolidone) with dye ligands is strong enough to prevent the non-specific binding of proteins to the dye ligands. On the other hand this interaction is less efficient than specific binding of nucleotide-dependent enzymes to the dye ligands. Hence, these enzymes bind to the dye-affinity column pretreated with the polymer. The interaction of PEI with the dye ligands was much stronger than that of poly(N-vinyl pyrrolidone) and poly(vinyl alcohol). Thus, PEI could not be used for polymer shielding because it bound so strongly that it prevented specific binding to the column. In contrast, the strength of PEI binding can be exploited for the displacement of proteins bound to the dye-affinity column.

When coupled to the chromatographic matrix Sepharose CL-4B, both dyes, CB and PR, were able to bind pure LDH from porcine muscle. Efficient PEI binding to these dye ligands was used for the displacement of bound LDH. A 1% PEI solution in the same buffer used for LDH binding (20 m*M* Tris · HCl pH 7.3) proved to be an efficient eluent. Displacement of LDH with PEI resulted in quantitative recovery of the enzyme from both Blue Sepharose and Red Sepharose as well as from Scarlet Sepharose. LDH was displaced with 1% PEI and eluted as a sharp peak without tailing as usually observed during non-specific elution with high salt concentration. For instance, practically all LDH bound to Blue Sepharose was eluted with 1% PEI in 2.5-fold less volume than with 1.5 *M* KCl.

Fig. 3 presents LDH elution profiles using linear gradients of PEI-35 000, PEI-2000 and PEI-700. Unexpectedly, PEI-35 000 was a slightly weaker displacer than PEI-2000 and PEI-700, though all the polymers used displaced LDH efficiently from the Red Sepharose column. The difference in behaviour may be attributed to

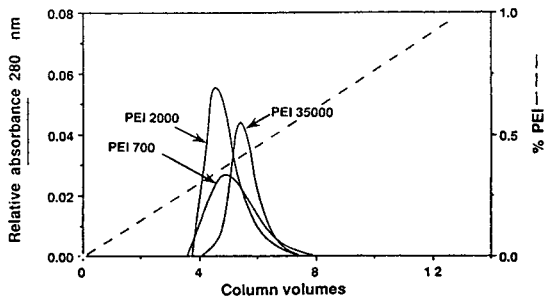

Fig. 3. LDH elution profile using a gradient of PEI. Experimental conditions: 1.5 × 1.0 cm I.D. Red Sepharose column. A 520-μl volume of pure LDH (1.1 mg/ml) was applied and eluted using a 0 to 1% linear PEI gradient at a flow-rate of 0.5 ml/min. The elution profiles are adjusted subtracting the contribution of PEI absorbance at 280 nm. Arrows indicate the molecular mass of PEI used.

some differences in polymer structure, e.g. degree of branching. The different PEI preparations are from different suppliers and sufficient documentation is not available to judge whether the preparations have the same degree of branching. On the other hand, LDH was not eluted with spermine, which can be regarded as a low-molecular-mass PEI analogue with degree of polymerization of 4. Thus, the polymeric nature of PEI and the possibility of multipoint interaction with the dye matrix was crucial for an efficient LDH elution.

Polymer bound strongly to the column after PEI elution and it was necessary to develop a proper column-regeneration protocol. Usually polycation displacers are washed out from cation exchangers with high-pH–high-salt buffer [18,19]. PEI ionization is suppressed at high pH and a high salt concentration decreases efficiency of ionic interaction. A 250-fold higher PEI concentration was required for complete "saturation" of spectral changes in CB solution at pH 12 (0.1 *M* glycine buffer, containing 1 *M* NaCl) comparing to that needed at neutral conditions. The PEI–CB complex was quite weak at these conditions and the polymer could be washed out from the column. Blue Sepharose column was successfully regenerated with 0.1 *M* glycine buffer pH 12 containing 1 *M* NaCl. On the contrary, the PR molecule bears more negative charges than the CB molecule and provides more oppor-

tunities for multipoint interactions with PEI. Even at these for complex formation unfavorable conditions, the PEI–PR complex is still strong enough resulting in significant spectral changes (data not shown). As a consequence the Red Sepharose column could not be regenerated with 0.1 *M* glycine buffer pH 12 containing 1 *M* NaCl.

It was necessary to make the mobile phase more attractive for PEI in order to remove it from the stationary phase. Addition of 1% polyacrylate (PAA) into the regeneration buffer was attempted. PAA is negatively charged at pH 12 and it does not bind to the negatively charged dye ligands, but is able to interact via hydrogen bonding with PEI, which is neutral at this pH. PEI-35 000 interacted strongly with PR even in the presence of 1% PAA, while the interaction of PEI-2000 with PR at these conditions was weaker. The interaction of PEI-700 with PR was abolished in the presence of 1% PAA (Fig. 4).The regeneration procedure using 1% PAA in 0.1 *M* glycine buffer pH 12 containing 1 *M* NaCl proved to be efficient after displacement of LDH with PEI-700 and PEI-2000 elution but not after displacement with PEI-35 000. A higher molecular mass of PEI results in more sites capable of interacting with dye ligands on the matrix. The polymer with higher molecular mass, PEI-35 000, binds to the dye matrix via a higher number of interactions and is therefore prevented from being washed out even by 1% PAA in 0.1 *M* glycine buffer pH 12 containing 1 *M* NaCl.

Two mechanisms can be assumed for the elution of LDH by PEI. According to the first mechanism the polymer binds to LDH thereby decreasing enzyme affinity towards the dye ligands. According to the second mechanisms. PEI binds to the dye ligands and thereby displaces LDH. PEI interacted strongly with dye ligands. The efficiency of these interactions is comparable to or even stronger than that of dye binding to LDH. PEI bound to the dye ligands prevented LDH from interaction with these ligands. LDH did not bind to the column after PEI elution and extensive washing with equilibrating buffer. A harsh regeneration procedure was required to remove bound PEI.

PEI interacted slightly with LDH, enzyme activity was decreased only 15–20% in the presence of 1% PEI. For comparison. LDH activity was decreased two-fold in 1.5 *M* KCl used for non-specific elution of enzyme. LDH was displaced with PEI and eluted as a concentrated solution, and usually only 10–100-μl samples

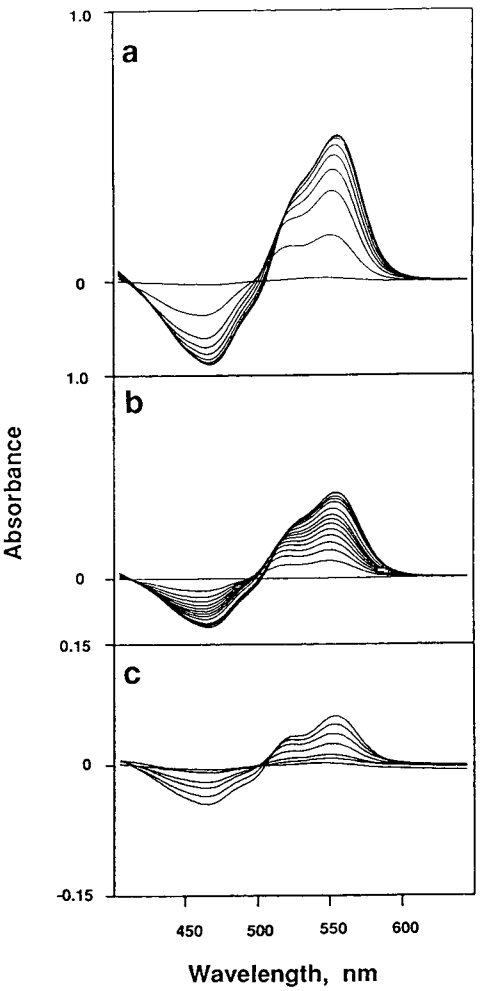

Fig. 4. Difference spectra obtained when Procion Red was titrated with increasing concentrations of (a) PEI-35 000, (b) PEI-2000 and (c) PEI-700. Both sample and reference cuvette contained 2 ml of 0.05 mg/ml Procion Red in 0.1 *M* glycine buffer pH 12, containing 1 *M* NaCl and 1% polyacrylate. Identical portions of buffer and of 10% PEI solution in 0.1 *M* glycine buffer pH 12, containing 1 *M* NaCl and 1% polyacrylate were added in the reference and sample cuvette respectively. Total 7×1 μl (a), 14×1 μl (b) and $1 + 1 + 5 + 5 + 10 + 10$ μl (c) aliquots of PEI solutions were added.

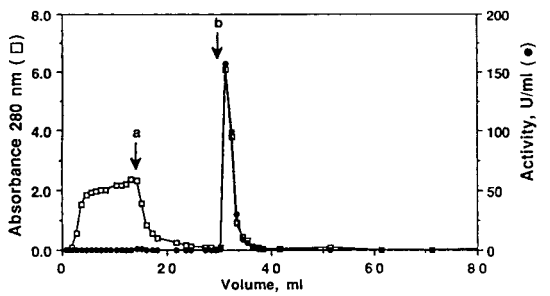

Fig. 5. LDH purification profile on Red Sepharose. Experimental conditions: 1.2 × 1.0 cm I.D.; flow-rate 0.5 ml/min. The crude extract was applied to a column until breakthrough. The arrows indicate: a = washing after breakthrough with 20 m*M* Tris · HCl, pH 7.3; b = elution with 1% PEI-700 in 20 m*M* Tris · HCl, pH 7.3. The column was regenerated with 1% polyacrylate in 0.1 *M* glycine buffer pH 12 containing 1 *M* NaCl and reequilibrated with 20 m*M* Tris · HCl buffer pH 7.3.

were used for assay of enzyme activity in a total assay volume of 1.5 ml. The 20–200 dilution of 1% PEI present in the eluent resulted in no measurable effect on LDH activity. Thus, we assume that LDH elution with PEI proceeds via the second mechanism, namely, via the displacement of enzyme by polymer due to the interaction of PEI with dye ligands.

Displacement with PEI-700 and subsequent column regeneration with 1% PAA in 0.1 *M* glycine buffer pH 12 containing 1 *M* NaCl was chosen for LDH purification from crude porcine muscle extract using Red Sepharose column. Crude extract was applied on a Red Sepharose column until breakthrough, the column was washed with buffer until no protein was eluted and LDH bound was eluted with 1% PEI-700 solution (Fig. 5).

Comparison with traditional strategies of LDH elution (Table 1) showed that displacement with PEI was more efficient than elution with 1.5 *M* KCl. It resulted in slightly better recoveries and sharper elution profiles. Displacement of LDH with PEI as well as 1.5 *M* KCl elution is non-specific and results in elution of all proteins bound on the column. On the other hand, specific elution proceeds via nucleotide competition with the dye ligand for the same protein sites. As a result, only proteins capable of nucleotide binding are eluted, the rest of the bound proteins should be eluted with high ionic strength to regenerate the column. Thus, the purification factors during specific elution with nucleotide (around 10) were higher than during both non-specific elution strategies (2.5–4). Though the structure of the dye resembles that of nucleotide, the dye is a pseudo-affinity ligand

Table 1
LDH purification on Red Sepharose with different elution strategies

Elution strategy	Capacity (units bound/ml matrix)	Recovery (%)	Elution volume (column volumes for 90% recovery)	Purification factor
PEI-700				
Run 1	320	100	3.0	4.0
Run 2	310	101	5.0	3.2
1.5 *M* KCl				
Run 1	310	81	[a]	2.5
Run 2	310	94	4.0	3.1
1 m*M* NADH + 10 m*M* oxamate				
Run 1	210	97	7.5	9.9
Run 2	270	92	10.0	9.5

Crude extract was applied until breakthrough at a flow-rate of 0.5 ml/min. The column was washed with 20 m*M* Tris · HCl buffer pH 7.3 until no protein was eluted and then eluted with either 1% PEI, or 1.5 *M* KCl, or 1 m*M* NADH + 10 m*M* oxamate, all in 20 m*M* Tris · HCl buffer pH 7.3.

[a] 81% recovery was obtained in 17.4 column volumes

and some relatively weak non-specific interactions of LDH with the dye are possible. These non-specific interactions resulted in broadened elution profiles. LDH was eluted specifically in 7–10 column volumes, while non-specifically it was eluted in 3–5 columns volumes.

Displacement chromatography has been regarded as a potentially very promising technique. Applications concerning the separation of small molecules have confirmed this statement, but it has been more difficult to attain all the advantages when separating crude protein mixtures. Only a few successful protein purifications using displacement chromatography have been reported [41]. A limiting factor has been that protein molecules are multifunctional and they interact with the support via a range of interactions. When using ion-exchange supports, there are many potential interactions that may take place and it is therefore difficult to obtain an idealized displacement behaviour. In theory it should be easier with hydrophobic sorbents since less potential interactions may occur, but the low solubility of highly hydrophobic displacers poses a problem. So far, a lot of effort has been invested but there are few successes in protein separation based on displacement chromatography.

The strategy adopted here is novel in the sense that conventional displacement is carried out, but the adsorption step has been chosen to include some more biospecificity than what is conventionally used. By means of this fewer potential interactions between the support and proteins are prevalent and the number of proteins binding to the adsorbent will be restricted. More efficient displacement steps may be achieved by this mode of operation.

4. Conclusions

Displacement of LDH from dye-affinity matrices with PEI was shown to be an effective elution strategy. It resulted in better recoveries and sharper elution profiles than traditional nonspecific elution with the same purification factors. The elution is supposed to proceed via displacement of bound protein by the polymer when the latter binds to the dye ligands. Complete elution of all bound protein is a characteristic feature of such a mechanism. Hence PEI displacement may be a promising strategy for eluting proteins with reported low recoveries in dye-affinity chromatography protocols.

Acknowledgements

The support of The Swedish Royal Academy of Sciences (KVA), the National Swedish Board for Technical and Industrial Development (NUTEK) and the Swedish Agency for Research Cooperation with Developing Countries (SAREC) is gratefully acknowledged. The authors thank Nandita Garg for linguistic advice.

References

[1] E. Boschetti, J. Chromatogr. A, 658 (1994) 207.
[2] M. Allary, J. Saint-Blancard, E. Boschetti and P. Girot, Bioseparation, 2 (1991) 167.
[3] E. Stellwagen, Methods Enzymol., 182 (1990) 343.
[4] S.R. Narayanan, J. Chromatogr. A, 658 (1994) 237.
[5] C.R. Lowe, S.J. Burton, N.P. Burton, W.K. Alderton, J.M. Pitts and J.A. Thomas, Trends Biotechnol., 10 (1992) 442.
[6] R.L. Easterday and I.M. Easterday, in R.B. Dunlap (Editor) Immobilized Biochemicals and Affinity Chromatography, Plenum Press, New York, 1974, p. 123.
[7] S. Roy and A. Nishikawa, Biotechnol. Bioeng., 21 (1979) 775.
[8] S. Whittle and A. Turner, J. Neurochem., 6 (1978) 1453.
[9] J. Barea and N. Giles, Biochim. Biophys. Acta, 524 (1978) 1.
[10] J. Barthova, M. Pecka and S. Leblova, Collect. Czech. Chem. Commun., 42 (1977) 3705.
[11] C. Tormanen, W. Redd, M. Srikantaiah and T. Scallen, Biochem. Biophys. Res. Commun., 68 (1976) 754.
[12] B. Champluvier and M.-R. Kula, Biotechnol. Bioeng., 40 (1992) 33.
[13] G. Gordon and H. Doelle, Eur. J. Biochem., 67 (1976) 543.
[14] R. Harkins, J. Black and M. Rittenberg, Biochemistry, 16 (1977) 3831.
[15] B.A. Notton, R. Fido and E. Hewitt, Plant. Sci. Lett., 8 (1977) 165.
[16] G. Vlatakis, G. Skarpelis, I. Stratidaki and V. Bouriotis, Appl. Biochem. Biotechnol., 15 (1987) 201.

[17] D. Burdette and J.G. Zeikus, Biochem. J., 302 (1994) 163.
[18] G. Jayaraman, S.D. Gadam and S.M. Cramer, J. Chromatogr., 630 (1993) 53.
[19] S.D. Gadam, G. Jayaraman and S.M. Cramer, J. Chromatogr., 630 (1993) 37.
[20] A.L.L. Abraham, W. Liao and C. Horváth, J. Chromatogr., 443 (1988) 31.
[21] S.C. David and N.G. Pinto, J. Chromatogr. Sci., 29 (1991) 478.
[22] S.-C.D. Jen and N.G. Pinto, J. Chromatogr., 519 (1990) 87.
[23] S. Ghose and B. Mattiasson, J. Chromatogr., 547 (1991) 145.
[24] A.R. Torres and E.A. Petterson, J. Chromatogr., 604 (1992) 39.
[25] R. Freitag and J. Breier, in D.L. Pyle (Editor), Separations for Biotechnology 3, SCI, Cambridge, 1994, p. 166.
[26] D. Klint, P. Arvidsson, Z. Blum and H. Eriksson, Protein Expres. Purific., 5 (1994) 569.
[27] S. Ghose and B. Mattiasson, Biotechnol. Appl. Biochem., 18 (1993) 311.
[28] I.Yu. Galaev and B. Mattiasson, in D.L. Pyle (Editor), Separations for Biotechnology 3, SCI, Cambridge, 1994, p. 179.
[29] S.J. Burton, S.B. McLoughlin, C.V. Stead and C. Lowe, J. Chromatogr., 435 (1988) 127.
[30] A.G. Mayes, R. Eisenthal and J. Hubble, Biotech. Bioeng., 40 (1992) 1263.
[31] S. Subramanian, Arch. Biochem. Biophys., 216 (1982) 116.
[32] S. Subramanian and B. Kaufman, J. Biol. Chem., 255 (1980) 10587.
[33] P.S. Appukuttan and B.K. Bachhawat, Biochim. Biophys. Acta, 580 (1979) 15.
[34] W. Heyns and P. DeMoor, Biochim. Biophys. Acta, 358 (1974) 1.
[35] C.C. Worthington (Editor), Worthington Manual–Enzymes and Related Biochemicals, Worthington Biochemical, Freehold, NJ, USA, 1988, p. 199.
[36] I.Yu. Galaev, N. Garg and B. Mattiasson, J. Chromatogr. A, 684 (1994) 45.
[37] I.Yu. Galaev and B. Mattiasson, J. Chromatogr., 648 (1993) 367.
[38] I.Yu. Galaev and B. Mattiasson, J. Chromatogr. A, 662 (1994) 27.
[39] N. Garg, I.Yu. Galaev and B. Mattiasson, Biotech. Techniques, 8 (1994) 645.
[40] I.Yu. Galaev and B. Mattiasson, Bio/Technology, 12 (1994) 1086.
[41] G. Subramanian and S.M. Cramer, Biotechnol. Progr., 5 (1989) 92.

ELSEVIER

Journal of Chromatography A, 710 (1995) 267–272

JOURNAL OF CHROMATOGRAPHY A

Chemically removable derivatization reagent for liquid chromatography
I. 2-(N-Phthalimido)ethyl 2-(dimethylamino)ethanesulfonate

Hwang-Shang Kou, Hsin-Lung Wu*, Yi-Fu Wang, Su-Hwei Chen, Shin-Sheng Wu

Graduate Institute of Pharmaceutical Sciences, Kaohsiung Medical College, Kaohsiung 807, Taiwan

First received 30 August 1994; revised manuscript received 19 April 1995; accepted 20 April 1995

Abstract

A sulfonate derivatization reagent, 2-(N-phthalimido)ethyl 2-(dimethylamino)ethanesulfonate, was synthesized and examined for use in liquid chromatography. The reagent contains two key moieties, a chromophore (phthalimido) necessary for detection and a dimethylamino function that is chemically removable after derivatization. The reagent was applied to the derivatization of 2,4,6-trichlorophenol as a model analyte. The results indicated that the reagent can be readily removed after derivatization by simple acid treatment.

1. Introduction

Analytical derivatization coupled with gas or liquid chromatography has found a wide range of applications in chemistry, biochemistry, pharmacology, toxicology, environmental science and many other disciplines; the relevant techniques for derivatization and chromatography have been extensively documented [1–6]. Basically, a large excess of derivatization reagent is used for the derivatization of an analyte at trace levels to give a derivative for sensitive analysis. Unfortunately, the excess of unreacted reagent often makes the chromatographic separation of the resulting derivative very difficult. Further disadvantages of an excess of derivatization reagent include the shortening of a column lifetime by a chemically reactive reagent and the shock to a sensitive detector caused by an intolerable input resulting from the excess of reagent.

Although several approaches have been applied for removal of excess reagent after derivatization, including using nitrogen purging for a volatile reagent [7], adding an additional chemical [8] to react with the reagent that is to be removed and column clean up [9–11]; these treatments are usually tedious, time consuming and expensive. Therefore, we sought to obtain a derivatization reagent with readily removable properties, and preliminary studies resulted in the synthesis of 2-(N-phthalimido)ethyl 2-(dimethylamino)ethanesulfonate (PEDAES). Using 2,4,6-trichlorophenol as a model organic analyte, PEDAES can be easily removed by simple acid treatment after derivatization, as illustrated in Fig. 1. This avoids interference due to reaction of the excess of the reagent with the derivative that is to be detected. The PEDAES reagent was

* Corresponding author.

0021-9673/95/$09.50
SSDI 0021-9673(95)00496-3

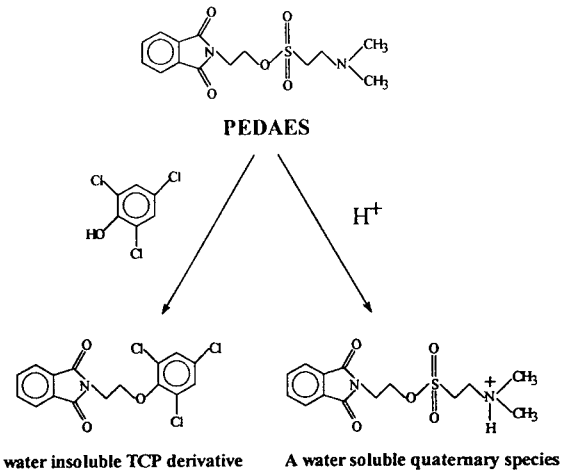

Fig. 1. Reaction scheme for PEDAES with 2,4,6-trichlorophenol and removal of excess PEDAES.

also reactive towards inorganic anions such as iodide in a biphasic water–toluene system using 18-crown-6 as the phase-transfer catalyst. The analytical derivatization of iodide will be reported elsewhere.

2. Experimental

2.1. Materials and reagents

The 2,4,6-trichlorophenol (TCP) derivative was synthesized in our laboratory and its structure was confirmed by mass and NMR spectrometry and elemental analysis. 2-Chloroethanesulfonyl chloride, N-hydroxyethylphthalimide, 18-crown-6, 4-chlorophenol (MCP), 2,4-dichlorophenol (DCP), TCP (TCI, Tokyo, Japan), dimethylamine (40%, w/v), trimethylamine (45%, w/v), toluene, potassium carbonate, sodium carbonate, sulfuric acid and silica gel 60 (70–230 mesh) (Merck, Darmstadt, Germany), diphenyl (Wako, Osaka, Japan), acetonitrile, chloroform and dichloromethane (Fisher, Fair Lawn, NJ, USA) were used without further treatment. All other chemicals were of analytical-reagent grade. Solutions of MCP, DCP, TCP, 18-crown-6 and PEDAES were prepared by dissolving the appropriate amounts in toluene and a solution of diphenyl (internal standard, I.S.) was prepared in acetonitrile.

2.2. HPLC conditions

A Waters–Millipore LC system with a U6K injector, a Model 510 pump and a Model 486 UV–Vis detector was used. A Nova-Pak C_{18} (4 μm) column (150 × 3.9 mm I.D.) and a mobile phase acetonitrile–water (55:45, v/v) at a flow-rate of 0.9 ml/min were used. The column eluate was monitored at 225 nm. The solvent was pretreated with a vacuum filter for degassing.

2.3. Synthesis of PEDAES

Synthesis of 2-(N-phthalimido)ethyl ethenesulfonate (PEES)

N-Hydroxyethylphthalimide (2.40 g, 12.55 mmol), 2-chloroethanesulfonyl chloride (2.65 ml, 25.20 mmol) and trimethylamine (7.79 ml, 50.40 mmol) were placed successively in a 100-ml reaction flask containing chloroform (60.0 ml) pre-cooled in an ice-bath. The reaction mixture was magnetically stirred at 0°C for 1.5 h, then the resulting mixture was washed successively with water (3 × 60 ml) and (10%, w/v) sodium carbonate solution (2 × 60 ml). The chloroform layer was treated with anhydrous sodium sulfate (ca. 2.5 g) and the filtrate was evaporated to dryness in a rotary evaporator. The residue dissolved in dichloromethane (4.0 ml) was purified by column chromatography (40 × 3 cm I.D.) on silica gel 60 (ca. 120 g) with dichloromethane as the eluent, to give PEES (1.48 g, 5.27 mmol) as a white powder, m.p. 87–88°C. ^{1}H NMR ($CDCl_3$): δ4.03 (t, 2H, N-CH_2, J = 5.43 Hz), 4.40 (t, 2H, CH_2-O, J = 5.46 Hz), 6.10 (d, 1H, *cis*-terminal vinyl proton, J = 9.38 Hz), 6.39 (d, 1H, *trans*-terminal vinyl proton, J = 16.64 Hz), 6.51 (dd, 1H, vinyl proton, J = 9.38 Hz), 7.72–7.90 (m, 4H, aromatic H). Analysis: calculated for $C_{12}H_{11}NO_5S$, C 51.25, H 3.91, N 4.98; found, C 51.08, H 3.90, N 4.97%. MS [fast atom bombardment (FAB)]: m/z 282 (M^+ + 1), 174

($M^+ - OSO_2CH=CH_2$), 107 (M^+ – phthalimidoethyl moiety).

Synthesis of PEDAES

PEES (1.42 g, 5.05 mmol) and dimethylamine (0.89 ml, 7.03 mmol) were placed in a 150-ml reaction flask containing dichloromethane (100 ml) pre-cooled in an ice-bath. The reaction mixture was magnetically stirred at 0°C for 1.5 h. The resulting mixture was treated with anhydrous sodium sulfate (ca. 2.5 g) and the filtrate was evaporated to dryness (1.59 g) in a rotary evaporator. An aliquot of the residue (1.0 g) recrystallized from 10 ml of *n*-hexane–chloroform (3:2, v/v) gave a colourless plate crystal (72% yield), m.p. 106–107°C. ^{1}H NMR ($CDCl_3$): δ2.22 (s, 6H, $N(CH_3)_2$), 2.75 (t, 2H, CH_2NMe_2, $J = 7.42$ Hz), 3.28 (t, 2H, CH_2SO_2, $J = 7.43$ Hz), 4.04 (t, 2H, CH_2N-phthalimido, $J = 5.31$ Hz), 4.50 (t, 2H, CH_2O, $J = 5.34$ Hz), 7.72–7.90 (m, 4H, aromatic). ^{13}C NMR ($CDCl_3$) from HETCO ($^{13}C/^1H$); δ37.25 [$CH_2N(CO)_2$], 45.00 (N-Me_2), 48.81 (CH_2SO_2), 52.84 (CH_2NMe_2), 65.56 (CH_2O), 123.50 and 134.24 (aromatic C other than that of angular C), 131.91 (angular aromatic C), 167.87 (imido C). Analysis: calculated for $C_{14}H_{18}N_2O_5S$, C 51.51, H 5.57, N 8.58, S 9.83; found, C 51.49, H 5.56, N 8.61, S 9.67%. MS [electron impact (EI)]: *m/z* 326 (M^+), 173 (phthalimidoethyl – H), 160 (phthalimidomethyl), 71 ($CH_2=CHNMe_2$), 58 (CH_2NMe_2).

2.4. Derivatization procedure

A 0.2-ml aliquot of TCP (50 μM) or other chlorophenol solution was added to a 10-ml screw-capped test-tube containing about 50 mg of potassium carbonate, then 0.1 ml of 18-crown-6 solution (100 mM) and 0.5 ml of PEDAES solution (60 mM) were added. The reaction mixture was shaken at 95°C for 4.0 h. After cooling, 0.4 ml of the reacted toluene solution was taken and washed with 1.0 ml of 1.0 M H_2SO_4 by vortex mixing for 30 s. A 0.1-ml aliquot of the acid-washed toluene layer was transferred into a test-tube and purged with a gentle stream of nitrogen to near dryness, then 0.1 ml of diphenyl solution (40 μM) was added and the resulting solution was used for HPLC analysis (about 15 μl).

3. Results and discussion

To study the chemical removability and reactivity of the newly synthesized reagent PEDAES, TCP was used as a model analyte in an amount of 10 nmol. The effects of reaction temperature, reaction time and amount of PEDAES on the derivatization of TCP in toluene were studied, using 18-crown-6 (10 μmol) and potassium carbonate (ca. 50 mg) as catalyst in a 0.8-ml reaction system. The resulting effects were evaluated by measuring the peak-area ratio of the derivative with respect to diphenyl (I.S.) The optimum amounts of 18-crown-6 and potassium carbonate were found to be $\geq$5 μmol and $\geq$25 mg, respectively, in the reaction system.

3.1. Effects of reaction temperature and reaction time

The reaction temperature and reaction time required to reach an equilibrium for the TCP derivative were studied. The results indicated that 4 h were needed for derivatization at 95°C, whereas with derivatization at 70°C, plateau formation of the derivative was not attainable in 6 h and a lower yield was obtained compared with reaction at 95°C. The derivatization yields of TCP at three levels (at 95°C) were all above 95% as shown in Table 1, based on the peak-

Table 1
Derivatization yield of 2,4,6-trichlorophenol

2,4,6-Trichlorophenol tested (nmol)	Derivative found[a] (nmol)	Yield (%)
8.02	7.81 ± 0.04	97.4
4.01	3.83 ± 0.01	95.5
1.00	0.98 ± 0.01	98.0

[a] Mean ± S.D. of triplicate analyses.

area ratios of the TCP derivative to the I.S. in comparison with that of the synthesized TCP derivative to the I.S.

3.2. Effect of amount of derivatizing agent

The amount of PEDAES required for the derivatization of TCP (10 nmol) to plateau formation of the derivative was about 27.5 μmol, equivalent to a molar ratio of PEDAES to TCP of about 2750, as shown in Fig. 2; however, an excess of the reagent (30 μmol) was selected for the derivatization of TCP.

3.3. Removability of derivatizing agent after derivatization

TCP (10 nmol), DCP (10 nmol) or MCP (15 nmol) was derivatized with excess of PEDAES as described in Section 2.4. After derivatization, the reaction mixture was either treated with or without 1.0 *M* H_2SO_4 (1 ml). The results are shown in Fig. 3. A broad and large reagent peak overlapped that of the chlorophenol derivatives resulting from the derivatization without treatment with acid solution. On the other hand, the interfering PEDAES peak in Fig. 3 can be easily removed after derivatization by simple treatment of the reaction solution with H_2SO_4, based on the protonation of the tertiary amino function of PEDAES to form a water-soluble quaternary species. The resulting quaternary species in water can be easily separated from the chlorophenol derivatives in the toluene layer.

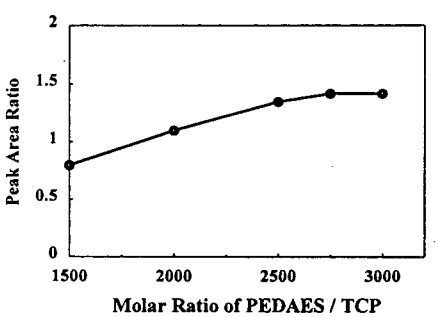

Fig. 2. Effect of molar ratio of PEDAES to 2,4,6-trichlorophenol on the formation of the TCP derivative. See text for conditions.

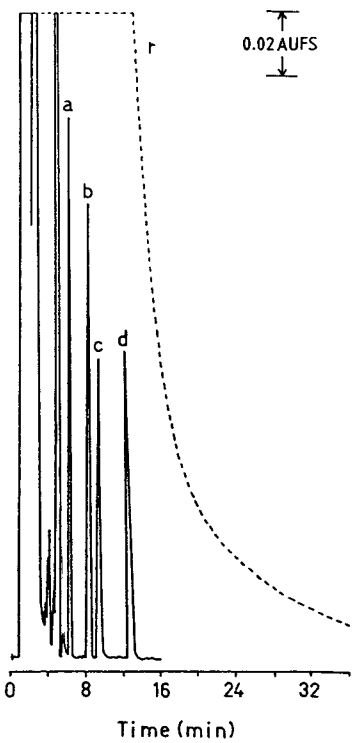

Fig. 3. Composite liquid chromatogram of 4-chlorophenol (MCP) (15 nmol), 2,4-dichlorophenol (DCP) (10 nmol) and 2,4,6-trichlorophenol (TCP) (10 nmol) derivatized with PEDAES with acid treatment (solid line) and without acid treatment (dashed line) after derivatization. Peaks: a = derivative of MCP; b = derivative of DCP; c = diphenyl (I.S.); d = derivative of TCP; r = excess of reagent. See text for conditions.

3.4. Mass spectra analysis of the derivatives

The derivative of TCP was synthesized by scaling up the amount of TCP (0.278 mmol) in toluene (20 ml) and using a similar procedure to that described in Section 2.4. The resulting derivative (m.p. 103–104°C) was examined by FAB-MS (JEOL JMX-HX 110 instrument) using thioglycerol as the sample matrix. The mass spectrum obtained exhibited a pseudo-molecular ion of *m/z* 370 (M′ = M + 1) and the typical ion peak proportions of M′: M′ + 2: M′ + 4 were equivalent to 100.0:98.0:36.0, revealing a characteristic species with three chlorine atoms, and a basal peak of *m/z* 174 was also found, corresponding to the N-phthalimidoethyl moiety.

This reasionally suggests that the resulting derivative is 2-(N-phthalimido)ethyl 2,4,6-trichlorophenyl ether. The retention time of peak d in Fig. 3 is identical with that of the synthesized derivative. The derivatives of MCP and DCP were not synthesized for retention time comparison, but peaks a and b in Fig. 3., equivalent to the derivatives of MCP and DCP, respectively, were elucidated by GC–EI-MS (Varian Star 3400 CX–Saturn 3 system). The mass spectra obtained for the derivatives of MCP and DCP exhibited their parent ions at m/z at 301 and 335, respectively, corresponding to the (N-phthalimido)ethyl ethers of the related chlorophenols.

3.5. Analytical calibration

Based on the optimum derivatization conditions for TCP as indicated in Section 2.4, the method was used to the determination of several chlorophenols, including TCP, DCP and MCP, to evaluate its quantitative applicability. The ranges of TCP, DCP and MCP levels used for the study were 0.1–10.0, 0.1–10.0 and 0.2–15.0 nmol, respectively. Five different amounts of each chlorophenol in the stated range were measured and the linearity between the peak-area ratios (y) and sample masses (x, nmol) was studied. The linear regression equations obtained were $y = (0.1423 \pm 0.0014)\ x - (0.0023 \pm 0.0002)$ with a correlation coefficient (r) of 0.999 for TCP, $y = (0.1519 \pm 0.0035)\ x + (0.0089 \pm 0.0008)$ with $r = 0.999$ for DCP and $y = (0.1012 \pm 0.0019)\ x + (0.0129 \pm 0.0009)$ with $r = 0.999$ for MCP, indicating good linearity of the method. The detection limits (signal-to-noise ratio = 5) for TCP, DCP and MCP were about 0.01, 0.01 and 0.02 nmol, respectively.

3.6. Application

The proposed method was cursorily applied to the determination of TCP spiked in water at concentrations of 50.6, 202.6 and 405.2 nM (prepared by dissolving and diluting suitable amounts of TCP in 0.01 M KOH solution). The procedure for the extraction of TCP is as follows: a 100-ml aliquot of the TCP (5.1, 20.3 or 40.5 nmol)-spiked water was acidified to pH 1 with 3 M H_2SO_4 and extracted with 1.0 ml of toluene by shaking for 5 min in a pear-shaped separating funnel. After suitable discharge of the lower water layer, a 0.2-ml aliquot of the toluene extract was directly subjected to derivatization and HPLC analysis as indicated in Section 2.4. The results are given in Table 2; the recoveries of the spiked TCP were all >92%. The method presented is very simple, using the same solvent (toluene) for the extraction and derivatization. A considerable increase in the sensitivity of the method is suggested by the extraction of a large volume of TCP-containing water sample with toluene and, in turn, concentration of the toluene extract for derivatization.

Table 2
Analytical results for 2,4,6-trichlorophenol-spiked water

Amount spiked (nmol)	Amount found[a] (nmol)	Recovery (%)	R.S.D. (%)
5.1	4.73 ± 0.07	92.7	1.48
20.3	19.12 ± 0.24	94.2	1.26
40.5	37.84 ± 0.38	93.4	1.00

[a] Mean ± S.D. of triplicate analyses.

In conclusion, the sulfonate reagent PEDAES was synthesized and its preliminary application to the derivatization of TCP, DCP and MCP was demonstrated. The results indicated that the excess of reagent can be readily removed by simple acid treatment after derivatization. This makes the separation of the resulting derivative for detection very simple. Further modification of the reagent for sensitive detection with a potential tag such as a chromophore, electrophore or fluorophore coupled with variation in the tertiary amino function for acid removal will be very attractive.

Acknowledgement

The authors are grateful to the National Science Council, ROC, for financial support of this work.

References

[1] J.F. Lawrence and R.W. Frei (Editors), Chemical Derivatization in Liquid Chromatography, Elsevier, Amsterdam, 1976.
[2] K. Blau and G.S. King (Editors), Handbook of Derivatives for Chromatography, Heyden, London, 1978.
[3] D.R. Knapp (Editor), Handbook of Analytical Derivatization Reaction, Wiley, New York, 1979.
[4] F. Lawrence, R.W. Frei and J.F. Lawrence (Editors), Chemical Derivatization in Analytical Chemistry, Vol I: Chromatography, Plenum Press, New York, 1981.
[5] J. Drozd (Editor), Chemical Derivatization in Gas Chromatography, Elsevier, Amsterdam, 1981.
[6] H. Lingeman and W.J.M. Underberg (Editors), Detection-Oriented Derivatization Techniques in Liquid Chromatography, Marcel Dekker, New York, 1990.
[7] J.M. Rosenfeld and J.L. Crocco, Anal. Chem., 50 (1978) 701–704.
[8] O. Gyllenhaal, H. Brotell and P. Hartvig, J. Chromatogr., 129 (1976) 295–302.
[9] L.G. Johnson, J. Assoc. Off. Anal. Chem., 56 (1973) 1503–1505.
[10] A. Vairavamurrthy, M.O. Andreae and J.M. Brooks, Anal. Chem., 58 (1986) 2684–2687.
[11] A. Sonesson, L. Larsson and J. Jimenez, J. Chromatogr., 417 (1987) 366–370.

ELSEVIER

Journal of Chromatography A, 710 (1995) 273–285

JOURNAL OF CHROMATOGRAPHY A

Liquid chromatographic–thermospray mass spectrometric analysis of sesquiterpenes of *Armillaria* (Eumycota: Basidiomycotina) species

Peadar Cremin[a], Dervilla M.X. Donnelly[a], Jean-Luc Wolfender[b], Kurt Hostettmann[b,*]

[a]*Department of Chemistry, University College Dublin, Dublin 4, Ireland*

[b]*Institut de Pharmacognosie et Phytochimie, École de Pharmacie, Université de Lausanne, CH-1015 Lausanne, Switzerland*

First received 17 January 1995; revised manuscript received 26 April 1995; accepted 26 April 1995

Abstract

Conventional HPLC analysis of the sesquiterpene aryl esters present in the crude extracts of the pathogenic basidiomycete *Armillaria* is complicated by difficulties in identification solely on the basis of retention time. On-line coupling of liquid chromatography with thermospray mass spectrometry (LC–TSP-MS) provides a means for their direct detection. Crude extracts of seven *Armillaria* species were analysed providing a semi-quantitative survey of sesquiterpene aryl ester production within the genus. The distribution of these metabolites and its significance with regard to species differentiation and pathogenicity are discussed. Unknown components were also detected by on-line LC–TSP-MS screening of extracts, facilitating a targeted isolation route.

1. Introduction

The pathogenic basidiomycete *Armillaria* is the cause of widespread root disease in deciduous and coniferous trees and can also exist as a saprophyte, particularly on tree stumps [1]. Five European and 20 worldwide species have been classified with virulence varying widely from species to species and within strains of the same species [2,3]. Our previous phytochemical examinations led to the isolation of several biologically active sesquiterpene aryl esters from *Armillaria* species [4]. These metabolites possess varying antibiotic and antifungal activity and comprise three major structural types represented by armillyl orsellinate (J), melleolide (I) and armillane (F) (Fig. 1). The structural similarity of this series of sesquiterpene aryl esters suggests a common biosynthetic pathway. However, the role played by each of these metabolites in this pathway and their relationship to pathogenicity within the genus are of interest.

An initial study of the distribution of sesquiterpene aryl esters within the genus involved a high-performance liquid chromatographic (HPLC) analysis of crude extracts of five *Armillaria* species [5]. This led to the tentative linking of higher concentrations of certain sesquiterpenes to virulent strains. However, retention time data alone are insufficient for the identification of the sesquiterpenes of interest because of

* Corresponding author.

0021-9673/95/$09.50
SSDI 0021-9673(95)00514-5

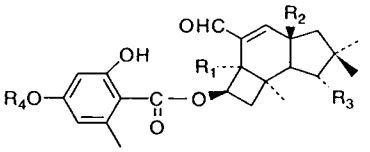

	R_1	R_2	R_3	R_4
A : melledonal	OH	OH	OH	H
C : 5'-methoxy melledonal	OH	OH	OH	OCH_3
D : 13-hydroxy-4-methoxymelleolide	OCH_3	OH	H	H
I : melleolide	OH	H	H	H
K : 4-methoxy melleolide	OCH_3	H	H	H
M : 4-dehydromelleolide	H	H	H	H

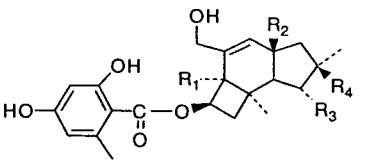

	R_1	R_2	R_3	R_4
B : 13-hydroxhdihydromelleolide	OH	OH	H	H
E : 14-hydroxydihydromelleolide	OH	H	H	OH
G : 10-hydroxydihydromelleolide	OH	H	OH	H
L : dihydromelleolide	OH	H	H	H
H : 4-dehydro-14-hydroxydihydromelleolide	H	H	H	OH
N : 4-dehydrodihydromelleolide	H	H	H	H

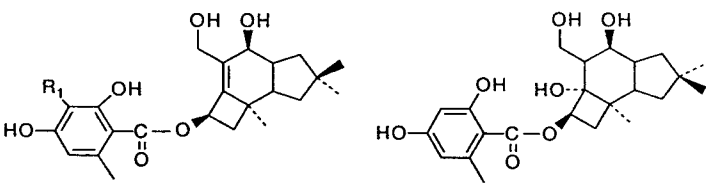

	R_1
J : armillyl orsellinate	H
O : armamiol	Cl

F : armillane

Fig. 1. Structures of the sesquiterpene aryl esters studied.

interference between the main sesquiterpenes and minor components.

Here we report on the liquid chromatographic–thermospray mass spectrometric (LC–TSP-MS) analysis of a standard mixture of 15 sesquiterpene aryl esters and crude extracts of seven *Armillaria* species (Table 1). This allowed a rapid semi-quantitative survey of sesquiterpene distribution within the genus. On-line coupling of liquid chromatography with ultraviolet spectrophotometry (LC–UV) and with mass spectrometry (LC–MS) in the analysis of crude plant extracts provides important structural information on metabolites directly in their biological matrices [6,7].

2. Experimental

2.1. Chemicals

HPLC-grade water was prepared by distillation on a Büchi (Flawil, Switzerland) Fontavapor 210 distillation instrument and passed through a 0.50-μm filter (Millipore, Bedford, MA, USA). HPLC-grade methanol from Maechler (Reinach,

Table 1
Armillaria genus: species and strains investigated

Species	Pathogenicity[a]	Host range	Strains examined[b]
Armillaria mellea	Pathogenic	Broadleaved, conifers, vines, fruit trees and shrubs	UCD 520, UCD 618, UCD 619, UCD 622, UCD 662, UF IM-CT-91, UF IM-SR-VIR, UF IM-QG-SAP
Armillaria ostoyae	Moderately pathogenic	Conifers (associated with fir species in Europe)	UCD 663, UCD 664, UCD 666, UCD 667, CBS 434.72
Armillaria tabescens (European)	Non-pathogenic	Broadleaved (associated with oak species in Europe)	UF IM-TAB-1, UF IM-TAB-202, UF IM-TAB-303, INRA PT 89.92, INRA PT 83.39, INRA PT 90.5
Armillaria monadelpha (*Armillaria tabescens*, N. American)	Pathogenic	Broadleaved, conifers, fruit trees and shrubs	CBS 132.72, CBS 129.26
Armillaria gallica	Non-pathogenic	Broadleaved (associated with oak species in Europe)	UF 303
Armillaria cepestipes	Non-pathogenic	Broadleaved and conifers	UF 505
Armillaria novae-zelandiae	Moderately pathogenic	Broadleaved (associated with species of southern beech)	CBS 432.72
Unknown	Unknown	Unknown	UF A79

[a] Based on widespread distribution and ability to cause disease in natural forests, plantations and amenity planting [1,3].
[b] Strains examined were from the following collections: UCD = Department of Botany, University College Dublin, Dublin 4, Ireland; UF = Dr. M. Intini, Patologia Vegetale, Università di Firenze, Florence, Italy; CBS = Centraalbureau voor Schimmelcultures, Baarn, Netherlands; INRA = Professor J.J. Guillaumin, INRA, Clermont-Ferrand, France.

Switzerland) was passed through a 0.45-μm filter. Ammonium acetate was obtained from Merck (Darmstadt, Germany). DIFCO potato dextrose broth was obtained from DIFCO Laboratories (Michigan, USA). Merck Kieselgel 60 and Sephadex LH-20 were used as stationary phases for open-column chromatography.

2.2. HPLC conditions

Separations were performed on a Hypersil ODS 5 column (250 × 4.66 mm I.D.) equipped with a Nova-Pak Guard precolumn. A gradient of methanol–water from 75:25 to 90:10 in 30 min (1 ml/min) was used.

2.3. LC–UV analyses

Eluent delivery was provided by an LC-9A HPLC pump (Shimadzu, Tokyo, Japan) equipped with an FCV-9AL low-pressure mixing valve and a Model 7125 injection valve with a 20-μl loop (Rheodyne, Cotati, CA, USA). UV spectra were recorded with an HP-1040A photodiode-array detector and the data were processed on an HP-1090 Chemstation (Hewlett-Packard, Palo Alto, CA, USA).

2.4. LC–TSP-MS analyses

A Finnigan MAT (San Jose, CA, USA) TSQ-700 triple quadrupole instrument equipped with a TSP 2 interface was used for the data acquisition and processing. The temperatures of the TSP were source block 200°C, vaporizer 95°C and aerosol 200–220°C (beginning–end of gradient). The electron multiplier voltage was 1800 V, dynode 15 kV and the filament and discharge were off. Full-scan spectra from m/z 140 to 600 in the positive-ion mode were obtained (scan

time 1.2 s). Concerning the LC part, the eluent delivery was provided by a 600-MS HPLC pump (Waters) equipped with a gradient controller. The UV trace was recorded on-line with a Waters 490-MS programmable multi-wavelength detector. Postcolumn addition of buffer (0.5 *M* ammonium acetate) was achieved with a Waters 590-MS programmable HPLC pump (0.2 ml/min) using a simple tee junction (Waters).

2.5. Samples

Sesquiterpene aryl esters A–O were obtained from previous isolation work and standard solutions prepared by dissolving 0.2 mg of each in 1 ml of methanol. Each strain of the *Armillaria* species listed in Table 1 was grown on DIFCO potato dextrose broth in 12 × 1 l Roux flasks (each containing 200 ml). After incubation in the dark for 35 days at 24°C, these were harvested by filtration. The mycelium was macerated in methanol (2 × 300 ml), evaporated to dryness and then partitioned into chloroform–methanol–water (65:35:20) (2 × 1500 ml). Evaporation of the combined chloroform layers yielded the crude mycelial extract. The culture broth was extracted with hexane (3 × 200 ml) followed by ethyl acetate (4 × 300 ml). Evaporation of the combined ethyl acetate layers yielded the crude culture broth extract. Solutions to be analysed were prepared by dissolving 30 mg of these crude extracts in 1 ml of methanol. The injection volume was 10 μl.

2.6. Armillaria novae-zelandiae samples

Gel filtration on Sephadex LH-20 (methanol) of 4.733 g of the mycelial extract of *Armillaria novae-zelandiae* (CBS 432.72) yielded five fractions. Fraction II (4.034 g) was chromatographed on silica gel with gradient elution from 100:1 to 10:1 chloroform–methanol. This yielded five sub-fractions. Analysis of these sub-fractions was achieved by dissolving 20 mg in 1 ml of methanol with an injection volume of 10 μl.

3. Results

3.1. LC–UV photodiode-array detection

Reversed-phase HPLC utilizing gradient elution with methanol–water was used to separate the 15 sesquiterpene aryl esters A–O (Fig. 1). This separation was monitored by on-line LC–UV photodiode-array detection (Fig. 2), which allows the measurement of the UV spectrum (170–400 nm) of each component eluted. These metabolites possess an identical basic aryl chromophore which renders on-line LC–UV detection ineffective for their differentiation. This structural similarity also leads to similar retention time characteristics and co-elution, render-

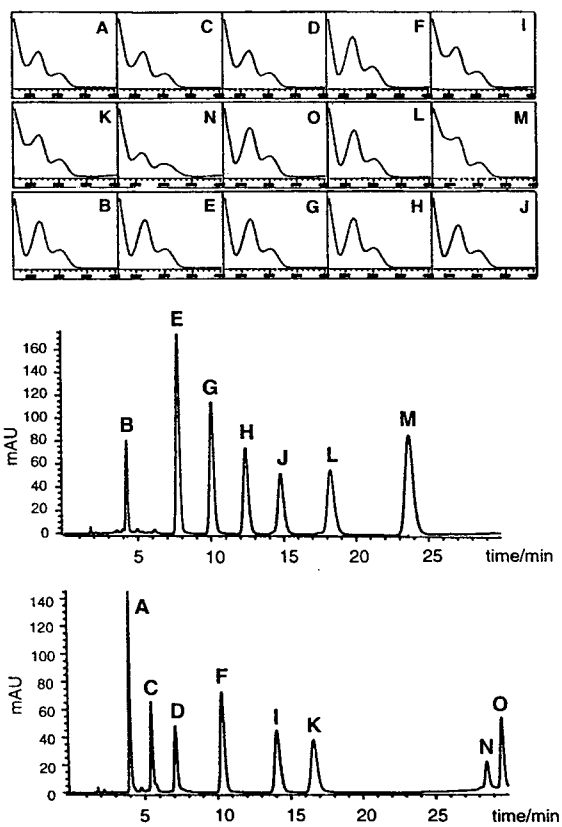

Fig. 2. Gradient HPLC–UV trace for sesquiterpene aryl esters A–O. For conditions, see Experimental. UV traces were recorded at 254 nm with UV spectra recorded from 170 to 400 nm. For peak identities, see Fig. 1.

ing some members of this group indistinguishable by conventional HPLC detection methods.

3.2. LC–MS thermospray tuning

LC–TSP-MS is a soft ionization technique that leads to the formation of adduct ions such as $[M + H]^+$ with molecules. These adduct ions allow the rapid determination of the molecular mass of a component directly after elution from the LC column. Sesquiterpene aryl esters are thermolabile and hence the ability to observe the adduct ions produced is a function of the temperatures set for the thermospray interface. The effect of variation of these parameters was investigated in the positive-ion mode with a solution of armillyl orsellinate (J: M_r 402) in methanol. Total ion current (TIC) and characteristic ion intensities as a function of ion source block temperature and as a function of thermospray vaporizer temperature were measured.

First the mass spectrum of armillyl orsellinate was measured at a source temperature of 200°C and a vaporizer temperature of 90°C for the purpose of determining the characteristic ions of this class of metabolites (Fig. 3). This showed an intense $[M + NH_4]^+$ ion as the base peak. The soft ionization characteristics of TSP-MS lead to a lack of fragmentation and the most intense fragment ions appear at m/z 385 (loss of water) and m/z 217 (loss of aryl group leading to protoilludane fragment ion). These characteristic ions were used to examine the dependence of the mass spectrum of armillyl orsellinate on the TSP-MS parameters. The variation in TIC and characteristic ion intensities as a function of ion source block temperature is illustrated in Fig. 4a. It is observed that although the TIC reaches a maximum at 240°C, at this temperature the base peak is at m/z 217, the protoilludane fragment ion, whereas below 220°C, the base peak is at m/z 420, the ammmoniated adduct of the molecular ion. A temperature of 200°C was then selected to maximize the response for the latter ion. Variation in TIC and characteristic ion intensities as a function of vaporizer temperature are shown in Fig. 4b. This plot indicates that the best ion intensities for the ammoniated ion are to

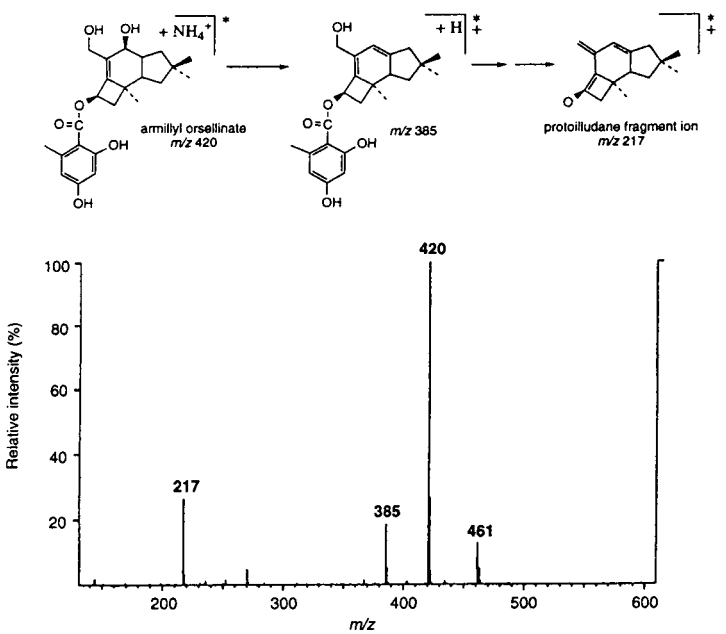

Fig. 3. LC–TSP mass spectrum of armillyl orsellinate (J).

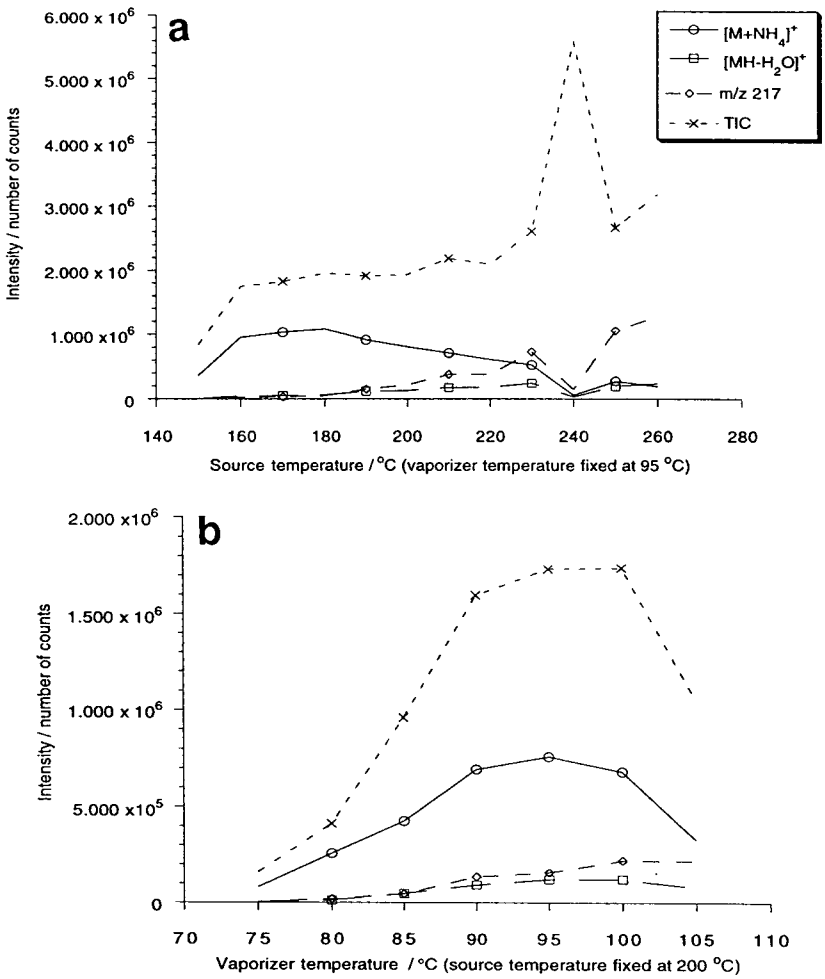

Fig. 4. Influence of (a) ion source temperature and (b) vaporizer temperature on the adduct molecular and fragment ions of armillyl orsellinate.

be obtained at a setting of 95°C. The mass spectrum of armillyl orsellinate was also recorded at different repeller potential values 0–200 V, with only a small variation in intensities observed at extreme values, i.e., less than 20 V or greater than 160 V. The repeller was then set to 100 V. Ammonium acetate was added as postcolumn buffer as this led to an increased intensity for the recorded ions. No improvements were observed using the filament-on or discharge-on modes under these conditions and the analysis was achieved in the filament-off mode.

3.3. LC–MS detection of sesquiterpene aryl esters

Fig. 5 shows the TIC and UV traces for a standard solution of eight of these sesquiterpene aryl esters and also the selected-ion monitoring traces for their adduct ions. A mass of 2 μg of each sesquiterpene was contained in the injection. The chromatographic characteristics and the positive-ion TSP-MS results for the 15 sesquiterpene aryl esters A–O are given in Table 2. The adduct ion $[M + NH_4]^+$ appears as the base peak in the TSP mass spectra for 13 of the

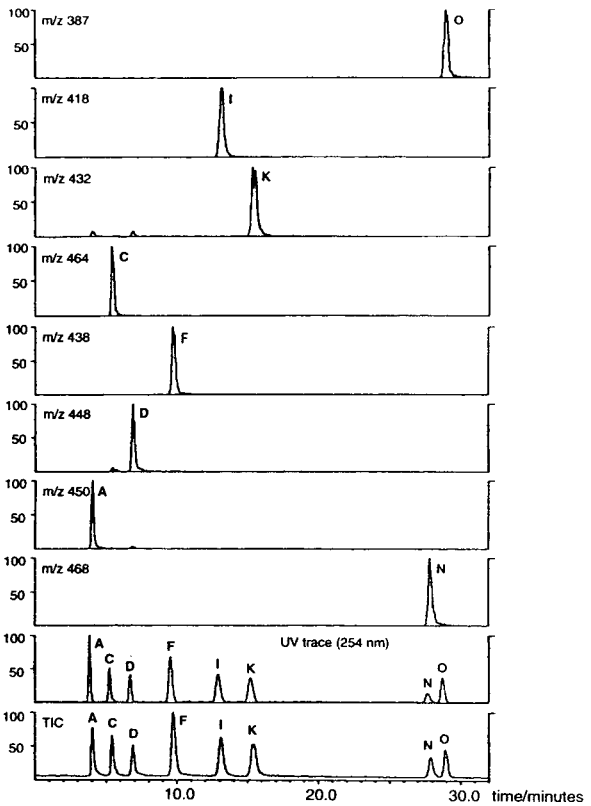

Fig. 5. LC–TSP-MS analysis for eight sesquiterpene aryl esters. For conditions, see Experimental. The UV trace at 254 nm and TIC trace for the standard solution are displayed, in addition to selected-ion traces corresponding to the adduct molecular ions of O, I, K, C, F, D, A and N.

sesquiterpene aryl esters. The abundance of ammoniated adducts in the TSP mass spectra has been explained by stabilization associated with the presence of a double bond and hydroxyl groups [8]. This is supported by the TSP mass spectra of 4-dehydromelleolide (M) and 4-dehydrodihydromelleolide (N), which do not possess a Δ^{2-3} double bond or oxygenation at position 3 and which exhibit the $[M + H]^+$ ion as the most intense peak rather than the ammoniated adduct.

The detection limit for these ions was investigated by injection of various amounts of armillyl orsellinate. This indicated that HPLC–TSP-MS could be used to detect these sesquiterpenes down to levels of 1 pg.

3.4. Extract analysis

Fig. 6 illustrates the analysis of a strain of the pathogenic *A. mellea* species (UCD 619). The LC–UV and TIC trace reveal a complex extract, with many sesquiterpene aryl esters present. However, their close retention times lead to considerable interference with each other and hence much confusion in assigning peaks. This is alleviated, however, by the selected-ion traces, in which each sesquiterpene aryl ester is clearly evident at its expected retention time free from interference. The selectivity of LC–TSP-MS in resolving overlapping components is demonstrated by the determination of armillane (F), *m/z* 420, and 10-hydroxydihydromelleolide (G), *m/z* 436, in this extract (Fig. 6). These two metabolites differ by about 20 s in elution times and can be distinguished by selective ion monitoring. They are indistinguishable, however, by conventional UV detection.

The sensitivity of LC–TSP-MS is useful for analysis of extracts in which these metbolites are present in trace amounts. Initial analysis of the mycelial extracts of INRA PT 90.5, a strain of the non-pathogenic species *A. tabescens*, established the presence of only two sesquiterpene aryl esters, armillyl orsellinate (J) and melleolide (I), which appear as the major components on the LC–UV and TIC traces (Fig. 7). However, selective ion monitoring at *m/z* 432 reveals the presence of an unknown component, P eluting at 26.12 min. Furthermore, selective ion monitoring at *m/z* 468 reveals the presence of arnamiol (O). These metabolites are not visible on the UV or TIC traces owing to the predominance of armillyl orsellinate (J) and melleolide (I).

The sesquiterpene aryl esters investigated in this study all exhibit a similar level of MS response. This facilitated a semi-quantitative analysis of their distribution based on observed ion intensities recorded in the analysis of *Armillaria* extracts. Selected-ion monitoring simplifies the process of recording the ion intensity of each sesquiterpene. Extracts of 25 strains were analysed. The intensities of the recorded ions were tabulated and results for some representative individual strains are illustrated in Table 3.

Table 2
Summary of the results of the LC–TSP-MS analysis of sesquiterpene aryl esters A–O

Code	Sesquiterpene	M_r	Retention time (min)	Major ions observed (m/z)[a]	
				$[M + NH_4]^+$	Others
A	Melledonal	432	3.8	450 (100)	433 (5):$[MH]^+$; 397 (1):$[MH - 2H_2O]^+$
B	13-Hydroxydihydromelleolide	418	4.0	436 (100)	419 (22):$[MH]^+$; 401 (80):$[MH - H_2O]^+$; 233 (55)
C	5-Methoxymelledonal	446	5.3	464 (100)	447 (10):$[MH]^+$; 217 (1)
D	13-Hydroxy-4-methoxymelleolide	430	6.8	448 (100)	431 (55):$[MH]^+$
E	14-Hydroxydihydromelleolide	418	7.3	436 (100)	383 (10):$[MH - 2H_2O]^+$; 233 (25)
F	Armillane	420	9.7	438 (100)	421 (25):$[MH]^+$; 251 (15)
G	10-Hydroxydihydromelleolide	418	9.4	436 (100)	419 (40):$[MH]^+$; 233 (50)
H	4-Dehydro-14-hydroxydihydromelleolide	402	11.6	420 (100)	403 (5):$[MH]^+$; 385 (30):$[MH - H_2O]^+$; 217 (80)
I	Melleolide	400	13.25	418 (100)	401 (25):$[MH]^+$; 250 (20):[MH-aryl]$^+$
J	Armillyl orsellinate	402	13.9	420 (100)	403 (5):$[MH]^+$; 385 (80):$[MH - H_2O]^+$; 217 (60)
K	4-Methoxymelleolide	414	15.7	432 (100)	415 (25):$[MH]^+$; 233 (5)
L	Dihydromelleolide	402	17.2	420 (100)	385 (20):$[MH - H_2O]^+$; 217 (55)
M	4-Dehydromelleolide	384	24.0	402 (80)	385 (100):$[MH]^+$; 217 (5)
N	4-Dehydrodihydromelleolide	386	28.7	404 (20)	387 (100):$[M - H]^+$; 369 (60):$[MH - H_2O]^+$; 343 (30):$[MH - CO_2]^+$
O	Arnamiol	449	29.7	468 (100)	217 (80)

[a] The relative intensity (%) of the ion is given in the parentheses after the m/z value.

These results were also averaged for each species to achieve an overall picture of the distribution of these metabolites within the genus (Table 4). This reveals that sesquiterpene aryl esters are produced by all members of the genus, but not in equal amounts. The species *A. mellea*, *A. tabescens* and *A. ostoyae* were examined in detail with strains from different sources included in the study. The results indicate that the culture broth and mycelial extracts of *A. mellea* possess a higher concentration level of all 15 sesquiterpene aryl esters than those of *A. ostoyae*, which

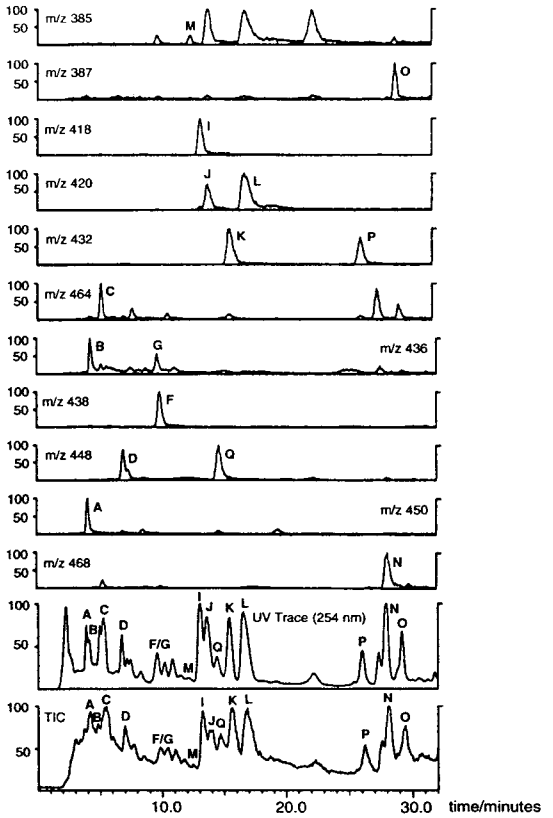

Fig. 6. LC–TSP-MS analysis of mycelial extract of *A. mellea* (strain UCD 619). The UV trace at 254 nm and TIC trace are displayed, in addition to selected-ion traces corresponding to adduct ions of sesquiterpene aryl esters A–O (sesquiterpenes H, *m/z* 420, and E, *m/z* 436, were undetected in this extract) and unknown components P and Q.

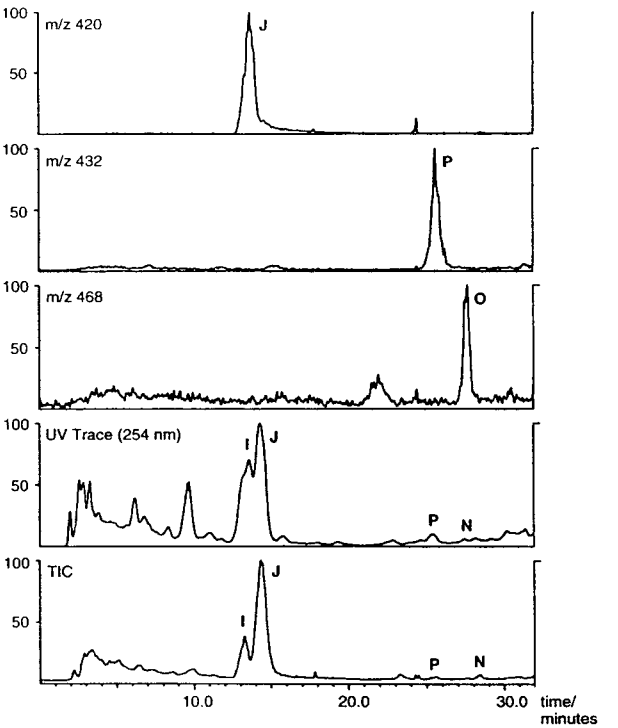

Fig. 7. LC–TSP-MS analysis of the mycelial extract of *A. tabescens* (strain INRA PT 90.5). The UV trace at 254 nm and TIC trace are displayed, in addition to selected-ion traces at *m/z* 420, armillyl orsellinate (J), *m/z* 432, component P, and *m/z* 468, arnamiol (O).

in turn possesses a higher concentration level of sesquiterpenes than extracts of *A. tabescens*. This variation in sesquiterpene aryl ester concentration mirrors the variation in reported pathogenicity of these species (Table 2). Hence the existence of a direct relationship between the level of these metabolites and pathogenicity is supported.

Two strains of *A. tabescens* (N. American), regarded as a serious pathogen in the southern USA, were examined. *A. tabescens* (European) is reported as possessing a low pathogenic ability [3]. Recent mycological studies led to the proposal that *A. tabescens* (N. American) is a distinct and different species from *A. tabescens* (European) and the name *A. monadelpha* is suggested for the former [1]. LC–TSP-MS analysis revealed a considerable difference in their metabolic profiles, with a far higher level of sesquiterpenes present in extracts of *A. monadelpha* in comparison with those of *A. tabescens* (Table 4). Hence our results indicate a possible chemotaxonomic basis for the differentiation of these two species.

One strain each of the species *A. gallica* and *A. cepestipes* were examined. Both of these species are considered as weak pathogens [3]. However, LC–TSP-MS analysis revealed a level of sesquiterpenes present comparable to that found in extracts of *A. mellea*. This suggests that these strains may be members of a pathogenic species based on our previous findings. The pathogenicity of these two strains has not been

Table 3
Occurrence of sesquiterpene aryl esters and components P and Q in extracts of six *Armillaria* strains[a]

Extract	A	B	C	D	E	F	G	H	I	J	K	L	M	N	O	P	Q
A. mellea UCD 520 culture broth	++	++	++	–	++	+	+	–	++	–	–	++	–	+	+	++	++
A. mellea UCD 520 mycelial	++	–	++	–	+	–	+	–	–	++	–	–	–	+	++	–	++
A. mellea UCD 619 culture broth	+++	+++	+++	++	++	++	+++	–	++	–	++	++	–	+	++	–	++
A. mellea UCD 619 mycelial	++	++	+++	+++	++	++	++	–	+++	+++	+++	+++	++	++	++	+++	+++
A. mellea UF IM-QG-SAP culture broth	+++	++	+++	–	+++	–	++	–	++	–	–	++	++	–	+	–	–
A. mellea UF IM-QG-SAP mycelial	++	++	++	++	++	–	++	–	++	++	++	++	++	++	++	++	++
A. ostoyae UCD 663 culture broth	++	–	++	–	–	–	–	–	++	–	–	–	–	–	–	–	++
A. ostoyae UCD 663 mycelial	++	–	++	–	–	–	–	–	+	–	+	–	–	–	+	–	–
A. monadelpha CBS 137.32 culture broth	++	++	++	++	++	++	++	–	++	++	++	++	++	++	–	–	–
A. monadelpha CBS 137.32 mycelial	++	++	++	+++	++	++	+++	–	+++	++	++	+++	++	++	–	–	–
A. tabescens INRA PT 90.5 culture broth	–	–	–	–	–	–	–	–	+	–	–	–	–	–	–	–	+
A. tabescens INRA PT 90.5 mycelial	+	–	++	++	–	+	–	–	+	++	–	–	–	–	++	++	++

[a] Plus and minus signs indicate the intensity values recorded for these compounds on the TIC trace. – = Intensity values undetectable; + = Intensity values less than $1 \cdot 10^4$ counts; ++ = Intensity values between $1 \cdot 10^4$ and $1 \cdot 10^6$ counts; +++ = Intensity values greater than $1 \cdot 10^6$ counts.

Table 4
Occurrence of sesquiterpene aryl esters and components P and Q in extracts of seven *Armillaria* species[a]

Species	A	B	C	D	E	F	G	H	I	J	K	L	M	N	O	P	Q
A. mellea culture broth	++	++	+++	+	++	+	+	–	++	–	+	++	+	+	+	+	+
A. mellea mycelial	++	+	++	+	++	+	+	–	++	++	++	++	+	++	++	++	++
A. ostoyae culture broth	++	+	++	+	+	+	+	+	+	+	–	+	–	+	+	+	++
A. ostoyae mycelial	++	+	++	+	–	+	–	–	+	+	–	–	–	+	–	++	+
A. tabescens culture broth	+	–	++	–	–	–	–	–	+	–	–	–	–	–	–	–	+
A. tabescens mycelial	–	–	–	–	–	–	+	+	–	–	–	–	–	+	–	+	–
A. monadelpha culture broth	++	++	++	++	++	++	++	+	+	+	+	+	++	–	+	–	–
A. monadelpha mycelial	++	++	++	+++	+	++	+++	+	+++	++	++	+++	++	+	++	–	–
A. gallica culture broth	+++	+++	++	–	++	++	–	–	++	–	–	++	++	–	–	+	++
A. gallica mycelial	+++	++	++	++	++	++	++	–	++	++	++	++	++	++	++	++	++
A. cepestipes culture broth	+++	++	++	–	++	++	–	–	++	–	–	++	–	++	–	++	++
A. cepestipes mycelial	++	–	+++	++	–	–	–	–	++	–	–	–	–	++	++	++	++
A. novae-zelandiae culture broth	+++	++	++	–	++	++	++	–	++	–	–	–	–	–	–	–	–
A. novae-zelandiae mycelial	+	+	++	+	–	+	+	–	+	+	–	+	–	–	–	–	+
A79 culture broth	++	–	+++	–	–	–	–	–	++	–	–	–	–	–	–	–	++
A79 mycelial	++	–	++	++	–	+	–	–	++	++	++	++	++	++	++	++	++

[a] See footnote to Table 3.

assessed in field tests and it is possible that they are virulent or aggressive members of an otherwise non-pathogenic species. Studies on further strains of *A. gallica* and *A. cepestipes* are necessary before their sesquiterpene metabolite production can be compared with that of other species.

One strain of *A. novae-zelandiae* was examined. The culture broth extract was found to possess a level of sesquiterpene aryl esters comparable to that in extracts of *A. ostoyae* examined (Table 4), with the mycelial extract exhibiting a lower level of concentration. Also examined was an isolate of *Armillaria*, strain A79 of unknown species (Table 1). The mycelial extract of A79 revealed an intermediate concentration of sesquiterpene aryl esters similar to that found in some strains of *A. mellea*. The level of sesquiterpene aryl esters present in the culture broth extract of A79 resembles the levels found in extracts of *A. ostoyae*. This suggests that A79 is a pathogenic rather than non-pathogenic strain and hence a strain of either *A. ostoyae* or *A. mellea* rather than the other species.

This study provides evidence for a direct link between the level of sesquiterpene aryl esters produced and the pathogenicity of the strain. Linking the presence and concentration of a specific metabolite or metabolites to virulence or locating the most important or 'killer toxin' is more problematic. Our previous HPLC–UV quantitative study linked higher concentrations of armillyl orsellinate (J) and arnamiol (O) to extracts of pathogenic species. Of the metabolites examined in this work, melledonal (A) and 5′-methoxymelledonal (C) possess the highest level of concentration in extracts of pathogenic species. Other sesquiterpene aryl esters, namely 13-hydroxydihydromelleolide (B), 14-hydroxydihydromelleolide (E), melleolide (I) and dihydromelleolide (L), possess a slightly lower level of concentration. 13-Hydroxy-4-methoxymelleolide (D), armillane (F), 10-hydroxydihydromelleolide (G), armillyl orsellinate (J), 4-methoxymelleolide (K), 4-dehydromelleolide (M) and arnamiol (O) exhibit the lowest concentration levels of the sesquiterpenes studied in extracts of pathogenic species. Preliminary studies on the biological activity of sesquiterpene aryl esters has indicated armillyl orsellinate (J) to be the most active of these metabolites, with melledonal (A) possessing no biological activity [9]. Biosynthetic studies have demonstrated that these sesquiterpene aryl esters are produced via a common biosynthetic pathway originating from the cyclization of humulene to give the protoilludyl cation [9]. It is possible that the end product of this pathway is the active armillyl orsellinate (J) and that high concentration levels of the inactive melledonal (A) and 5′-methoxymelledonal (C) in extracts of pathogenic species may indicate that these compounds act as stores or key intermediates to armillyl orsellinate.

While the level of these metabolites may show variations, they all appear to follow a similar gradient of higher concentration in pathogenic, lower in moderately pathogenic and lowest in non-pathogenic species. An exception is 4-dehydro-14-hydroxydihydromelleolide (H), which is either undetectable or at low levels in all extracts. This metabolite has been isolated from *A. monadelpha* and is unknown in other species.

3.5. Variations within each species

Considerable variation in sesquiterpene production exists amongst strains of the same species. For example, of the *A. mellea* strains, UCD 619 produces a high level of almost all 15 sesquiterpene aryl esters, whereas UCD 520 and UF IM-QG-SAP exhibit more varied sesquiterpene profiles (Table 3). We believe that this variation in sesquiterpene aryl ester production reflects the variation in virulence within the species, a factor which has confounded foresters in assessing the threat posed by an infestation, since although one strain may be non-pathogenic, another of the same species may be strongly pathogenic. This variation may depend on factors such as host type, its condition and the habitat. *A. tabescens* (European) has long been accepted as non-pathogenic on its natural host, *Quercus* spp., in northern Europe. However, it has been reported as highly pathogenic on *Eucalyptus* spp. in southern France [10] and

Citrus spp. in Corsica [11]. This southward distribution of root disease also appears in reports upon the behaviour of *A monadelpha* [*A. tabescens* (N. American)] [12] and is noteworthy because observations in China [13] associated severe root infection by *A. tabescens* with high soil temperature. Thus environmental factors appear to have a direct relationship on the pathogenic ability of these species. It may be that these factors directly or indirectly affect the metabolic pathways and production of the basidiomycete. A study involving strains of *A. tabescens* (European) and *A. monadelpha* from differing hosts and conditions is under way to assess the impact of these factors on sesquiterpene aryl ester production.

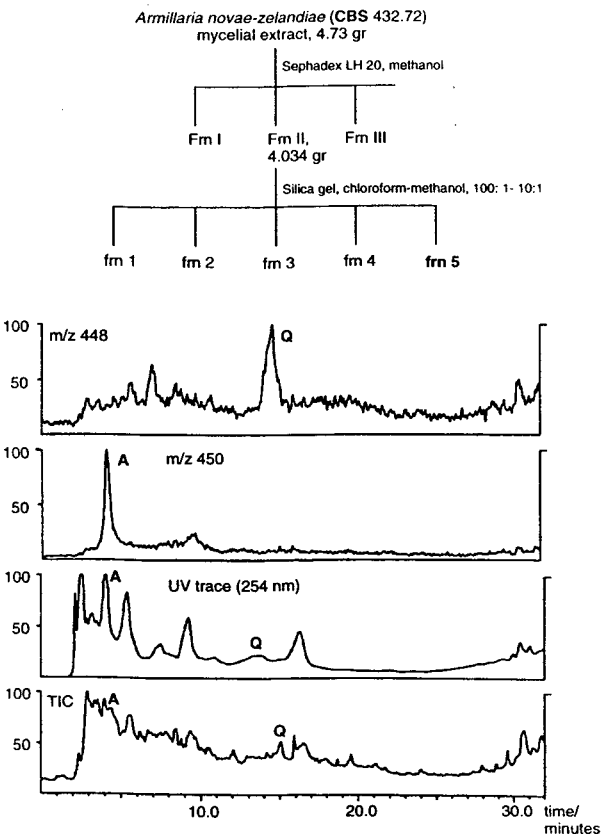

Fig. 8. LC–TSP-MS analysis of subfraction 5 of chromatographic separation of mycelial extract of *A. novae-zelandiae* (strain CBS 432.72) (see inset). The UV trace at 254 nm and TIC trace are displayed, in addition to selected-ion traces corresponding to adduct ions of 13-hydroxy-4-methoxymelleolide (D) and melledonal (A).

3.6. Unknown components

Selected-ion monitoring of extracts for the presence of 4-methoxymelleolide (K) at m/z 432 and for 13-hydroxy-4-methoxymelleolide (D) at m/z 448 revealed the presence of two unknown components, P and Q, respectively (Fig. 6). The clear ionization of P eluting at 26.12 min and Q eluting at 14.6 min under these conditions as well as their distribution within the extracts (Tables 3 and 4) suggest that they may be sesquiterpene components. Given that ammoniated adducts are the norm in this study, this suggests a relative molecular mass of 414 for P and 430 for Q. These molecular masses may correspond to a number of sesquiterpene aryl esters previously isolated from *Armillaria* species. The low fragmentation characteristics of thermospray ionization is limiting in further structural elucidation of such components. However, its usefulness in their isolation is illustrated by the analysis of fractions I–V collected from a successive separation of a mycelial extract of *A. novae-zelandiae* on Sephadex and silica (Fig. 8). Subfraction 5 is clearly targeted as having the highest level of species Q and isolation work on this fraction is continuing.

4. Conclusion

The results indicate that LC–TSP-MS can be successfully applied to the identification of sesquiterpene aryl esters of extracts of *Armillaria* species. Previously developed HPLC procedures for sesquiterpene aryl ester analysis have been successfully coupled with TSP to provide an on-line analysis. The advantages of our conventional HPLC analysis is thus retained, namely speed of analysis, reproducibility and ability to handle small amounts of sample. LC–TSP-MS further allows the identification of components not just on the basis of retention time but also from on-line molecular mass information. Thus

another dimension is provided through which we can observe these metabolites.

Fungal extracts are complicated biological matrices and the isolation of the biologically active components present is often a complex and tedious process. The developed method allows us to determine these components in a semi-quantitative fashion from direct analysis of the extracts. This is particularly useful in conjunction with standard isolation techniques. Components of interest can be determined rapidly and, although the structural information on these components may be limited, extracts and/or fractions which are rich in these components can be readily targeted.

That *Armillaria* species can cause serious disease has been known for over a century, but its propensity to do so has been a matter of controversy. This analysis supports a direct relationship between the level of sesquiterpene aryl ester metabolites produced by a strain and its virulence. LC–TSP-MS analysis may thus provide a direct method of determining the pathogenic ability of any strain of this wood-rotting basidiomycete. This technique is also applicable to the analysis of infected wood tissue. The level and identity of sesquiterpene aryl esters present may be established and hence the threat posed by an infestation of *Armillaria* assessed.

References

[1] G.A. Kile, J.J. Guillaumin, C. Mohammed and R. Watling, in M. Johansson and J. Stenlid (Editors), Proceedings of the Eighth IURFO International Conference on Root and Butt Rots, 1993, pp. 411–436.
[2] J. Rishbeth, Plant Pathol., 31 (1982) 9–17.
[3] C.G. Shaw and G.A. Kile, Agricultural Handbook No. 691, Forest Service, USDA, Washington, DC, 1991.
[4] D.M.X. Donnelly and D.J. Coveney, in K. Hostettmann and P.J. Lea (Editors), Proceedings of the Phytochemical Society of Europe, 1987, pp. 19–32.
[5] O. Dunne, Ph.D. Thesis, National University of Ireland, 1993.
[6] J.L. Wolfender and K. Hostettmann, J. Chromatogr., 647 (1993) 191.
[7] M. Maillard, J.L. Wolfender and K. Hostettmann, J. Chromatogr., 647 (1993) 147.
[8] E.B. Hansen, J. Abian, T.A. Getek, J.S. Choinski and W.A. Korfmacher, J. Chromatogr., 603 (1992) 157.
[9] R.H. Hutchinson, Ph.D. Thesis, National University of Ireland, 1990.
[10] B. Lung-Escarmant, D. Poincot and B. Taris, presented at the 27th Colloquium of the Société Française de Phytopathologie, Agronomie, 5 (1985) 559.
[11] E. Laville and R. Vogel, Arboric. Fruit., 31 (1984) 34.
[12] A.S. Rhoads, Lloydia, 19 (1956) 193.
[13] L.W. Chang, Q.F. Liu and G. Li, Acta Phytopathol. Sin., 12 (1982) 41.

ELSEVIER

Journal of Chromatography A, 710 (1995) 287–295

JOURNAL OF CHROMATOGRAPHY A

Enantiomeric resolution of derivatized DL-amino acids by high-performance liquid chromatography using a β-cyclodextrin chiral stationary phase: A comparison between derivatization labels

Andreas M. Rizzi*, Sabine Cladrowa-Runge, Helén Jonsson[1], Susanne Osla[1]

Institute of Analytical Chemistry, University of Vienna, Währingerstraße 38, A-1090 Vienna, Austria

First received 24 June 1994; revised manuscript received 21 April 1995; accepted 21 April 1995

Abstract

A chiral stationary phase with immobilized β-cyclodextrin was used for the liquid chromatographic separation of amino acid derivatives into their enantiomers. Several reagents differing in size, structure and linking group (i.e. the isothiocyanates PITC, NITC, DNITC and DABITC, the activated ester AQC, and the sulfonyl chlorides DNS-Cl and DABS-Cl) were used to derivatize the amino groups of α-amino acids prior to separation. A compilation of the selectivity data obtained with the different labels is given as guideline in selecting appropriate labels for a particular separation problem.

1. Introduction

The analysis of amino acid enantiomers belongs to the very early examples of chromatographic separations of enantiomers and still plays an important role. The amount of certain D-amino acids in various types of samples has found to be of relevance for many aspects of biochemical and molecular biological research [1,2], in the control of food and beverages [3,4], as well as in age determination [5–7]. Various chiral separation methods are available for the enantiomeric resolution of amino acids. Methods based on chiral ligand-exchange [8–11] and on the formation of inclusion complexes with cyclodextrins (CD) [12–14] have received the most attention. Cyclodextrins were employed in their native form or after modification by methylation, acetylation or by binding other structural moieties to the hydroxyl groups of the glucose [15–17]. Cyclodextrin systems, especially when using stationary phases with immobilized cyclodextrins, are easy to use, and separations can be carried out in a rather simple, and when employing aqueous/alcoholic mixed eluents, rather inexpensive way. This method turned out to be of particular interest for many separation problems. Furthermore, it can easily be combined with a non-chiral preseparation in a two-column set-up [18–21].

Bonded β-CD stationary phases are commercial available. These phases are not necessarily

* Corresponding author.

[1] On leave from the Institute of Chemistry, University of Uppsala, Uppsala, Sweden.

0021-9673/95/$09.50
SSDI 0021-9673(95)00498-X

identical in their separation characteristics, as they might use different linking groups between spacer and selector and exhibit different selector densities. The enantioselectivity coefficients may vary to some extent when using β-CD stationary phases from different suppliers. Recently, a new material has become available from the E. Merck company under the trade name ChiraDex [22]. This stationary phase is used for the present investigation.

Amino acids are usually analyzed after pre-column derivatization in order to allow more sensitive detection and/or to make them more suitable for the chromatographic separation. The chiral separability of the derivatives is generally dependent on the type of derivatization, especially when using chiral selectors operating in a host–guest mechanism. Separations of amino acids as dansyl derivatives and OPA derivatives by means of β-CD-chiral stationary phases (CSPs) have been reported [12,14,15,21,23]. The popular FMOC derivatives cannot be separated by β-CD systems, with a few exceptions; they are, however, readily separable in γ-CD systems [24].

There are a number of other derivatization reagents available which can be utilized for the enantioseparation of amino acids in β-CD systems, and the present paper deals with an investigation of the enantioseparation attainable by means of some of these derivatizations. The investigation covers the following derivatization reagents: 5-dimethylaminonaphthalene-1-sulfonyl chloride (DNS), 4-dimethylaminoazobenzene-4′-sulfonyl chloride (DABS), phenyl isothiocyanate (PITC), 1-naphthyl isothiocyanate (NITC), 4-dimethylaminoazobenzene-4′-isothiocyanate (DABITC), 4-dimethylamino-1-naphthyl isothiocyanate (DNITC), and the newly introduced 6-aminoquinolyl-N-hydroxysuccinimidyl carbamate (AQC) [17,25]. The structures of the amino acid derivatives are shown in Fig. 1. With the DNS and DABS reactions, the labels are linked by a sulfonamide group, with the others either by a thiourea (PITC, NITC, DNITC, DABITC) or an urea group (AQC). Many of these derivatives offer specific advantages (e.g. high absorbance, strong fluorescence, fast reaction rate, stable products, minimum peak interferences caused by the reagent) and suffer from specific limitations (e.g. limited stability, limited degree of reaction, side reactions, slow reaction rates, etc.). The aim of the present paper is to offer some guidelines for selecting the labels appropriate for a particular amino acid separation problem, and, secondly, to contribute to the discussion of the effect of the derivatization labels on chiral recognition by β-CD host–guest complexation.

2. Experimental

2.1. Apparatus

The liquid chromatographic system consisted of a pump (L-6200, Intelligent Pump, Merck-Hitachi, Tokyo, Japan), a syringe valve injector (Rheodyne 7125, Cotati, CA, USA) equipped with a 20-μl loop and an UV detector (L-4000, Merck-Hitachi) connected to an integrator (D-2000, Chromatointegrator, Merck-Hitachi). Column temperature was controlled by a water jacket around the column using a thermostat (LTD, 6, Grant, Herts, UK).

2.2. Columns

A stainless-steel column (250 × 4.0 mm I.D.) prepacked with immobilized β-CD, mean particle diameter 5 μm, (Chiradex, E. Merck, Darmstadt, Germany) was used.

2.3. Chemicals

Methanol (MeOH) and acetonitrile of LiChrosolv grade and triethylamine (TEA) of pro analysi grade were obtained from E. Merck. Water was twice distilled from a quartz apparatus and processed through an Elgastat UHQ apparatus (Elga, High Wycombe Bucks, UK). The eluents were premixed and degassed in an ultrasonic bath before use. Standard samples of free amino acids as well as DNS amino acids

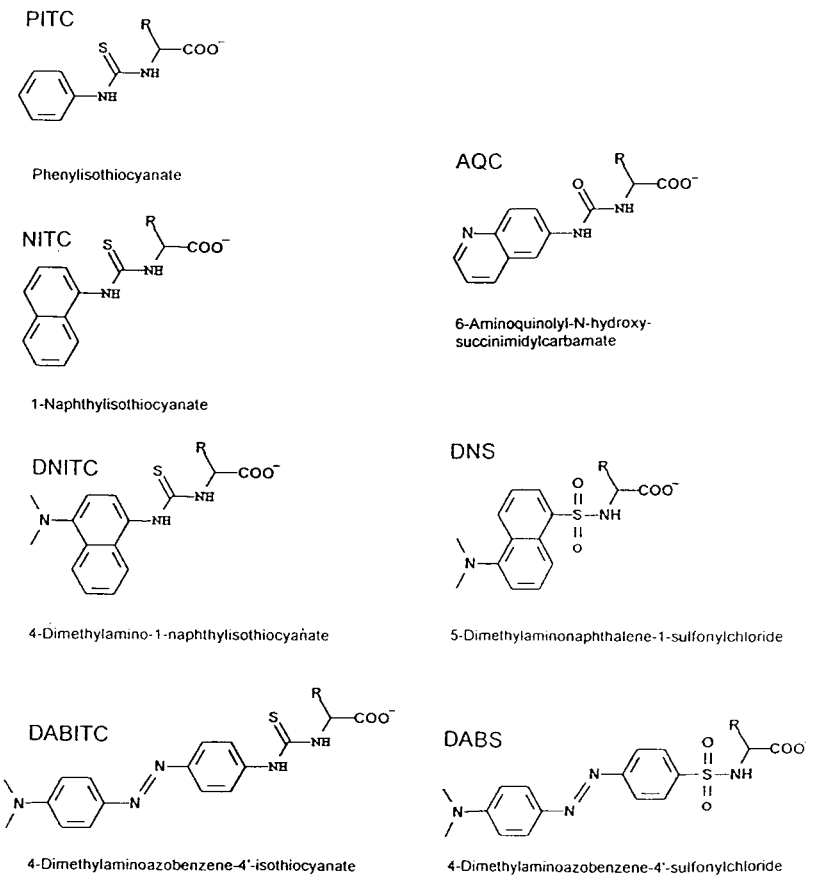

Fig. 1. Chemical structures of the amino acid derivatives investigated, R = amino acid side chain. Abbreviations refer to the reagents employed.

were obtained from Sigma (Deisenhofen, Germany).

The derivatization reagents 5-dimethylaminonaphthalene-1-sulfonyl chloride (DNS-Cl), PITC, and NITC were purchased from Sigma. DNITC, DABITC and 4-dimethylaminoazobenzene-4′-sulfonyl chloride (DABS-Cl) were purchased from Fluka (Buchs, Switzerland). AQC with the trade name AccQ-Fluor™ was obtained from Waters (Bedford, MA, USA).

Boric acid (H_3BO_3), ammonium acetate (NH_4Ac), sodium hydroxide (NaOH), disodium hydrogenphosphate (Na_2HPO_4), sodium dihydrogenphosphate (NaH_2PO_4), pyridine, acetone, and hydrochloric were obtained from E. Merck in pro analysi grade.

2.4. Derivatization procedures

DNS derivatives [26]

Approximately 5 mg of the amino acids were dissolved in 460 μl borate buffer (0.1 *M* boric acid, adjusted to pH 9 by addition of NaOH) and 300 μl of 0.1 *M* DNS-Cl dissolved in acetone were added. The sample was kept in the dark for 2 h at room temperature to complete the reaction. Then the sample was dried by vacuum centrifugation, washed once by adding 500 μl of a mixture of acetone–1 *M* HCl (19:1, v/v) and centrifuged for 5 min to eliminate the unreacted reagent and insoluble salts. The liquid was again dried by vacuum centrifugation. After resolubilization of the derivatized amino acids in the

mobile phase the samples were ready for injection.

DABS derivatives [27]

Approximately 5 mg of the amino acid were dissolved in phosphate buffer (0.1 *M* Na_2HPO_4 adjusted with 0.1 *M* NaH_2PO_4 to pH 7), and 100 μl reagent (100 mg DABS-Cl in 10 ml acetone) were added. The sample was kept at 65°C for 30 min to complete the reaction and then dried by vacuum centrifugation. Resolubilization as above.

PITC-, NITC-, DABITC- and DNITC derivatives [28]

A buffer solution was prepared by mixing 5 ml methanol, 2.5 ml pyridine, 1 ml triethylamine and 1.5 ml water. A 500-μl volume of 0.1 *M* solution of the reagents dissolved in acetonitrile was added to the buffer. A 200-μl aliquot of this resulting reagent solution was added to a few milligrams of the amino acids. To complete the reaction, samples were kept at room temperature for 5–10 min under protection from light. The samples were dried by vacuum centrifugation and aliquots were resolubilized in the mobile phase.

AQC derivatives [29,30]

"AccQ.Fluor Reagent" was completely reconstituted in 1 ml "AccQ.Fluor Reagent Diluent", yielding approximately 10 m*M* 6-aminoquinolyl-N-hydroxysuccinimidyl carbamate (AQC) in acetonitrile. The sample was reconstituted in 70 μl "AccQ.Fluor Borate Buffer" and 20 μl "AccQ.Fluor Reagent" was added. After vortexing, the samples were allowed to stand for one min at room temperature and then heated in an oven for 10 min at 55°C.

2.5. Chromatographic conditions

The mobile phases consisted of aqueous buffer solutions (0.1 *M* ammonium acetate and 0.1% v/v TEA and adjusted to pH 5.5–6.5 with acetic acid) which were mixed with methanol. The methanol concentrations were kept constant within the series of the various types of derivatives. They are specified in the tables and figures given. Temperature was carefully maintained at 20 ± 0.1°C. Flow-rates of 0.5 ml/min were used, unless indicated otherwise. Amounts of injected amino acid derivatives ranged between 20 and 200 ng. The detection wavelength was 254 nm for all derivatives except for DABS, where 456 nm was used.

Plate number calculation was based on peak-width data measured at 0.607 of the peak hight.

3. Results and discussion

3.1. Selection of derivatization reagent

Enantioselectivity data (separation factors) and capacity factors of the derivatized amino acids measured under the chosen experimental conditions (water–methanol mixed mobile phases, modifier content between 40 and 90% v/v as specified, temperature of 20°C) are listed in the Tables 1 and 2. The experimental conditions were kept constant for a series of amino acids carrying an identical derivatization label. Methanol concentrations were chosen in order to obtain rather short retention times, i.e. 10 to 20 min for most compounds applying a flow-rate of 0.5 ml/min. A compilation of those amino acid derivatives which, under the chosen conditions, can completely or almost completely be resolved to baseline is given in Table 3. Appropriate excitation and emission wavelengths for the fluorescence detection are shown in Table 4. Tables 1–3 are aimed to provide a guideline facilitating the selection of derivatization labels well suited for the solution of a given separation problem. The following résumé can be drawn from the given data.

(i) Amino acids carrying a dansyl-label are enantioseparated in all instances, except for DNS-DL-Trp. Baseline separation is achieved under the chosen experimental conditions if the separation factor is higher than ca. 1.18. Under these conditions the column exhibits approximately 3000–4000 theoretical plates per 25 cm. Due to the high methanol concentration rather low capacity factors are obtained (between 1 and

Table 1
Enantioselectivity coefficients, $\alpha = k_2'/k_1'$[a], for differently labeled DL-amino acids at 20°C

Amino acid	DNS	DABS	PITC	NITC	DNITC	DABITC	AQC
Ala	1.08	1.14	1.17	1.06	1.00	1.00	1.08
Val	1.22	1.64	1.30	1.10	1.00	1.00	1.00
Leu	1.75	1.19	1.00	1.14	1.40	1.43	1.39
Ile	1.32		1.21	1.00	1.08	1.10	1.13
Pro	1.10	1.00	1.14	1.22	1.10	1.44	1.10
Met	1.24	1.31	1.06	1.08	1.18	1.19	1.08
Cys	1.15	1.00	1.82	1.07	1.00	1.33	1.08
Ser	1.16	1.15	1.11	1.07	1.00	1.00	1.07
Thr	1.29	1.13	1.25	1.06	1.00	1.00	1.07
Lys	1.10	1.20	1.28	1.14	1.11	1.12	1.16
Lys[b]		1.25			1.32		1.07
Arg	1.16	1.22	1.24	1.13	1.13	1.14	1.13
Asn	1.11	1.10	1.25		1.17	1.18	1.11
Gln	1.14	1.16	1.16		1.04	1.07	1.06
Asp	1.13		1.24		1.10		1.20
Glu	1.15		1.14	1.04	1.00	1.05	1.00
Phe	1.43	1.13	1.21	1.13	1.14	1.16	1.13
Trp	1.00	1.19	1.24	1.35	1.00	1.00	1.04
His	1.07	1.14	1.18	1.12	1.08	1.09	1.06
Tyr	1.25	1.20	1.06	1.00	1.10	1.11	1.25

Chromatographic conditions: immobilized β-cyclodextrin stationary phase (ChiraDex). Eluent composition: DNS-derivatives, aqueous buffer [(0.1 *M* NH_4Ac, 0.1% TEA, pH 5.5)–MeOH (30:70, v/v)]; DABS-derivatives, aqueous buffer [(0.1 *M* NH_4Ac, 0.1% TEA, pH 5.5)–MeOH (10:90, v/v)]; PITC-, NITC-, DABITC-, DNITC-derivatives, aqueous buffer [(0.1 *M* NH_4Ac, pH 6.5)–MeOH (60:40, v/v)]; AQC-derivatives, aqueous buffer [(0.1 *M* NH_4Ac, 0.1% TEA, pH 6.5)–MeOH (50:50, v/v)].

[a] k_1' and k_2' are the capacity factors of the first and second enantiomer, respectively. The hold up time was obtained by assuming a column porosity of 0.75.

[b] N^{α},N^{ϵ} derivatized compound.

3), except for the two acidic amino acids Asp and Glu.

(ii) Phenylisothiocyanate-derivatized amino acids are enantioseparated in all instances, except for PITC-DL-Leu. Again, the capacity factor values are low under the selected mobile phase conditions allowing analysis times of ca. 20 min at the given flow; the only exceptions were Asp and Glu and the two aromatic amino acids Phe and Trp. The highest enantioselectivity coefficients for a particular amino acid are usually achieved by using either PITC or DNS. PITC turned out to be the best derivatization agent for Ala and Glu, the two amino acids which are of special interest in the context of D-amino acid analysis in bacterial cell membranes. Separations of a few PITC amino acids are shown in Fig. 2.

(iii) DABS-labeled amino acids are enantioseparated in many instances. For DL-Met and DL-Val the best separations have been achieved using this label. As general drawback, these derivatives are eluted with long retention times, and the large capacity factors could not be reduced by variation of the eluent composition.

(iv) NITC-, DNITC- and DABITC-derivatized amino acids, all of them exhibiting a thiourea linkage group, are resolved with separation factors generally lower than those of the corresponding PITC analytes, with the exceptions of Leu, Pro, Met, Tyr and Trp. NITC-DL-Trp and DABITC-DL-Pro were separated with the highest separation factors achievable amongst all the labels investigated. Nevertheless, except for the analytes mentioned, there is no observed advantage in the use of these types of derivatizations over PITC with respect to separation selectivity. Clearly, however, the fluorescence activity of the NITC, DNITC and DABITC moiety allows one

Table 2
Capacity factors of the second eluted enantiomer, k'_2, of differently labeled amino acids, at 20°C

Amino acid	DNS	DABS	PITC	NITC	DNITC	DABITC	AQC
Ala	2.52	9.57	3.01	2.93	1.98	3.18	2.45
Val	2.03	12.34	3.34	2.79	2.19	2.72	2.15
Leu	2.54	14.05	5.00	4.90	4.58	6.86	4.89
Ile	1.68		4.22	3.32	2.84	4.19	3.16
Pro	1.40	18.21	3.13	3.81	3.79	6.92	2.51
Met	1.33	11.37	3.86	3.94	3.32	4.89	2.90
Cys	2.99	8.32	6.68	4.91	3.58	5.58	2.40
Ser	1.37	13.39	3.11	3.17	2.28	3.39	2.50
Thr	1.46	10.10	2.93	2.77	2.14	3.00	2.29
Lys	1.22	5.23	1.61	1.48	1.63	1.86	4.86
Lys[a]		21.28			4.97		
Arg	0.84	3.68	1.42	1.42	1.60	1.85	1.44
Asn	1.68	19.89	3.68		3.06	4.65	2.46
Gln	1.38	12.84	2.69			3.39	2.05
Asp	18.03		29.69		19.26		16.64
Glu	9.17	>30.00	17.65	15.82	11.66	20.44	10.08
Phe	2.42	13.23	8.11	8.54	4.66	7.07	7.06
Trp	1.63	14.65	7.87	10.34	5.10	7.75	4.82
His	1.66	14.75	3.00	3.12	2.96	3.64	2.50
Tyr	2.67	15.30	5.33	4.94	2.95	4.37	5.19

Chromatographic conditions as in Table 1.
[a] N^{α},N^{ε} derivatized compound.

Table 3
Guidelines for the separation of differently labeled amino acids by use of the β-cyclodextrin chiral stationary phase

Amino acid	DNS	DABS	PITC	NITC	DNITC	DABITC	AQC
Ala	(+)	+	+ +				(+)
Val	+	+ +	+	(+)			
Leu	+ +	(+)		(+)	+	+ +	+
Pro	(+)		(+)	+		+ +	
Met	+	+ +			(+)	+	
Cys			+ +			+	
Ser	+[a]	+	(+)				
Thr	+[a]	(+)	+				
Lys	(+)	+	+ +		+		
Arg	+	+ +	+ +		(+)	(+)	(+)
Asn	(+)	(+)	+		(+)	+	
Gln	(+)	(+)	+ +				
Asp	(+)		+		(+)		+ +
Glu	+		+ +				
Phe	+ +	(+)	+	+	(+)	+	(+)
Trp		+	+ +	+			
His		(+)	+ +[a]	(+)			
Tyr	+ +	+				(+)	+ +

+ = complete resolution; (+) = nearly baseline resolution; + + = best separation achieved for a particular amino acid. Chromatographic conditions as given in the Tables 1 and 2.
[a] Lower methanol concentration recommended than given in Table 1.

Table 4
Excitation and emission wavelengths to be considered for the various fluorescent derivatization labels

Derivatization	Wavelength (nm)	
	Excitation	Emission
DNS	325	350[a]
NITC	250	410
DNITC	240	490
DABITC	240	480
AQC	250	395[b]

[a] Ref. [31].
[b] Ref. [17].

to take advantage of improved detection sensitivity.

(v) AQC derivatives, exhibiting an urea linkage, are separated with separation factors very similar to those obtained with the thiourea-linked labels NITC, DNITC and DABITC. This means that in most instances the selectivity coefficients achieved are not sufficiently high to achieve baseline separation of the enantiomers under the given conditions (cf. Table 3). It might be of interest that enantioseparation of AQC amino acids in the reversed-phase mode (using eluent mixtures of methanol and aqueous buffer) is reported for Leu only [17] when using a different type of stationary phase where native β-CD is immobilized via epoxyalkylsiloxanes.

Examples for amino acid separations readily achievable after DABS-, NITC- and AQC derivatization are illustrated by the chromatograms in Fig. 3.

3.2. Influence of eluent composition

All data given in the Tables are collected at constant eluent composition within a series of analytes. It can be assumed that the chosen separation conditions were not necessarily optimum for all analytes. A certain, though limited, improvement of the resolution can still be expected in several instances when optimizing

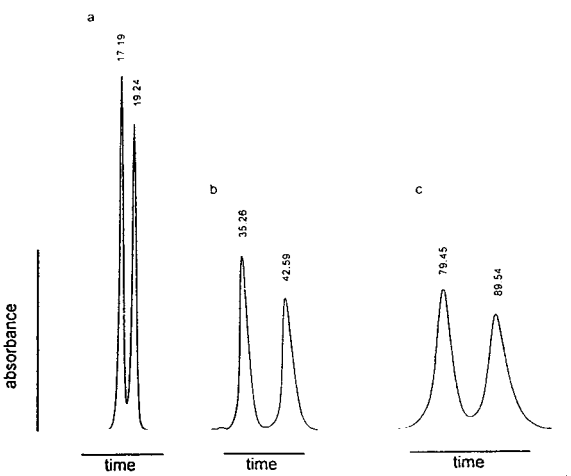

Fig. 2. Section of chromatograms of PITC-derivatized amino acids (a) DL-alanine, (b) DL-tryptophane, (c) DL-glutamic acid. Retention times in minutes. Flow-rate: 0.5 ml/min; eluent composition, aqueous buffer [0.1 *M* NH_4Ac pH 6.5–MeOH (60:40, v/v)]. Other chromatographic conditions as specified in Experimental.

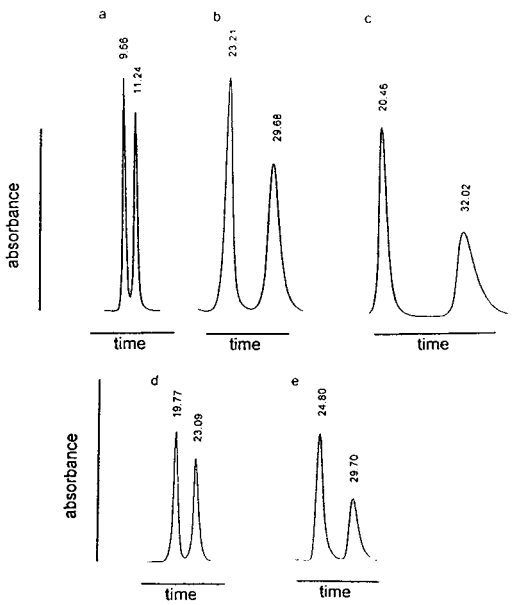

Fig. 3. Sections of chromatograms of selected DABS-, AQC- and NITC-derivatized amino acids readily separable under the chosen eluent and temperature conditions. (a) DABS-DL-arginine, (b) DABS-DL-methionine, (c) DABS-DL-valine, (d) NITC-DL-proline, and (e) AQC-DL-tyrosine. Eluent conditions: (a,b,c) aqueous buffer [0.1 *M* NH_4Ac pH 5.5–methanol (10:90, v/v)]; (d,e) aqueous buffer [0.1 *M* NH_4Ac pH 6.5–methanol (60:40 and 50:50, v/v)], respectively. All other conditions as specified in Experimental.

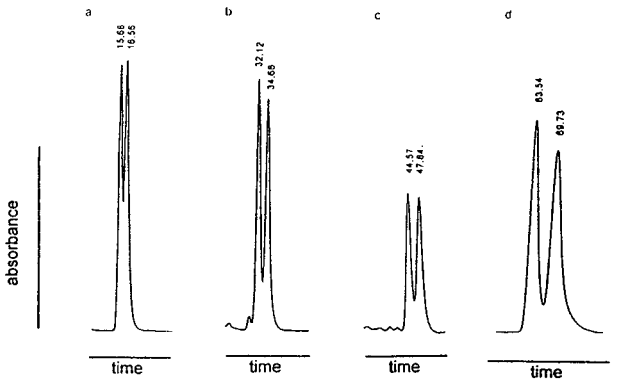

Fig. 4. Section of chromatograms of AQC-DL-alanine using the following chromatographic conditions: (a) 50% (v/v) methanol, 20°C, 0.5 ml/min; (b) 20% (v/v) methanol, 20°C, 0.7 ml/min; (c) 10% (v/v) methanol, 20°C, 0.8 ml/min; (d) 20% (v/v) methanol, 10°C, 0.5 ml/min.

the eluent composition and exploiting temperature effects. An example of the influence of modifier concentration and temperature is given in Fig. 4 for AQC-DL-alanine.

Analytes with sulfonamide linked labels, i.e. DNS- and DABS amino acids, are found to require a higher modifier concentration in order to be eluted with retention times comparable to analytes carrying the corresponding thiourea linked labels. The two acidic amino acids Glu and Asp exhibit very high capacity factors, k', in all instances. For these analytes faster analysis will be obtained by using β-cyclodextrin as mobile phase additive [21].

4. Conclusions

The chromatographic resolution which can be achieved for a given pair of enantiomers is found to be significantly dependent on the derivatization label used. For the selection of the derivatization labels most appropriate for the enantiomeric resolution of particular amino acids, the selectivity and capacity factor data in the Tables 1–3 can serve as a guideline.

All derivatizations discussed here, except PITC derivatization, yield fluorescent derivatives, thus enabling the use of the significantly higher sensitivity and better selectivity of fluorescence detection if required. Another advantage of the AQC reagent is that its hydrolysis products are only weakly fluorescent and do not cause peak interferences in the chromatogram. Concerning the effort and time requirements for the derivatization procedure, there is a significant advantage in using the AQC reagent, as the whole derivatization procedure is completed in a few minutes and is easy to handle. Considering the stability of the products, the thiourea and urea derivatives obtained by the various isothiocyanate and the AccQ-Tag reagents respectively, are stable for weeks, even in solution. The stability of DNS amino acids in solution is much worse and cooling at −20°C is required for longer storage.

No simple rules can be given regarding the relationship between the structural features of the analytes and the achieved enantioselectivity. This relationship is apparently complex for separations based on a host–guest mechanism. Small changes in the analyte structure often result in major changes in the enantioselectivity coefficients. Therefore, only a few remarks are made on the given results: (i) Sulfonamide and thiourea linking groups are not comparable at all with respect to their effect on chiral discrimination. This is probably due to both electronic and steric reasons. Large differences are seen in the pattern of the selectivity data when comparing the series of DNS derivatives with that of the DNITC derivatives although these compounds have very similar fluorescent moieties; this also holds for a comparison between the series of DABS- with that of DABITC derivatives. In the majority of cases the derivatives carrying a sulfonamidic linking group exhibit the higher separation factors. (ii) The separation factors obtained for the DABITC- and DNITC derivatives of the same amino acid are very similar although their fluorescent moieties are very different with respect to size and shape. These similarities are also found for the AQC derivatives. In these cases thiourea and urea linking groups are comparable with respect to chiral recognition. On the other hand, the data of the PITC derivatives show very few similarities to those of the other thiourea compounds. We

hypothesize that the global orientation adopted by most of the amino acid derivatives in their interactions with the β-CD selector is similar for the DNITC-, DABITC- and AQC derivatives, but different for the PITC derivatives.

Acknowledgements

The authors are grateful to the E. Merck company, Darmstadt, for providing the β-CD column, and to Millipore-Austria for providing the AccQ-Tag Fluor reagent.

References

[1] G.C. Barret (Editor), Chemistry and Biochemistry of Amino Acids, Chapman and Hall, New York, NY, 1985, p. 8.
[2] K.H. Schleifer and E. Stackebrandt, Ann. Rev. Microbiol., 37 (1983) 143.
[3] H. Brückner, R. Wittner and H. Godel, Chromatographia, 32 (1991) 383.
[4] M. Langer, R. Wittner, P. Jack, H. Godel and H. Brückner, in W. Baltes, T. Eklund, R. Fenwick, W. Pfannhauser, A. Ruiter and H.P. Thier (Editors), Strategies for Food Quality Control and Analytical Methods in Europe, Proceedings of the 6th European Conference on Food Chemistry, Hamburg, September 22–26, 1991, B. Behr's Verlag, Hamburg, 1991, pp. 385–390.
[5] R. Hardial and C.F. Simpson, Anal. Proc., 26 (1989) 57.
[6] S. Ohtani and K. Yamamoto, J. Forensic Sci., 36 (1991) 792.
[7] V.R. Meyer, in S. Ahuja (Editor), Chiral Separations by Liquid Chromatography, ACS Symp. Ser., Vol. 471, American Chemical Society, Washington, DC, 1991, pp. 217–227.
[8] V.A. Davankov, Adv. Chromatogr., 18 (1980) 139.
[9] Y. Tapuhi, N. Miller and B.L. Karger, J. Chromatogr., 205 (1981) 325.
[10] N. Oi, H. Kitahara and R. Kira, J. Chromatogr., 592 (1992) 291.
[11] S. Lam, F. Chow and A. Karmen, J. Chromatogr., 199 (1980) 295.
[12] W.L. Hinze, T.E. Riehl, D.W. Armstrong, E. DeMond, A. Alak and T. Ward, Anal. Chem., 57 (1985) 237.
[13] S. Li and W.C. Purdy, J. Chromatogr., 543 (1991) 105.
[14] N. Thuaud, B. Sebille, A. Deratani and G. Lelievre, J. Chromatogr., 555 (1991) 53.
[15] S.H. Lee, A. Berthod and D.W. Armstrong, J. Chromatogr., 603 (1992) 83.
[16] J. Zukowski, M. Pawlowska and D.W. Armstrong, J. Chromatogr., 623 (1992) 33.
[17] M. Pawlowska, S. Chen and D.W. Armstrong, J. Chromatogr., 641 (1993) 257.
[18] L.-E. Edholm, C. Lindberg, J. Paulson and A. Walhagen, J. Chromatogr., 424 (1988) 61.
[19] A. Walhagen, L.-E. Edholm, B.N.M. Kennedy and L.C. Viao, Chirality, 1 (1989) 20.
[20] A.M. Rizzi and C. Plank, J. Chromatogr., 557 (1991) 199.
[21] A.M. Rizzi, P. Briza and M. Breitenbach, J. Chromatogr., 582 (1992) 35.
[22] K. Cabrera, D. Lubda and G. Jung, Poster 1-144 at the 17th International Symposium on Column Liquid Chromatography, Hamburg, 1993.
[23] I. Merino Merino, E. Blanco Gonzales and A. Sanz-Medel, Anal. Chim. Acta, 234 (1990) 127.
[24] K. Cabrera, D. Lubda, S. Bohne and M. Schäfer, Poster 1-143 at the 17th International Symposium on Column Liquid Chromatography, Hamburg, 1993.
[25] S.A. Cohen, K.M. DeAntonis, J. Chromatogr. A, 661 (1994) 25.
[26] E. Bayer, E. Cran, B. Kaltenegger and R. Ulmann, Anal. Chem., 48 (1976) 1106.
[27] E.H.J.M. Jansen, R.H. Van den Berg, R. Both-Miedema and L. Doorn, J. Chromatogr., 553 (1991) 123.
[28] B.A. Bidlingmeyer, S.A. Cohen and T.L. Tarvin, J. Chromatogr., 336 (1984) 93.
[29] S.A. Cohen, D.P. Michaud, Poster 361 presented at 16th international Symposium on Column Liquid Chromatography, 1992, Baltimore, USA.
[30] S.A. Cohen and D.M. Michaud, Anal. Biochem., 211 (1993) 279.
[31] R. Kuhn and S. Hoffstetter-Kuhn, Capillary Electrophoresis: Principle and Practice, Springer Verlag, Berlin, 1993, p. 281.

ELSEVIER

Journal of Chromatography A, 710 (1995) 297–302

JOURNAL OF CHROMATOGRAPHY A

High-performance liquid chromatographic method for the separation of the optical isomers of γ,γ′-di-*tert.*-butyl-D,L-γ-carboxyglutamic acid and D,L-γ-carboxyglutamic acid

Antal Péter[a,*], Csaba Somlai[b], Botond Penke[b]

[a]*Department of Inorganic and Analytical Chemistry, József Attila University, Dóm tér 7, H-6720 Szeged, Hungary*
[b]*Department of Medical Chemistry, Albert Szent-Györgyi Medical University, Dóm tér 8, H-6720 Szeged, Hungary*

First received 31 January 1995; revised manuscript received 19 April 1995; accepted 19 April 1995

Abstract

The chemical synthesis of γ,γ′-di-*tert.*-butyl-γ-carboxyglutamic acid is accompanied by extensive racemization, and very careful resolution is needed to obtain D- and L-γ,γ′-di-*tert.*-butyl-γ-carboxyglutamic acids in high chiral purity. A novel method was devised for the separation of enantiomers of γ,γ′-di-*tert.*-butyl-γ-carboxyglutamic acid and γ-carboxyglutamic acid, applying precolumn derivatization with 1-fluoro-2,4-dinitrophenyl-5-L-alanine amide and 2,3,4,6-tetra-O-acetyl-β-D-glucopyranosyl isothiocyanate as chiral reagents, with subsequent reversed-phase high-performance liquid chromatographic separation of diastereomeric compounds. The effects of organic modifiers, of the mobile-phase composition and of the pH on the separation of the diastereomers were investigated.

1. Introduction

γ-Carboxyglutamic acid (Gla), an acid-labile derivative of glutamic acid (Glu), exhibits a very strong and specific affinity for calcium ions. A number of Gla residues are present in the calcium-binding region of Gla-containing polypeptides [1–4] and proteins [5], and as a result the interactions between the bivalent ions and the cumulated carboxylic side-chains are extensively enhanced. These proteins and peptides are known to be responsible for many biological functions, and consequently there is a considerable interest in the biological study of Gla-containing peptides. The synthesis of Gla-containing peptides requires protected Gla derivatives, which are not always readily available commercially. In our laboratory γ,γ′-di-*tert.*-butyl-D- and -L-γ-carboxyglutamic acids (DTBGLA) have been synthesized with high efficiency.

According to the literature the chromatographic analysis of Gla can be divided into three main phases: (1) separation on an anion-exchange column, with subsequent postcolumn derivatization with ninhydrin or *o*-phthalaldehyde [5–23] (Low et al. [24] used thin-layer chromatography), (2) RP-HPLC methods, with precolumn derivatization with *o*-phthalaldehyde in the presence of thiols [25–30], phenyl isothiocyanate [31], 1,1-diphenylboronic acid [32] or 4-dimethylamino-4-azobenzenesulfonyl chloride [33] and (3) identification of D- and L-isomers of Gla and Gla derivatives after their conversion to Glu. For the separation of D- and

* Corresponding author.

0021-9673/95/$09.50
SSDI 0021-9673(95)00494-7

L-Glu, Rivier et al. [34] and Nishiuchi et al. [35,36] used 1-fluoro-2,4-dinitrophenyl-5-L-alanine amide (FDAA) as chiral reagent, while Kurihara et al. [37] used 2,3,4,6-tetra-O-acetyl-β-D-glucopyranosyl isothiocyanate (GITC).

The method described in the present paper allows the analysis of the optical isomers of DTBGLA and Gla without conversion to Glu. The amino acids were derivatized directly with FDAA and GITC, and the D- and L-diastereoisomers were separated by an RP-HPLC method.

2. Experimental

2.1. Chemicals and reagents

Chirally pure enantiomers of DTBGLA were synthesized via a seven-step route with preparatively advantageous modification of the general literature procedures [38–41].

D- and L-Gla were synthesized by acidic treatment of DTBGLA with hydrogen fluoride at 0°C for 30 min. The chiral purity of D- and L-DTBGLA and D- and L-Gla was determined by our new method.

GITC was purchased from Aldrich (Steinheim, Germany), FDAA from Pierce Chemical Company (Rockford, IL, USA), potassium dihydrogenphosphate, phosphoric acid of analytical reagent grade, acetonitrile and methanol of HPLC grade from Merck (Darmstadt, Germany). Buffers were prepared by means of dissolving 0.01 mol potassium dihydrogenphosphate in water, adjusting the pH with 5.0 *M* phosphoric acid or 0.5 *M* sodium hydroxide and diluting to the final volume of 1 l.

2.2. Apparatus

The HPLC analyses were performed on an M-600 low-pressure gradient pump fitted with an M-996 photodiode-array detector and a Millennium 2010 Chromatography Manager data system (Waters Chromatography, Division of Millipore, Milford, MA, USA) and on an L-6000 liquid chromatographic pump (Merck Hitachi, Tokyo, Japan) fitted with a UV 308 detector (Labor MIM, Budapest, Hungary) and an HP 3395 integrator (Hewlett-Packard, Waldbronn, Germany).

The column used was Lichrospher 100 RP-18 (125 × 4 mm I.D.), 5 μm particle size (Merck, Darmstadt, Germany).

2.3. Derivatization of amino acids for chromatographic analysis

An amount of 2–4 μmol of DTBGLA or Gla was derivatized with FDAA by the Marfey method [42]. The molar ratio of FDAA/amino acid in the mixture was kept at 1.4:1. For derivatization with GITC, 2–4 μmol of DTBGLA or Gla was used, applying the method of Nimura et al. [43]. In both derivatization methods, after completion of the reaction, the reaction mixture was diluted with the eluent 2–10 fold and 10-μl aliquots were used for injection onto the HPLC system.

3. Results and discussion

To keep the ionization of the free carboxylate groups of Gla and DTBGLA at a constant level within the column, and to achieve good run-to-run reproducibility, buffering of the aqueous–organic modifier phase system is required. Protonation of the free carboxylate groups changes the hydrophobicity and hence the retention behaviour. On the other hand, Gla and its derivatives are sensitive to hydrolysis under acidic conditions [17]. Thus, the correct choice of the buffer system and the conditions used can be rather important. The application of potassium dihydrogenphosphate as buffer appeared favourable. Under the conditions used for the analysis of Gla and DTBGLA, any Glu peak could readily be observed in the chromatograms.

3.1. Separation of D,L-DTBGLA–FDAA derivatives

The chromatographic analysis was carried out in different phosphate buffer (pH 2–6)–organic

modifier (acetonitrile or methanol) systems. Data obtained in the phosphate buffer–acetonitrile system indicate that, with a decrease of the acetonitrile content at a given pH, k' increases and the α and R_s values improve. The k' and R_s values increased considerably on decrease of the pH of the aqueous phase from 6 to 2. At a constant phosphate buffer–acetonitrile ratio, e.g. 60:40 (v/v), the k' values of the L- and D-isomers increased from 1.3 to 16.0 and from 2.1 to 24.5, while R_s increased from 1.1 to 4.9 (Fig. 1A). This behaviour is probably correlated with protonation of the α-carboxylate group. The protonation microconstant for the α-carboxylate group of Gla in aqueous solution is $\log k^{\alpha} = 2.66$ [44]. There is no general rule for the conversion of the protonation constants obtained in aqueous solution to those in an aqueous–organic modifier system [45], but the increase in the retention time at low pH is probably connected with the increased hydrophobicity of the adduct. On the other hand, a resolution higher than 2 can also be achieved with a relatively low k' ($k' < 5$) at higher pH, by keeping the acetonitrile content below 40% (v/v).

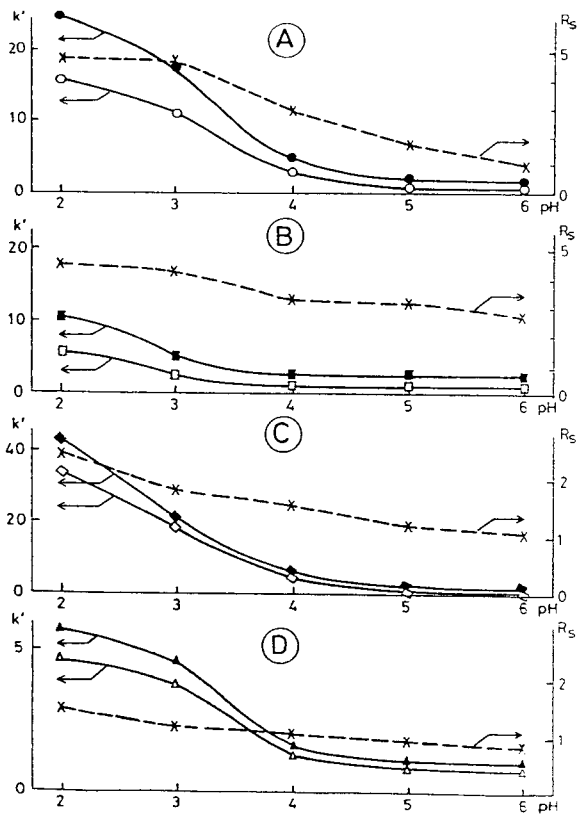

Fig. 1. Dependence of retention factor (k') and resolution (R_s) of DTBGLA–FDAA and DTBGLA–GITC derivatives on pH at a given eluent composition. Column, Lichrospher 100 RP-18; flow-rate, 0.8 ml/min. (A,B) DTBGLA–FDAA derivatives; (C,D) DTBGLA–GITC derivatives. Mobile phase, 0.01 *M* potassium dihydrogenphosphate (pH 2–6)–organic modifier; (A,C) buffer–acetonitrile 60:40 (v/v), (B,D) buffer–methanol 35:65 (v/v); (○, □, ◇, △) retention factor (k') of L-isomer, (●, ■, ◆, ▲) retention factor (k') of D-isomer; (×) R_s value of L/D isomers.

The general observations for the phosphate buffer–methanol system are similar to those obtained with acetonitrile as organic modifier. With respect to the separation capabilities of the two systems, the phosphate buffer–methanol system seems more efficient than the acetonitrile-containing one. To compare the two systems (see Fig. 1A and B), in the methanol-containing system a resolution of higher than 2.5 can be achieved at every pH with low values of the corresponding retention factor. Figs. 2A and 2B show characteristic chromatograms of DTBGLA–FDAA derivatives obtained in the acetonitrile- or methanol-containing eluent systems. The elution sequence on the chromatograms is L-isomer before D-isomer. The described method is suitable for the determination of a content of the minor enantiomer of less than 0.05% of that of the major enantiomer.

3.2. Separation of D,L-DTBGLA–GITC derivatives

The results of the separation in the phosphate buffer–acetonitrile or methanol systems of the GITC derivatives show that with a decrease in the organic modifier concentration, k', α and R_s increase at every pH. The effect of pH at a given phosphate buffer–organic modifier ratio is similar to that observed for the FDAA derivatives (Fig. 1C,D). With regard to separations carried out with the two derivatizing reagents: FDAA and GITC at the same eluent composition, phosphate buffer–acetonitrile 60:40 (v/v), and at the same pH, the GITC derivatives generally

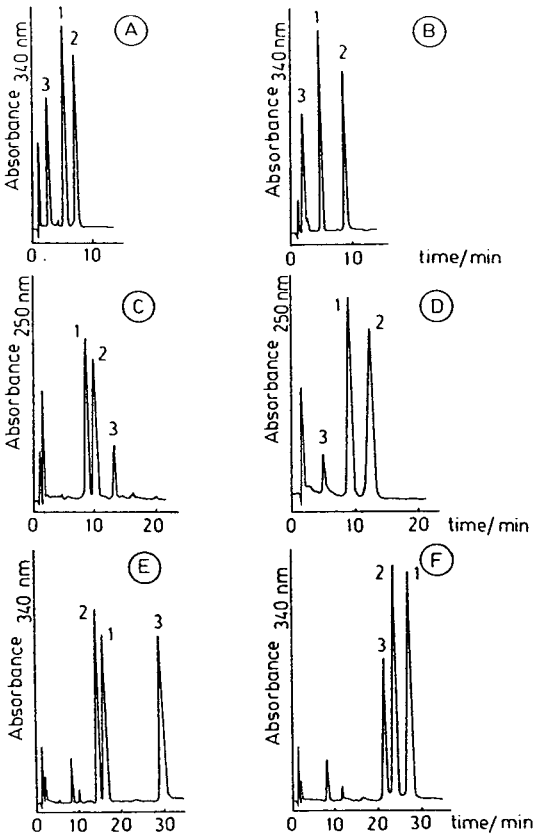

Fig. 2. Chromatograms of D,L-DTBGLA and D,L-Gla derivatives. Column, Lichrospher 100 RP-18; flow-rate, 0.8 ml/min; detection, 340 nm (FDAA derivatives), 250 nm (GITC derivatives). (A,B) D,L-DTBGLA–FDAA derivatives; (C,D) D,L-DTBGLA–GITC derivatives; (E,F) D,L-Gla–FDAA derivatives. Mobile phase, A, phosphate buffer (pH 3)–acetonitrile 50:50 (v/v); B, phosphate buffer (pH 3)–methanol 35:65 (v/v); C, phosphate buffer (pH 5)–acetonitrile 65:35 (v/v); D, phosphate buffer (pH 6)–methanol 45:55 (v/v); E, phosphate buffer (pH 2)–acetonitrile 80:20 (v/v); F, phosphate buffer (pH 2)–methanol 70:30 (v/v). Peaks: 1 = L-isomer, 2 = D-isomer, 3 = unreacted reagent. Molar ratio of D/L isomers is 1:1.

have higher k' and lower R_s values than the FDAA derivatives (Fig. 1A,C). In the phosphate buffer–methanol system at a given eluent composition of 35:65 (v/v) and at the same pH, the GITC derivatives have lower k' and R_s than the FDAA derivatives (Fig. 1B,D). On the basis of these results, a baseline separation ($R_s > 1.5$) of DTBGLA–GITC derivatives can be obtained with relatively low k' values ($k' < 5$). For this purpose the pH of the phosphate buffer should be kept at a relatively high value (pH 5–6) and the organic-modifier content of the eluent at a relatively low concentration (Fig. 2C,D). The elution sequence of the isomers on the chromatograms is L-isomer before D-isomer. The chiral purity of DTBGLA enantiomers can also be determined by application of GITC as derivatizing reagent. The detection limit is lower than 0.05% of the minor isomer in the presence of the major enantiomer.

3.3. Separation of D,L-Gla–FDAA and D,L-Gla–GITC derivatives

The separations were carried out in phosphate buffer–acetonitrile or methanol systems (Fig. 2E,F). The separation of D- and L-diastereoisomers could be achieved only when the pH of the phosphate buffer was near 2. The distribution curves of the Gla species [44] indicate that the formation of more hydrophobic (protonated) species is favourable at low pH ($pH \ll 2$) in aqueous solution.

In the aqueous–organic modifier system, the pK values of the carboxylate groups of Gla are higher, but the increase at 20–30% organic-modifier content is probably not considerable [45]. Thus the observed chromatographic behaviour of Gla derivatives is in agreement with the expectations.

Of the two organic modifier systems, acetonitrile and methanol, the acetonitrile-containing system seems more efficient. A similar resolution in acetonitrile can be achieved at lower k', and the main peak of the unreacted reagent elutes very close to the D-diastereoisomer in methanol. The elution sequence is the reverse of that observed for the DTBGLA–FDAA derivatives: the D-isomer elutes before the L-isomer. The application of this separation method allows the determination of a minor enantiomer content less than 0.05% of that of the major isomer.

The separation experiments for D,L-Gla–GITC derivatives were carried out in different phosphate buffer–acetonitrile or methanol systems.

Both systems were unsuccessful with respect to the separation of GITC derivatives.

4. Conclusion

The described procedure can be applied for the separation of optical isomers and for the determination of the enantiomeric content of DTBGLA and Gla without conversion to Glu. In the case of DTBGLA, FDAA seemed more suitable than GITC as derivatizing reagent, and a better resolution could be achieved within a shorter time. Concerning the two organic modifiers, the methanol-containing systems seemed more favourable than the acetonitrile-containing ones. In the separation of Gla enantiomers, FDAA was much more favourable as derivatizing reagent than GITC, while of the two organic modifiers, acetonitrile was more advantageous than methanol.

The pH of the phosphate buffer was a very important factor in the separation. The elution sequence for the L- and D-diastereomers of DTBGLA was the opposite of that for Gla.

Acknowledgement

This work was supported in part by a grant from the Hungarian Research Foundation (OTKA 71/91 and T 14898).

References

[1] J. Stenflo, P. Fernlund, W. Egan and P. Roepstorff, Proc. Natl. Acad. Sci. USA, 71 (1974) 2730.
[2] G.L. Nelsestuen, T.H. Zytkovicz and J.B. Horward, J. Biol. Chem., 249 (1974) 6347.
[3] S. Magnusson, L. Sottrup-Jensen, T.E. Peterson, H.R. Morris and A. Dell, FEBS Lett., 44 (1974) 189.
[4] J.J. van Buskirk and W.M. Kirsch, Biochem. Biophys. Res. Commun., 82 (1978) 1329.
[5] P.V. Hauschka, J.B. Lian and P.M. Gallop, Proc. Natl. Acad. Sci. USA, 72 (1975) 3925.
[6] T.H. Zytkowicz and G.L. Nelsestuen, J. Biol. Chem., 250 (1975) 2968.
[7] P. Fernlund, Clin. Chim. Acta, 72 (1976) 147.
[8] H. Tabor and O.W. Tabor, Anal. Biochem., 78 (1977) 554.
[9] P.V. Hauschka, Anal. Biochem., 80 (1977) 212.
[10] T. Yamagata, H. Kasai and T. Okuyama, Bunseki Kagaku, 26 (1977) 819.
[11] D.A. Madar, P.A. Willis, K.A. Koehler and R.G. Hiskey, Anal. Biochem., 92 (1979) 466.
[12] C.M. Gundberg, J.B. Lian and P.M. Gallop, Anal. Biochem., 98 (1979) 219.
[13] L.B. James, J. Chromatogr., 175 (1979) 211.
[14] L.M. Canfield, J. Ma and E.G. Sander, Vitamin K Metabolism, Vitamin K-Dependent Proteins, Proc. 8th Steenboch Symp. 1979, 1980, p. 505.
[15] P. Fernlund, Vitamin K Metabolism, Vitamin K-Dependent Proteins, Proc. 8th Steenboch Symp. 1979, 1980, p. 166.
[16] R. Kuttan, N. Wilson and R. Tenni, J. Chromatogr., 223 (1981) 182.
[17] P.V. Hauschka, E.B. Henson and P.M. Gallop, Anal. Biochem., 108 (1980) 57.
[18] Y. Ishikawa and R.E. Wuthier, Anal. Biochem., 114 (1981) 388.
[19] K.T.D. Lin, J. Chromatogr., 227 (1982) 341.
[20] M. Kuwada and K. Katayama, Anal. Biochem., 117 (1981) 259.
[21] P.P. Price, Methods Enzymol., 91 (1983) 13.
[22] Y. Ghirane, S. Nakamura, K. Hiraishi and K. Kurokawa, Rinsho Kagaku, 12 (1983) 297.
[23] C.C. Chin, Methods Enzymol., 92 (1984) 106.
[24] M. Low, J.J. Van Buskirk and W.M. Kirsch, Vitamin K Metabolism, Vitamin K-Dependent Proteins, Proc. 8th Steenboch Symp. 1979, 1980, p. 150.
[25] Y. Haroon, Anal. Biochem., 140 (1984) 343.
[26] M. Kuwada and K. Katayama, J. Chromatogr., 308 (1984) 398.
[27] R.W. Etheredge and M.J. Glimcher, Calcif. Tissue Int., 39 (1986) 239.
[28] B. Fournier, E. Gyneyts and P.D. Delmas, Clin. Chim. Acta, 182 (1989) 173.
[29] C. Colette, A. Benmbarek, H. Boniface, C. Astre, N. Pares-Herbute, L. Monnier and J. Guitter, Clin. Chim. Acta, 204 (1991) 43.
[30] J.R. Cairns, M. Williamson and P.A. Price, Anal. Biochem., 199 (1991) 93.
[31] D.M. Smalley and P.C. Preusch, Anal. Biochem., 172 (1988) 241.
[32] C.J. Strong, E. Henson, Y. Okamoto, M. Paz and P.M. Gallop, Anal. Biochem., 178 (1989) 276.
[33] K. Muramoto and H. Kamiya, Anal. Sci., 7 (1991) 939.
[34] J. Rivier, R. Galyean, L. Simon, L.J. Cruz, B.M. Olivera and W.R. Gray, Biochemistry, 26 (1987) 8508.
[35] Y. Nishiuchi, M. Nakao, M. Nakata and S. Sakakibara, J. Pept. Synth., (1992) 61.
[36] Y. Nishiuchi, M. Nakao, M. Nakata, T. Kimura and S. Sakakibara, Int. J. Pept. Protein Res., 42 (1993) 533.
[37] T. Kurihara, F. Taniyama, M. Hare, T. Saito, S. Hirose and S. Ohashi, Int. J. Pept. Protein Res., 43 (1994) 367.

[38] W. Märki, M. Oppliger and R. Schwyzer, Helv. Chim. Acta, 58 (1975) 1471; 59 (1976) 901.
[39] W. Märki and R. Schwyzer, Helv. Chim. Acta, 59 (1976) 1591.
[40] S. Bajusz and A. Juhász, Acta Chim. Acad. Sci. Hung., 88 (1976) 161.
[41] Cs. Somlai, A. Péter and B. Penke, J. Pract. Chem., in press.
[42] P. Marfey, Carlsberg Res. Commun., 49 (1984) 591.
[43] M. Nimura, H. Ogura and T. Kinoshita, J. Chromatogr., 202 (1980) 375.
[44] K. Burger, P. Sipos, M. Véber, I. Horváth, B. Noszál and M. Lõw, Inorg. Chim. Acta, 151 (1988) 239
[45] B.L. Karger, J.N. LePage and N. Tanaka, in Cs. Horváth (Editor), High-Performance Liquid Chromatography, Advances and Perspectives, Vol. 1, Academic Press, London, 1980, p. 113.

ELSEVIER

Journal of Chromatography A, 710 (1995) 303–308

JOURNAL OF CHROMATOGRAPHY A

Quantitative analysis of fluorinated ethylchloroformate derivatives of non-protein amino acids using positive and negative chemical ionization gas chromatography–mass spectrometry

Ping Cao, Mehdi Moini*

Department of Chemistry and Biochemistry, University of Texas at Austin, Austin, TX 78712, USA

First received 9 January 1995; revised manuscript received 12 April 1995; accepted 12 April 1995

Abstract

The GC–MS characterization of the ethylchloroformate derivatives of amino acids in an aqueous medium has been applied to non-protein amino acids. Derivatization of non-protein amino acids using ethylchloroformate, trifluoroethanol, and pyridine produced strong $[M+1]^+$ and $[M-1]^-$ ions in positive and negative chemical ionization (CI) modes, respectively. Twenty-one out of the twenty-three non-protein amino acids studied produced detectable ion chromatograms in both ionization modes when methane was used as the CI reagent gas. Mass spectra of these non-protein amino acid derivatives showed characteristic $[M-19]^+$, $[M+1]^+$, $[M+29]^+$, and $[M+41]^+$ peaks in the positive chemical ionization mode, and $[M-1]^-$, and $[M+35]^-$ peaks in the negative chemical ionization mode. The detection limits and the linear dynamic range of trifluorethanol ethylchloroformate derivatives of non-protein amino acids were studied using positive chemical ionization. The detection limits are mostly in the femtomole range.

1. Introduction

Recently, Husek introduced a derivatization procedure for gas chromatographic (GC) analysis of protein amino acids using ethylchloroformate (ECF) [1] which was based on his previous study of chloroformate-induced esterification of the carboxylic groups of fatty acids [2]. The main advantages of this technique include: (1) simultaneous N(O,S)-derivatization of amino acids in one step, (2) derivatization of amino acids in aqueous solution, (3) reaction time of only a few seconds, (4) derivatization with inexpensive reagents, and (5) GC [1–3] or GC–MS [4–6] identification of products.

It was shown by this lab [6] that ECF derivatization of protein amino acids in a solution of water, trifluoroethanol, and pyridine, followed by GC–MS analysis of the products using positive and/or negative chemical ionization (CI) mode increases the sensitivity of detection and simplifies the identification of these derivatized amino acids.

To date, most of the reported data shows the

* Corresponding author.

0021-9673/95/$09.50
SSDI 0021-9673(95)00476-9

application of ECF derivatization to protein amino acids. Here we report the application of the ECF derivatization to non-protein amino acids using trifluoroethanol as the esterifying agent.

2. Experimental

The twenty-three non-protein amino acids were provided by Professor Mabry, Department of Botany, The University of Texas at Austin. A solution containing 250 ng/ml of each of the non-protein amino acids in 0.1 *M* HCl was used for the qualitative analysis. The ethylchloroformate was purchased from Sigma (St. Louis, MO, USA). The trifluoroethanol was purchased from Aldrich (Milwaukee, WI, USA). The ECF derivatives were prepared according to the procedure reported previously [1]. Analysis by GC–MS was carried out on a Finnigan MAT TSQ-70 MS (San Jose, CA, USA) coupled to a Varian 3400 GC (Palo Alto, CA, USA). The GC separation employed a 25-m DB-1701 fused-silica capillary column with 0.32 mm I.D. and 1 μm film coating (SGE, Austin, TX, USA). Mass spectrometric conditions were as follows: scan range of 120–500 u, scan rate of 1 scan/s (3 scans/s for quantitative analysis), methane gas at a pressure of ca. 2 Torr used as the CI reagent gas, and an interface temperature of 270°C. GC conditions were as follows: initial column temperature of 80°C, 2 min delay, final column temperature of 270°C, and a column ramp rate of 10°C/min. A 1-μl aliquot of the solution was injected in direct (splitless) injection mode for each analysis. For quantitative study, the stock solution (250 ng/ml, the upper limit of the dynamic range study) of non-protein amino acids was diluted by two to five orders of magnitude using 0.1 *M* HCl solution. These solutions were then derivatized and analyzed according to the above procedure.

3. Results and discussion

The reconstructed total ion chromatograms (RIC) of the twenty-one ECF + trifluoroethanol + pyridine derivatives of non-protein amino acids under positive and negative chemical ionization modes are shown in Figs. 1 and 2, respectively. Under the experimental conditions employed here, each derivatized non-protein

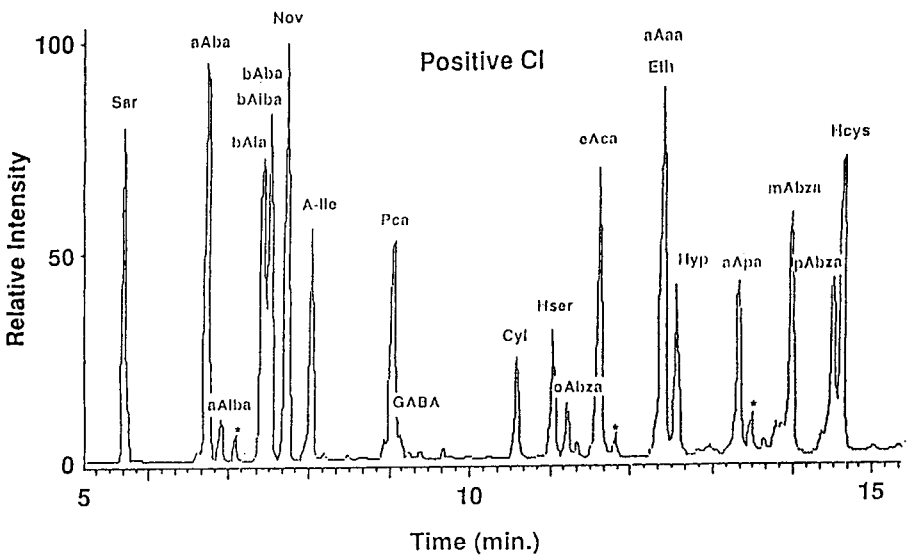

Fig. 1. Reconstructed TIC of positive chemical ionization GC–MS of the trifluoroethanol ECF derivatized non-protein amino acids. Peaks marked with an asterisk were not identified.

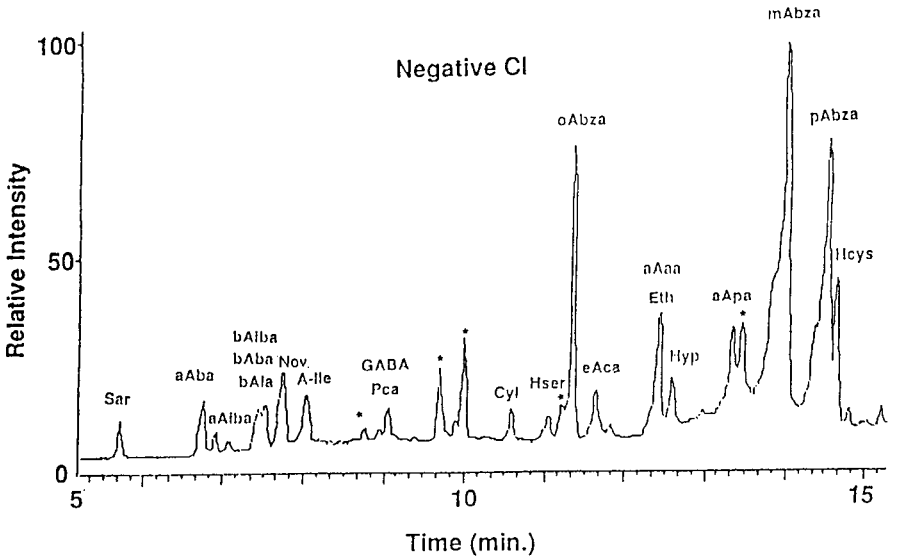

Fig. 2. Reconstructed TIC of negative chemical ionization GC–MS of the trifluoroethanol ECF derivatized non-protein amino acids. Peaks marked with an asterisk were not identified.

amino acid produced a separated peak except for three pairs whose peaks overlapped: β-aminoisobutyric acid and β-aminobutyric acid, DL-α-aminoadipic acid and DL-ethionine, and pipecolinic acid and γ-aminobutyric acid. However, the overlapping peaks were identified when their ion chromatograms were plotted. In cases where derivatized non-protein amino acids had the same molecular mass, their ion chromatograms and retention time were used for identification. Comparison between the GC–MS results in the positive and negative chemical ionization modes (Figs. 1 and 2, respectively) indicates that, in general, the positive CI chromatogram has lower background chemical noise and higher signal intensity than negative CI except for anthranilic acid, *p*-aminobenzoic acid, and *m*-aminobenzoic acid. Anthranilic acid in the positive CI mode did not produce a significant peak in the corresponding total ion chromatogram. In the negative CI mode, however, these three compounds showed strong peaks. The most likely explanation for this behavior is that these three non-protein amino acids all have an aromatic ring which increases the electron capture cross-section and/or stabilizes the negatively charged ions, therefore giving higher signal intensity with respect to non-aromatic non-protein amino acids. L-Citrulline and taurine did not produce detectable peaks in the total ion chromatograms of either ionization mode.

The results of the mass spectrometric study of the ECF derivatives of non-protein amino acids using trifluoroethanol in positive and negative CI modes are tabulated in Table 1. Similar to the analysis of the protein amino acids, $[M+1]^+$ is the base peak in all of the positive CI spectra. The positive CI spectra show a common fragmentation pattern for all of the non-protein amino acids, with major fragments originating from the loss of HF from $[M+1]^+$. In addition, with methane as a regent gas, all of the non-protein amino acid derivatives formed $[M+29]^+$ and $[M+41]^+$ ions, the $C_2H_5^+$ and $C_3H_5^+$ adducts of the molecules. Existence of the $[M-F]^+$, $[M+1]^+$, $[M+29]^+$ and $[M+41]^+$ peaks immediately distinguishes the fluorinated derivatives of non-protein amino acids from other side products or impurities which produce peaks in the chromatograms. As an example, Fig. 3 shows the mass spectrum of derivatized sarcosine (Sar) under the positive CI mode using methane as reagent gas.

The negative CI spectra show that $[M-1]^-$ is

Table 1
Characteristic ion peaks in positive CI spectra of trifluoroethanol ECF derivatives of non-protein amino acids

Non-protein amino acid	M_r	Derivative $[M+1]^+$	Base peak (m/z)	Other important ions (m/z)
Sarcosine (Sar)	89	244	244	224,272,284
β-Alanine (bAla)	89	244	244	224,272,284
α-Aminobutyric acid (aAba)	103	258	258	238,286,298
α-Aminoisobutyric acid (aAiba)	103	204	204	232,244
β-Aminobutyric acid (bAba)	103	258	258	238,286,298
β-Aminoisobutyric acid (bAiba)	103	258	258	238,286,298
L-Norvaline (Nov)	117	272	272	252,300,312
DL-Homoserine (Hser)	119	174	174	202,214
Pipecolinic acid (Pca)	129	284	284	264,312,324
Cycloleucine (Cyl)	129	230	230	258,270
ε-Amino-η-caproic acid (eAca)	131	286	286	266,314,326
L-*allo*-Isoleucine (A-Ile)	131	286	286	266,314,326
Hydroxy-L-proline (Hyp)	131	286	286	266,314,326
DL-Homocystein (Hcys)	135	362	362	342,390,402
m-Aminobenzoic acid (mAbza)	137	292	292	272
p-Aminobenzoic acid (pAbza)	137	292	292	272,320,332
Anthraniline (oAbza)	137	292	292	272,320,332
DL-α-Aminoadipic acid (aAaa)	161	398	398	378,426,438
DL-Ethionine (Eth)	163	318	318	346,358
γ-Aminobutyric acid GABA)	103	258	258	238,286,298
DL-α-Aminopinelic acid (aApa)	175	412	412	392,440,452

the base peak in all of the non-protein amino acids except DL-α-aminopinelic acid which gave the HCl adduct as the base peak. The negative CI spectra also show characteristic $[M+35]^-$ peaks arising from $[M+Cl]^-$ ions formed from the loss of a proton from the HCl adducts of the molecules under negative CI conditions. This is consistent with our previous results [6], that under the experimental conditions of this study protein and non-protein amino acids are present as HCl adducts.

In accordance with the previous studies of the

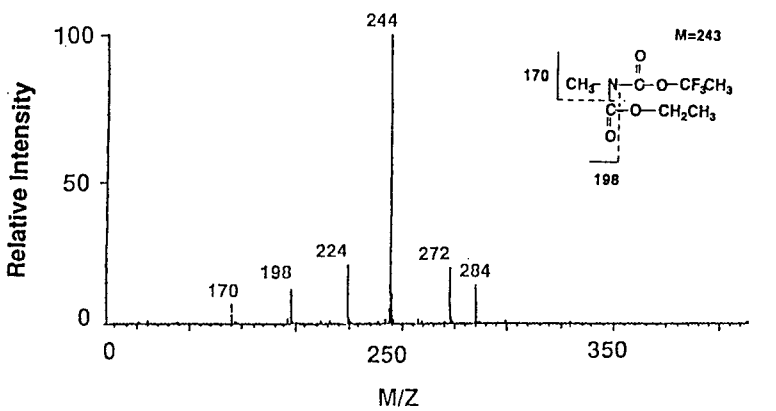

Fig. 3. Positive CI spectrum of derivatized sarcosine using methane as reagent gas. The m/z 224, 244, 272, and 284 are $[M-F]^+$, $[M+H]^+$, $[M+C_2H_5]^+$, and $[M+C_3H_5]^+$ peaks, respectively.

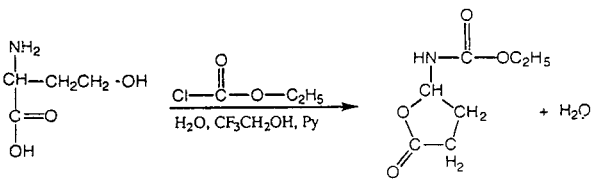

Fig. 4.

ECF derivatization of protein amino acids [5], the substituted alkyl group on the carboxylic side of the amino acids is provided by the alcohol, and the substituted alkyl group for the amine side is provided by the alkyl group of the chloroformate. A minor amount of derivatives are also found where the substituted alkyl group on both the carboxylic side and the amine side are provided by the alkyl group of the chloroformate. Derivatization of both the carboxylic side and the amine side by the alkyl group of ECF, however, gave the main products for α-aminoisobutyric acid and cycloleucine. In addition, we also observed that a lactone is the major derivatization product of DL-homoserine due to the stable structure of a five membered ring as shown in Fig. 4.

The detection limits and linear dynamic range of the ethylchloroformate derivatives of non-protein amino acids were studied using chemical ionization in the positive ion mode. The results are given in Table 2. As is shown, the detection limits are mostly in the femtomole range. Chemical ionization of the ECF trifluoroethyl ester derivatives of non-protein amino acids, therefore, is the technique of choice for detection of trace amounts of non-protein amino acids.

Acknowledgement

We thank Drs. Chang-Hwan Oh and Tom J. Mabry, Department of Botany, University of Texas at Austin, for their kind submission of non-protein amino acids and helpful discussion.

References

[1] P. Husek, J. Chromatogr., 552 (1991) 289.
[2] P. Husek, J.A. Rijks, P.A. Leclercq and C.A Cramers, J. High Res. Chromatogr., 13 (1990) 633.

Table 2
Detection limits and linear dynamic ranges of trifluoroethyl ester ECF derivative non-protein amino acids

Non-protein amino acid	Detection limit (ng)	Linear dynamic range (orders of magnitude)	Correlation coefficient
α-Aminobutyric acid (aAba)	5.00E − 03	3.7	0.988
L-Norvaline (Nov)	5.00E − 03	3.7	0.9848
β-Alanine (bAla)	5.00E − 03	3.7	0.9854
DL-Homocystein (Hcys)	5.00E − 03	3.7	0.992
m-Aminobenzoic acid (mAbza)	5.00E − 03	3.7	0.9747
p-Aminobenzoic acid (pAbza)	5.00E − 03	3.7	0.9914
DL-Ethionine (Eth)	5.00E − 02	3	0.9917
DL-α-Aminopimelic acid (aApa)	5.00E − 02	3	0.9986
Sarcosine (Sar)	5.00E − 02	3	0.982
Hydroxy-L-proline (Hyp)	5.00E − 02	3	0.98
α-Aminoisobutyric acid (aAiba)	5.00E − 02	3	0.9933
DL-Homoserine (Hser)	5.00E − 02	3	0.9877
Pipecolinic acid (Pca)	5.00E − 02	3	0.9916
Cycloleucine (Cyl)	5.00E − 02	3	0.9924
L-*allo*-Isoleucine (Alle)	5.00E − 02	3	0.9975
ε-Amino-η-caproic acid (eAca)	0.25	2.7	0.9948
DL-α-Aminoadipic acid (aAaa)	0.25	2.7	0.9988

[3] P. Husek and C.C Sweeley, J. High Res. Chromatogr., 14 (1991) 751.
[4] Z.H. Huang, J. Wang, D.A. Cage, J.T. Watson, C.C Sweeley and P. Husek, J. Chromatogr., 635 (1993) 271.
[5] J. Wang, Z.-H. Huang, D.A. Gage and J.T. Watson, J. Chromatogr. A, 663 (1994) 71.
[6] M. Vatankhah and M. Moini, Biological Mass Spectrom., 23 (1994) 277.

ELSEVIER

Journal of Chromatography A, 710 (1995) 309–321

JOURNAL OF CHROMATOGRAPHY A

Systematic study of field and concentration effects in capillary electrophoresis of DNA in polymer solutions

Liouba Mitnik[a,b], Laurence Salomé[c], Jean Louis Viovy[a,b], Christoph Heller[b,d,*]

[a]*Laboratoire de PhysicoChimie Théorique (URA CNRS 1382), Ecole Superieure de Physique et de Chimie Industrielles de la Ville de Paris, 10 rue Vauquelin, 75231 Paris cedex 05, France*

[b]*Laboratoire de PhysicoChimie Structurale et Macromoléculaire (URA CNRS 278), Ecole Superieure de Physique et de Chimie Industrielles de la Ville de Paris, 10 rue Vauquelin, 75231 Paris cedex 05, France*

[c]*Centre de Recherches Paul Pascal, CNRS, Avenue A. Schweitzer, 33600 Pessac, France*

[d]*Laboratoire de Physique des Surfaces et Interfaces (URA CNRS 1379), Institut Curie, 11 rue Pierre-et-Marie Curie, 75005 Paris, France*

First received 7 March 1995; revised manuscript received 21 April 1995; accepted 21 April 1995

Abstract

A systematic study of the separation of double-stranded DNA in hydroxypropylcellulose (HPC) with a molecular mass of 10^6 was undertaken, using a variety of concentrations (from 0.1 to 1%) and different electric fields (from 6 to 540 V/cm). The data show that at high polymer concentrations ($\geq$0.4%) and low fields, the separation mechanism is similar to that occurring in gels. The results are in good agreement with theoretical models, and in particular with a recently proposed theory for gels with a pore size smaller than the persistence length of DNA. For more dilute solutions and high fields, however, the separation pattern cannot be explained by existing theories. The existence of an original mechanism was confirmed by the direct observation of the conformation of double-stranded DNA molecules in the polymer solution by fluorescence videomicroscopy. Practical conclusions for the capillary electrophoretic separation of duplex DNA are drawn.

1. Introduction

Capillary electrophoresis (CE) has rapidly become a powerful and attractive separation technique because of its sensitivity, rapidity and the possibility of automation. The first separations of DNA by CE were performed in gels. However, the preparation of a gel-filled capillary is delicate. Air bubbles and inhomogeneities can be formed during the polymerization inside a capillary or during the electrophoresis. The structure of the gel may also vary along the capillary. The use of polymer solutions instead of gels as a sieving medium avoids these problems and permits the experimental protocols to be simplified. It can be especially effective for large and flexible DNA molecules. Indeed, several studies yielded a good separation for DNA restriction fragments up to 23 kilo-base pairs (kbp) in different polymer solutions (e.g., [1,2]).

Some theoretical approaches that permit one to predict the separation and to evaluate the optimum separation conditions for different sizes of DNA molecules in polymer solutions of different concentrations have been proposed recently. The first theoretical description, to our knowl-

* Corresponding author.

0021-9673/95/$09.50
SSDI 0021-9673(95)00500-5

edge, of DNA electrophoresis in polymer solutions was proposed by Grossman and Soane [3]. A more detailed theoretical model was developed by Viovy and Duke [4].

In order to check the conformity with experimental data and to establish if the models used for DNA electrophoresis in gels would be applicable to those in polymer solutions, we undertook a systematic study of the separation of double-stranded DNA in hydroxypropylcellulose (HPC) using a variety of concentrations and field strengths.

Also, we present here some data on the direct observation of DNA molecules during their migration in polymer solutions, obtained by epifluorescence microscopy. The observation of conformations of individual DNA molecules undergoing electrophoresis can be helpful in the understanding of migration mechanisms.

2. Theory

We recall in the following some proposed models for DNA separation in polymer solutions, in order to compare them with our experimental data.

2.1. Polymers

Three regimes of polymer solutions can be distinguished: dilute, semi-dilute and concentrated. However, for CE, only the dilute and semi-dilute regimes are relevant. The crossover between these regimes is characterized by the overlap concentration, c^* (see Fig. 1).

Other important parameters in the theory of polymer solutions are the square-averaged radius of gyration, $\langle R_g^2 \rangle$, and the screening length, ξ.

If the molecular mass, M_w, is known, a simple experimental way to determine the radius of gyration of a polymer is to measure the intrinsic viscosity $[\eta]$ in the dilute regime [5]:

$$[\eta] \approx 6.2 R_g^3 N_A / M_w \quad (1)$$

where N_A is Avogadro's number. If the radius of gyration is known, this permits in turn the calculation of c^*, which is defined as

$$c^* \approx 3M_w / 4\pi N_A R_g^3 \approx 1.5[\eta]^{-1} \quad (2)$$

The screening length, ξ, is the distance above which the excluded volume interactions are screened by other chains. Grossman and Soane [3] proposed the use of this parameter as the effective "pore size" of the transient network. Viovy and Duke [4] proposed that the so-called "blob size", ξ_b (see Fig. 1), should be used instead. It is related to ξ by a universal prefactor [6]:

$$\xi_b = 2.86\xi = 1.43 R_g (c/c^*)^{-3/4} \quad (3)$$

Therefore, this difference affects predictions quantitatively but not qualitatively.

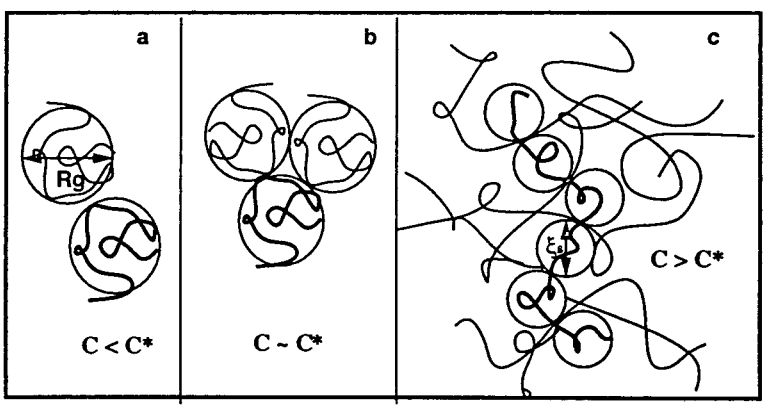

Fig. 1. Schematic representation of flexible polymers in solution. (a) Dilute solutions; (b) solutions at entanglement threshold c^*; (c) semi-dilute solutions. One chain is drawn as a thick line for easier visualization. The small circles in c represent the "blobs" of size ξ_b.

2.2. Molecular mechanisms of size separation in polymer solutions

The first mechanism proposed for the description of gel electrophoresis, the Ogston model [7], assumes that the mobility of a particle is proportional to the fraction of the volume available to it in the gel. Using purely geometric arguments, Ogston derived an expression for the mobility of a globular particle in a random array of fibres:

$$\mu = \mu_0 \exp(-K_R C) \tag{4}$$

where μ_0 is the mobility in pure solvent, K_R is the retardation coefficient and C is the gel concentration. In order to apply the Ogston model to DNA separation, one assumes that the DNA migrates as a random coil. Then K_R should be

$$K_R \approx (R_{DNA} + r)^2 \tag{5}$$

where r is the radius of the gel fibres and R_{DNA} is the radius of gyration of the DNA molecule. Since the Ogston model is in principle applicable to rigid fibre-like obstacles, it is not obvious what should play the role of the "fibre radius", r, in a solution of very flexible polymers. The molecular radius of HPC is of the order of 10–15 Å, i.e., negligible in comparison with the radius of gyration of DNA. Even in the opposite view, in which one considers that the blob size should play the role of the fibre radius, r would be much smaller than R_{DNA} for all experiments we performed, except for the smallest DNA in the most dilute solutions, where we shall see that there is virtually no separation. Therefore, r can be safely neglected in Eq. 5.

The Ogston model does not account correctly for the mobility of large DNA molecules in gels, so that a second type of model, the biased reptation model, was proposed. In the original biased reptation model (BRM), the DNA chain is assumed to thread its way, without changing its length, through a "tube" defined by the fibres (for a rigid mesh) or the "blobs" (for a flexible network) surrounding it. To facilitate the description of the DNA mobility, we introduce in the following two dimensionless parameters. These are the mesh size normalized to the Kuhn length b of DNA, $\bar{\xi} = \xi_b / b$, and $\varepsilon_0 = Eq_k b/kT$, the electric potential energy per Kuhn length scaled to the thermal energy (q_k is the effective charge per DNA Kuhn segment).

The biased reptation model predicts that the electrophoretic mobility $\mu(N,E)$ in DNA gel electrophoresis is approximately related to the DNA molecular size N and the electric field E by [8]

$$\mu(N, E) \approx \frac{A}{N} + B(E) \tag{6}$$

with $B(E)$ proportional to E^β, where the exponent β equals 2 for low electric fields (i.e., far from saturation). When expressed in terms of molecular parameters, A and B should be $A \approx \bar{\xi}\mu_0/3$ and $B \approx \mu_0 \varepsilon_0^2 \bar{\xi}^4/6$, where μ_0 is the mobility in free solution.

For small molecular sizes, Eq. 6 predicts that $\mu(N)$ scales as $1/N$; for large sizes it predicts a plateau mobility.

This theory was recently improved by Duke et al. [9] to include the fluctuations in the length of the DNA molecule. This new model, called "biased reptation with fluctuations" (BRF), considers two different cases, as follows.

Mesh size larger than the Kuhn length of DNA ($\bar{\xi} > 1$)

For $\bar{\xi} > 1$, the BRF theory gives for the mobility μ_{rep}

$$\mu_{rep}/\mu_0 \approx \frac{\bar{\xi}}{3}[(1/N_k) + \varepsilon_0 \bar{\xi}] \tag{7}$$

where N_k is the number of Kuhn segments. Therefore, the BRF model predicts two regimes for the mobility in constant field. For small DNA and/or a low electric field, the first term in Eq. 7 dominates (this regime is called: "reptation without orientation"); in this regime, the mobility varies as $\mu \propto 1/N_k$, and separation is possible. For a longer DNA and/or a higher electric field, a second regime, called "reptation with orientation", is reached, where the second term in Eq. 7 dominates. This leads to a mobility independent of size. There is a crossover point between

these regimes, which marks the DNA size beyond which the separation power of electrophoresis becomes weaker and weaker and finally disappears. It occurs at

$$N_k^* \approx \varepsilon_0^{-1} \bar{\xi}^{-1} \quad (8)$$

These predictions are in good agreement with experimental results for DNA separation in agarose gels [10–12].

Mesh size smaller than the Kuhn length ($\bar{\xi} < 1$)

In this case, reptation without orientation still occurs below a critical size N_k^*, but the mobility in this regime should be independent of the pore size [4]:

$$\mu_{rep}/\mu_0 \cong \frac{1}{3N_k} \qquad N_k < N_k^* \quad (9)$$

The theoretical values for the critical size and for the mobility beyond the crossover depend on ε_0 and $\bar{\xi}$:

(i) If $\varepsilon_0 < \bar{\xi}^{3/2}$:

$$\mu_{rep}/\mu_0 \cong \frac{\varepsilon_0}{3} \cdot \bar{\xi}^{3/2} \qquad N_k > N_k^* \quad (10)$$

and $N_k^* \approx \varepsilon_0^{-1} \bar{\xi}^{-3/2}$.

(ii) If $\bar{\xi}^{3/2} < \varepsilon_0 < \bar{\xi}^{-1}$

$$\mu_{rep}/\mu_0 \cong \frac{\varepsilon_0^{2/5}}{3} \cdot \bar{\xi}^{12/5} \qquad N_k > N_k^* \quad (11)$$

and $N_k^* \approx \varepsilon_0^{-2/5} \bar{\xi}^{-12/5}$.

(iii) Finally, if $\varepsilon_0 > \bar{\xi}^{-1}$:

$$\mu_{rep}/\mu_0 \cong \frac{\varepsilon_0^2}{3} \cdot \bar{\xi}^4 \qquad N_k > N_k^* \quad (12)$$

and $N_k^* \approx \varepsilon_0^{-2} \bar{\xi}^{-4}$.

All the theories mentioned above take no account of the mobile nature of the obstacles. In order to apply them to entangled polymer solutions, Viovy and Duke [4] suggested that, even in the absence of self-reptation or Ogston sieving, there is a finite mobility related to constraint release (CR), i.e., the self-renewal of obstacles due to the motions of the polymers in the matrix. They calculated this mobility as

$$\mu_{CR}/\mu_0 \approx (c/c^*)^{-15/4} \bar{\xi} \quad (13)$$

and proposed that, to a first approximation (i.e., for low enough electric fields and large enough DNA), the overall mobility is approximately

$$\mu = \mu_{rept} + \mu_{CR} \quad (14)$$

3. Experimental

3.1. Viscosity measurements

The viscosity of aqueous solutions of HPC covering the concentration range 0.05–2% was determined using an Ubbelohde capillary viscometer positioned in a thermostatically controlled water-bath at 26.0 ± 0.1°C. In this method, a liquid is allowed to flow through a fine-bore tube, and the viscosity is determined from the flow-rate, the gravitational pressure applied and the tube dimensions. Flow times for each solution were measured three times and readings agreed to within ±0.05%.

The intrinsic viscosity [η] obtained for HPC (M_w 10^6) (Aldrich) is 0.41 l/g. Using Eqs. 1 and 2, this yields a radius of gyration R_g = 48 nm and an overlap threshold c^* = 0.37%. These values should be taken as orders of magnitude, however, because the sample is not monodisperse.

3.2. Instrumentation and chemicals

The DNA samples used were 1-kbp DNA ladder (Gibco BRL), ϕX174/*HaeIII* digest (Gibco BRL) and Lambda/*HindIII* digest (New England Biolabs) at concentrations ranging from 10 to 100 μg/ml.

Analysis of the DNA fragments was accomplished using an automated capillary electrophoresis instrument (P/ACE 2100; Beckman Instruments, Palo Alto, CA, USA). The runs were performed in 37 cm long (30 cm to the detector) coated capillary tubes of 100 μm I.D. (DB-1 and DB-17; J & W Scientific, Folsom, CA, USA).

The running buffer was 1 × TBE (89 m*M* Tris–boric acid–2.5 m*M* EDTA) containing HPC (M_w 10^6) at different concentrations (0.1–

1%) and 10 μM ethidium bromide. All solutions were filtered and degassed before use.

The DNA samples were introduced into the capillary by electrokinetic injection at 175 V/cm for 10–30 s and separated at fields varying from 6 to 540 V/cm (negative polarity) at 25°C. For low electric fields, an external power supply was used instead of the built-in power supply. Detection was performed by UV absorption measurements at 254 nm.

3.3. Microscopic observations

An inverted microscope (Diaphot, Nikon) equipped for epifluorescence and with a Fluor 100 oil-immersion objective (Nikon) was coupled to a CCD camera with an image intensifier (Hamamatsu).

The following DNA samples were used: T4 phage DNA, 166 kbp (Amersham), and Lambda phage DNA, 48.5 kbp (Appligene). The DNA molecules were stained with an intercalating dye, oxazole yellow homodimer (YOYO, Molecular Probes), at a ratio of ca. 1 YOYO molecule per 10 bp. The DNA–polymer mixtures were placed between two cover-slips, which had been pretreated by overnight incubation in 1% methylcellulose 4000 (Serva) followed by thorough rinsing with Milli-Q-purified water. This treatment renders electroosmosis negligible, as checked by the measurement of the velocity profile across the cell [13]. The whole assembly was mounted in a special electrophoresis chamber, adapted to the microscope.

4. Results and discussion

To establish the conformity of the theoretical approach mentioned above to experimental data, we undertook a series of mobility measurements of DNA fragments (size range from 72 bp to 23 kbp) in solutions of 0.1, 0.2, 0.4 and 1% HPC at different field strengths. Typical examples of separations under different conditions are given in Figs. 2 and 3.

4.1. Mobility versus molecular mass

Fig. 4 shows double logarithmic plots of mobility versus molecular mass. The results show the usual sigmoidal dependence of the mobility on molecular mass: medium-sized molecules are well resolved in all cases, whereas shorter and larger molecules assume nearly constant mobilities.

For 1% HPC (well above c^*), and 0.4% HPC (slightly above c^*) (Fig. 4c and d), the double logarithmic mobility versus molecular mass plot is very similar to that obtained by separation in gels [12], with a well defined reptation regime (slope $= -1$) and a plateau mobility for large DNA at low electric fields. At high electric fields, however, a separation is achieved for large DNA, a behaviour opposite to the biased reptation prediction, that the limit of separation decreases with increasing field (Fig. 3c and d).

For 0.1% and 0.2% HPC (i.e., below c^*) (Fig. 4a and b), the result is different. Even at low electric fields, the slope never reaches -1, suggesting that in this case, reptation is not the main separation mechanism. Especially at higher field strengths, the mobility of the larger fragments never levels off totally, i.e. these fragments can still be separated.

4.2. Mobility versus electric field

The same data were replotted in order to demonstrate the dependence of the mobility on the electric field (Fig. 5). Again, the separation in 0.4% and 1% HPC is qualitatively very similar to that in gels (Fig. 5c and d): at low electric fields and/or low molecular mass, the mobility remains constant, i.e., is independent of the electric field, but it depends on size. Long chains (i.e., $N > N^*$), in contrast, show a linear log(mobility) versus log(electric field) dependence. At 1% HPC, the slope is 0.4, in excellent agreement with Eq. 11.

For 0.1% and 0.2% HPC (Fig. 5a and b), the picture is qualitatively similar, but the slope of the mobility versus electric field plot for the large molecules is even lower, with a value of about 0.2–0.3. Unsurprisingly, this behaviour is not

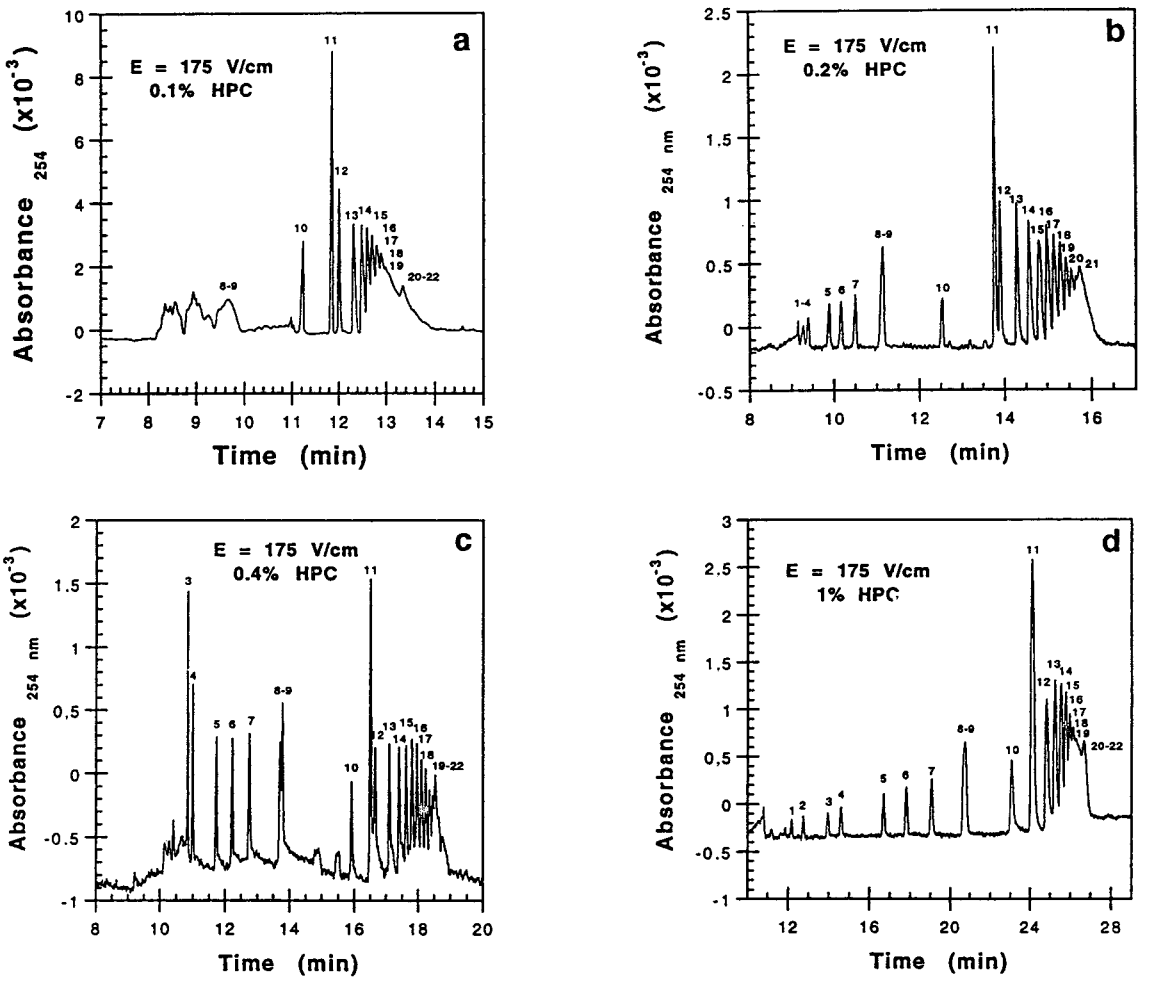

Fig. 2. Capillary electrophoresis of 1-kbp ladder ranging in size from 134 to 12 216 bp at different HPC concentrations, but with the same electric field: (a) 0.1%, (b) 0.2%, (c) 0.4% and (d) 1% HPC in 89 m*M* Tris–89 m*M* boric acid–2.5 m*M* EDTA–10 μM etidium bromide. Common conditions: coated capillary, DB-17; distance to detector, 30 cm; total length, 37 cm; I.D., 100 μm; field strength, 175 V/cm; temperature, 25°C. Peaks: 1 = 134; 2 = 154; 3 = 201; 4 = 220; 5 = 298; 6 = 344; 7 = 394; 8 = 506; 9 = 517; 10 = 1018; 11 = 1635; 12 = 2036; 13 = 3054; 14 = 4072; 15 = 5090; 16 = 6108; 17 = 7126; 18 = 8144; 19 = 9162; 20 = 10 180; 21 = 11 198; 22 = 12 216 bp.

predicted by the reptation theory, since at this concentration, the HPC used in these experiments is not fully entangled.

4.3. Reptation plot

Recently, a new representation of electrophoretic data as mobility times molecular size versus molecular size was proposed [8]. The existence of straight lines converging to a single point on the ordinate is expected to provide a "signature" of reptation behaviour, and allow a direct evaluation of the parameters entering mobility equations of the type of Eq. 6 or 7. On plotting our data using this so-called "reptation plot" [8], we indeed obtain straight lines, which seem to converge well towards a single point on the ordinate (not shown). Strikingly, this is true even for the data obtained at low HPC concentrations, for which the log–log representation (Fig.

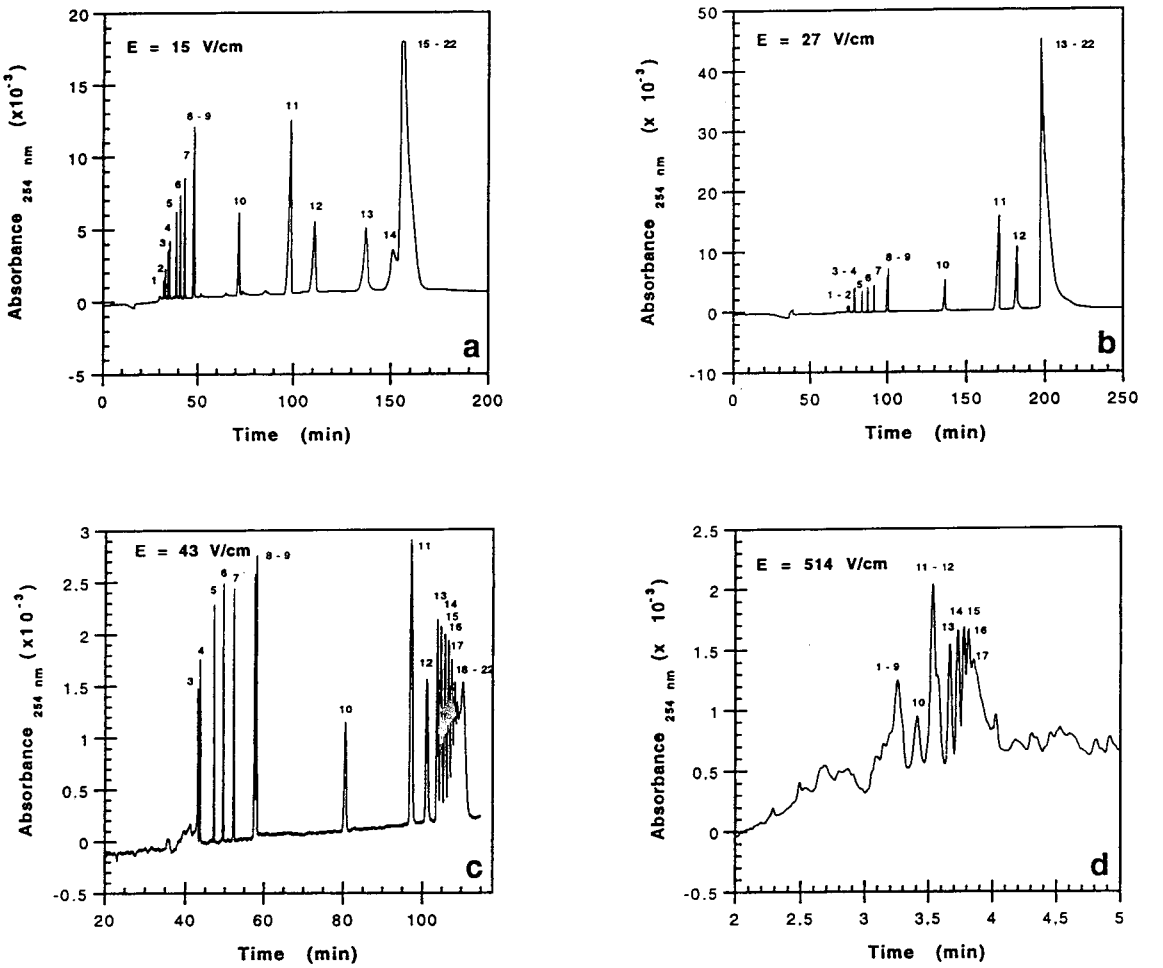

Fig. 3. Capillary electrophoresis of 1-kbp ladder under different electric field strengths, but at same polymer concentration (0.4% HPC), in 89 m*M* Tris–89 m*M* boric acid–2.5 m*M* EDTA–10 μM ethidium bromide. Conditions and peaks as in Fig. 2.

5a and b) provides no domain where the mobility is inversely proportional to the size. We conclude that the reptation plot is actually not a very accurate way of checking for reptation behaviour, probably because it puts relatively too much weight on data corresponding to the largest DNA. Fig. 6 presents a log–log plot of the slopes of the reptation plots, $B(E)$, versus the electric field which allows us to calculate the parameter β [8]. For the 1% HPC solution we obtain a slope of 0.4, in good agreement with the value obtained using the more classical log–log plot (Fig. 5d). For the 0.4%, 0.2% and 0.1% HPC solutions, the slope is 0.3, 0.27 and 0.07, respectively. In no case could we observe a square dependence of $B(E)$ on the field, as would be predicted by the biased reptation model without fluctuations (Eq. 6).

4.4. Ogston model

We also plotted the data for the lowest and highest HPC concentrations (0.1% and 1%) as log μ versus N (Fig. 7), in order to compare them with the predictions of the Ogston model. In both cases, considerable curvature is obtained

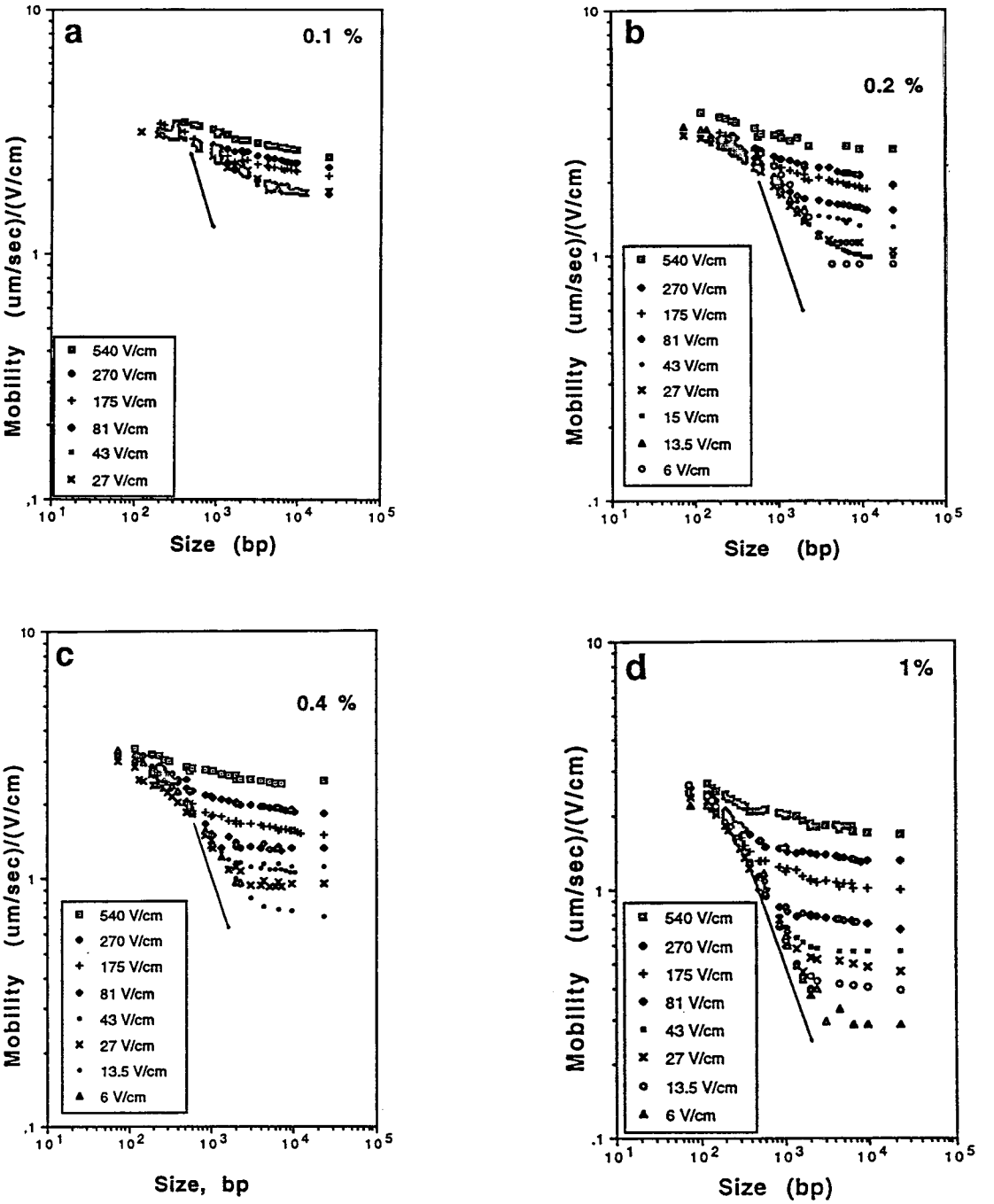

Fig. 4. Dependence of the electrophoretic mobility of linear double-stranded DNA fragments on the molecular mass in (a) 0.1, (b) 0.2, (c) 0.4 and (d) 1% HPC solutions at different electric field strengths in 1 × TBE containing 10 μM ethidium bromide at 25°C. The lines have a slope of −1.

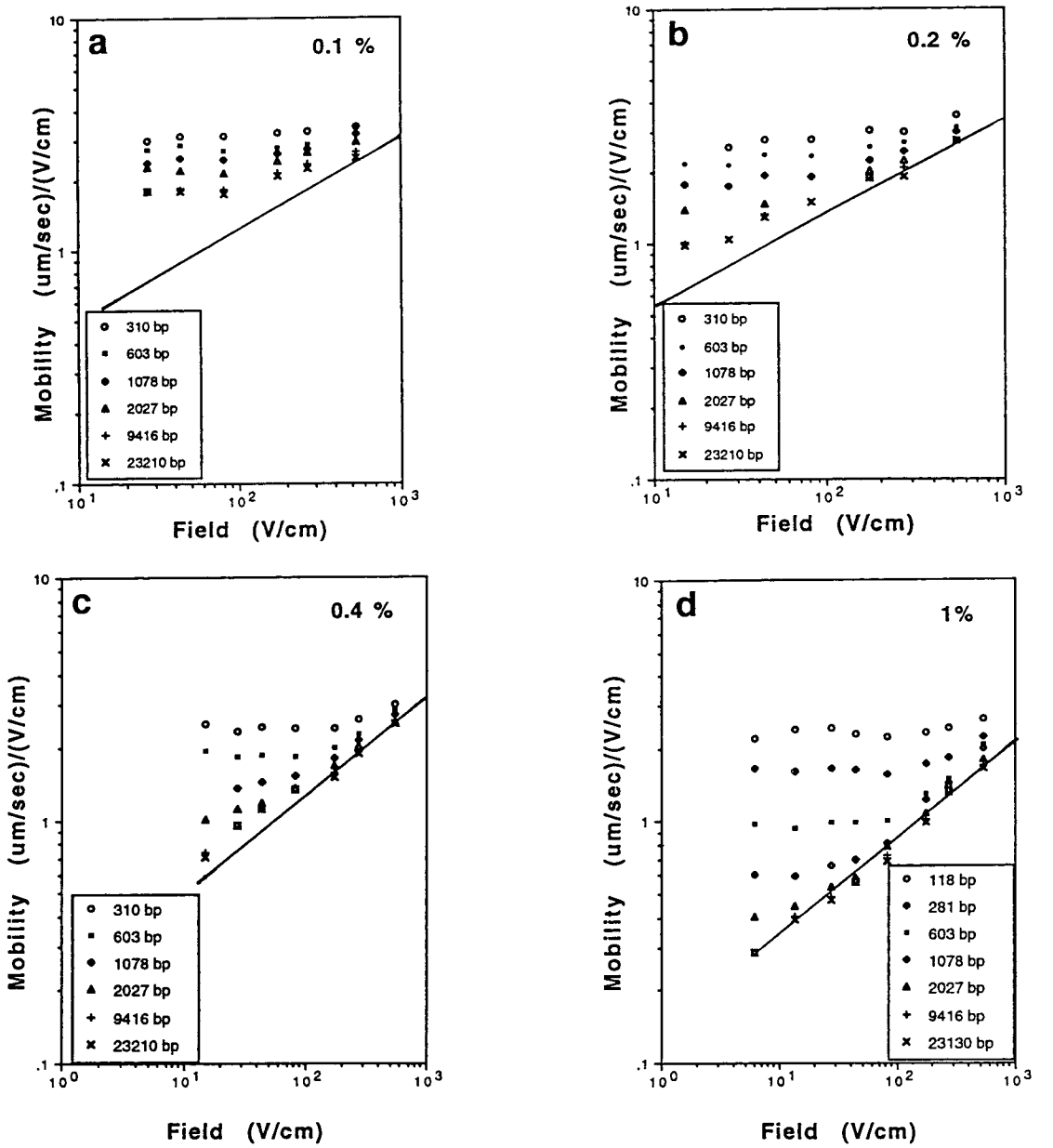

Fig. 5. Dependence of the electrophoretic mobility of linear double-stranded DNA fragments on the electric field in (a) 0.1, (b) 0.2, (c) 0.4 and (d) 1% HPC. The lines have a slope of 0.4. Same conditions as in Fig. 4.

above a critical size smaller than 1 kbp, confirming that the Ogston model does not describe the mobility of DNA better in polymer solutions than it does in gels. Only the mobility of the smallest fragments yields approximately a straight line. The deviation from linearity occurs at around 500 bp in 1% HPC and around 1 kbp in 0.1% HPC solution.

It is worth pointing out that, even for small DNA, only the data obtained at 1% HPC show a

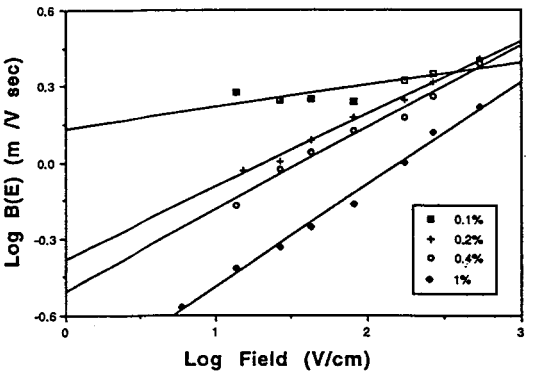

Fig. 6. Log–log plot of $B(E)$ versus electric field.

mobility independent of the electric field (as it should be according to the Ogston model). For low concentrations, the mobility depends on the electric field for large fields. This behaviour, which is not predicted by the Ogston model, suggests that the mobility of the DNA may in part be determined by the mobile nature of the obstacles ("constraint release").

4.5. Quantitative comparison with reptation and constraint release models

One important advantage of reptation and constraint release models is that they involve only molecular parameters with a clear significance. The mobility can in principle be predicted without any adjustable parameter, using only independently measured quantities. This is obviously an ambitious goal, because theoretical modelling always involves oversimplifications. However, we believe that a semi-quantitative agreement obtained in such conditions is a more stringent and more convincing test than a quantitative agreement obtained with several adjustable parameters.

For the BRF, four parameters are needed: the mobility of the DNA in free solution, μ_0, its Kuhn length (twice the persistence length), b, the effective charge of the DNA per Kuhn segment, q_k, and the pore size of the separating matrix, ξ.

The Kuhn length of duplex DNA varies with the ionic strength of the buffer. In 1 × TBE, it is equal to 100 ± 20 nm (or around 300 base pairs). From several experiments, and in particular from videomicroscopic measurements of chain stretching under the influence of an electric field [14], the effective charge is now evaluated as typically 0.1 ± 0.05 e$^-$ per base pair. Using the definition of ε_0, this yields $\varepsilon_0/E \approx 1.2 \cdot 10^{-2}$ cm/V.

In our case, the effective pore sizes ξ_b, evaluated using Eqs. 2 and 3, are 185, 110, 65 and 32 nm for 0.1, 0.2, 0.4 and 1% HPC, respectively. The corresponding values of $\bar{\xi}$ are 1.85, 1.10, 0.65 and 0.32. This suggests that for $c > 0.2\%$, our experiments correspond to the regime in

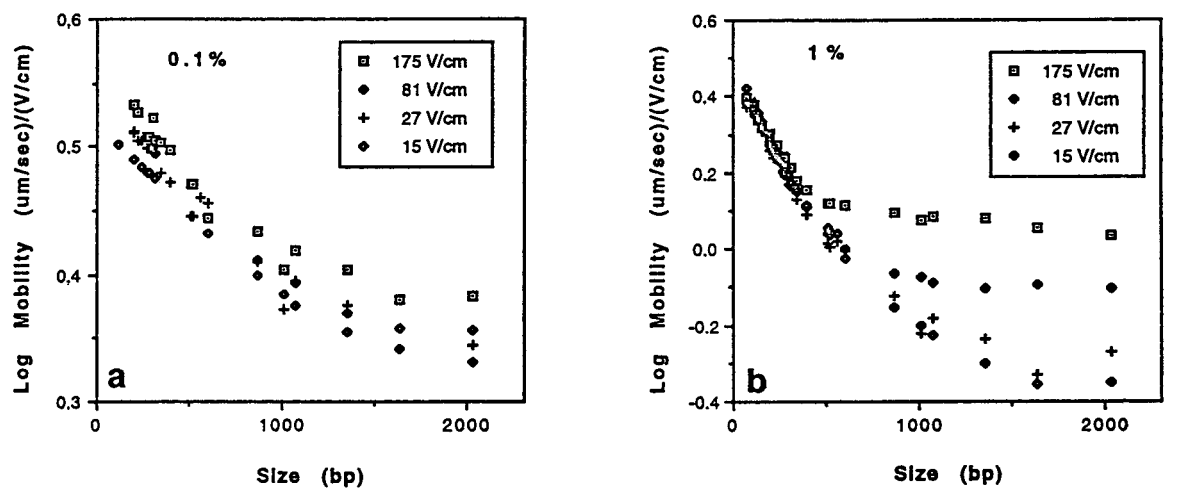

Fig. 7. Log–linear plot of the mobility of DNA versus molecular size. (a) 0.1% and (b) 1% HPC.

which the pore size is smaller than the Kuhn length of DNA (Eqs. 9–12).

The absolute mobility in free solution, μ_0, was evaluated from experiments by Olivera et al. [15]. In 1 × TBE, it should be around 3 ± 0.5 10^{-4} cm^2/V·s. Inserting this values in Eq. 9, one obtains, in the linear regime (i.e. $N_k < N_k^*$),

$$\mu_{theor,lin} \approx (1/N_k) \cdot 10^{-4} \text{ cm}^2/\text{V} \cdot \text{s} \quad (15)$$

In the double logarithmic mobility versus size plot, this regime can be associated with the portion in which the mobility is independent of field and inversely proportional to size (slope −1). In 1% solutions, where gel electrophoresis theories are most likely to apply, we find from Fig. 4d,

$$\mu_{exp,lin} \approx (1/N_k) \cdot 2 \cdot 10^{-4} \text{ cm}^2/\text{V} \cdot \text{s} \quad (16)$$

Considering that the numerical prefactors in the reptation theory are not well known, this is a fairly good agreement.

In the non-linear regime (i.e. $N_k > N_k^*$), the theory predicts a plateau mobility, which is indeed observed. The field dependence of this plateau when $\bar{\xi} < 1$ is expected to be complex, as can be seen from Eqs. 10–12. Using the absolute parameters for μ_0, ε_0/E and $\bar{\xi}$ determined independently, one expects the mobility to be proportional to E when $\varepsilon_0 < \bar{\xi}^{3/2}$ (i.e. $E < 45$ V/cm at 0.4% and $E < 15$ V/cm at 1% HPC), proportional to $E^{2/5}$ for $\bar{\xi}^{3/2} < \varepsilon_0 < \bar{\xi}^{-1}$ (i.e. 45 V/cm $< E <$ 130 V/cm at 0.4% and $15 < E < 240$ V/cm at 1% HPC) and proportional to E^2 (i.e. $E > 130$ V/cm and $E > 240$ V/cm, respectively). Experiments (for 1% HPC) show that the mobility is proportional to $E^{0.4}$ for the whole range, i.e., from 6 to 540 V/cm (Fig. 5d). This is in reasonable agreement with the theoretical predictions.

Finally, it is worth pointing out that the absolute values of the mobility of long DNA that can be predicted from Eq. 11 using the above-mentioned values of ε_0, $\bar{\xi}$ and μ_0 (not shown) are about three (for 1% HPC) to ten times (for 0.4% HPC) smaller than the measured values (Fig. 5c and d). It is unlikely that this discrepancy is due only to the poor knowledge of prefactors in the theory, because the BRF model was able to predict the absolute mobility in agarose gel electrophoresis within a factor of about two [16]. More probably, this discrepancy is due to the labile nature of the obstacles in a polymer solution as compared with permanent gels, i.e., to constraint release processes. Viovy and Duke [4] proposed a linear theory of constraint release and derived an expression for the constraint release mobility in terms of molecular parameters (Eq. 13). When the values of c/c^* and $\bar{\xi}$ are introduced into this expression, however, one finds a mobility which is still smaller than that observed experimentally, and which depends much more strongly on the concentration than observed experimentally. Moreover, the constraint release mobility predicted by the theory is independent of the field strength and of the molecular mass of the DNA, whereas the measured mobility depends on E and also depends weakly on the DNA size for strong fields. We conclude that the constraint release theory used in the currently available models [4], which neglects deformations of the polymer matrix by the DNA, and coupling between the DNA dynamics and the matrix dynamics, cannot account for the observed discrepancy between the predicted and measured values of the absolute mobility of large DNA. To try to understand the actual mechanism at play in these separations, we turned to a very different set-up, in which the molecules themselves can be observed in the course of migration.

4.6. Microscopic observations

The existence of an original migration mechanism at a polymer concentration around c^* was confirmed by the direct videomicroscopic observation of DNA molecules in the course of migration. In free liquid, molecules migrate in a random coil conformation (Fig. 8b) essentially identical with that which they adopt in the absence of field (Fig. 8a). Strikingly, however, at concentrations below c^*, molecules can become significantly extended, and often adopt U-shapes reminiscent of those observed in real gels [17] (Fig. 9). The DNA molecules progressively slide

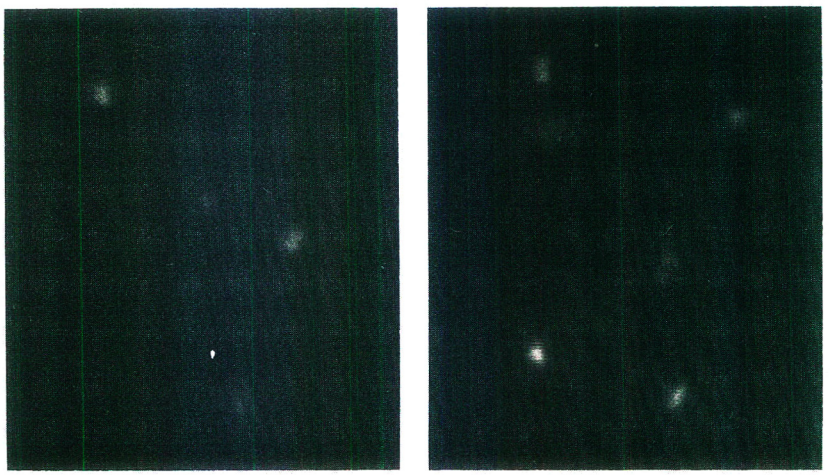

Fig. 8. Microscopic observation of Lambda DNA molecules. Conditions: (left) conformation in free liquid in the absence of field; (right) migration in free liquid at $E = 10$ V/cm. In both cases, the DNA molecules adopt a random coil conformation.

along their own contour to yield J-shapes, and finally adopt an extended conformation again. There are two differences between the U shapes observed in solutions below c^* and in gels, however. First, the conformations in polymer solutions are more open than in gels. Second, the top of the U (or the "pulley" around which the DNA slides) is itself moving downfield while the DNA disengages from it, whereas in gels it is immobile. The relative velocity of this downfield motion compared with that of the sliding motion decreases when the concentration of the polymer solution is increased. These qualitative observations are compatible with a mechanism in which the DNA molecule has to slide its way among the polymer obstacles, but also deforms and drag them along at the same time. This would also explain why the mobility observed in polymer

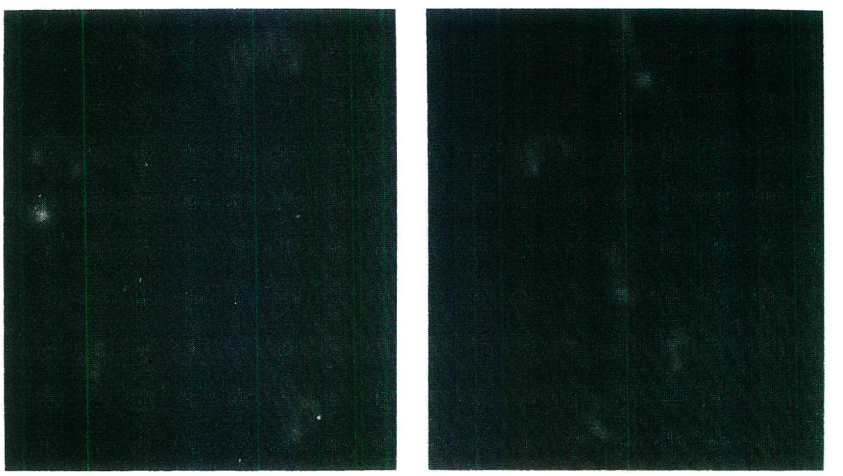

Fig. 9. Microscopic observation of Lambda DNA molecules in a 0.2% HPC solution at $E = 10$ V/cm. The two photographs display the same portion of the cell at different times, showing examples of U-shapes, J-shapes and extended conformations adopted by the molecules.

solutions is larger than predicted by the linear reptation and constraint release models, and why it depends on the electric field (the stronger is the field, and the more the DNA is able to deform the matrix). This dragging along of polymers is similar to the "entanglement coupling" mechanism recently proposed by Barron et al. [18] for dilute solutions, but the additional curvilinear sliding of DNA complicates the mechanism.

5. Conclusions

We performed a systematic study of the migration and separation properties of DNA in a high-molecular-mass water-soluble polymer, hydroxypropylcellulose. This study considered the effect of concentration, going well into the entangled regime, and the effect of the field strength over two orders of magnitude. The results were compared with theoretical predictions. For the first time in CE in non-gel media, we could observe regimes qualitatively consistent with the migration mechanism known in gel electrophoresis [biased reptation with fluctuations (BRF)]. This is probably due to the fact that we used an unusually large polymer at a high concentration (about four times the overlap concentration, c^*) and low electric fields. We demonstrated that such highly entangled solutions are able to provide a better resolution than more dilute ones, although on a narrower range of sizes. Our results also confirm that even unentangled solutions can separate DNA, as demonstrated recently by Barron et al. [18]. The choice of highly entangled or dilute solutions for a given application, essentially depends on the range of sizes to be separated and on the quality of the resolution required: dilute solutions are better for low resolution over a wide range, and entangled solutions for high resolution over a narrow range. Our results also point out the limited success of existing theories for describing electrophoresis in polymer solutions and suggest a new mechanism of migration, which combines a sliding of DNA molecules around obstacles and a dragging of these obstacles by the DNA. Theoretical work is in progress to describe the mobility of DNA in unentangled or weakly entangled polymer solutions [19].

Acknowledgements

This work was partly supported by Beckman France and by an EC (DG XII) "Human Genome" grant, No. CT93-0018. We thank Xavier Chaudot and Emmanuel Nonnet for their assistance.

References

[1] M. Strege and A. Lagu, Anal. Chem., 63 (1991) 1233.
[2] M. Chiari, M. Nesi and P.G. Righetti, J. Chromatogr. A, 652 (1993) 31.
[3] P.D. Grossman and D.S. Soane, Biopolymers, 31 (1991) 1221.
[4] J.L. Viovy and T.A.J. Duke, Electrophoresis 14 (1993) 322 (note that Eqs. 10 and 12 in this paper contain erroneous numerical prefactors; Eqs. 1 and 2 in the present paper contain the correct prefactors).
[5] M. Doi and S.F. Edwards, The Theory of Polymer Dynamics, Clarendon Press, Oxford, 1986.
[6] D. Broseta, L. Leibler, A. Lapp and C. Strazielle, Europhys. Lett., 2 (1986) 733.
[7] A.G. Ogston, Trans. Faraday Soc., 54 (1958) 1754.
[8] P. Mayer, G.W. Slater and G. Drouin, Appl. Theor. Electrophoresis, 3 (1993) 147.
[9] T.A.J. Duke, J.L. Viovy and A.N. Semenov, Biopolymers, 34 (1994) 239.
[10] W.L. Fangman, Nucleic Acids Res., 3 (1978) 653.
[11] H. Hervet and C. Bean, Biopolymers, 26 (1987) 727.
[12] C. Heller, T. Duke and J.L. Viovy, Biopolymers, 34 (1994) 249.
[13] L. Mitnik, J.L. Viovy and L. Salomé, paper presented at the 33rd IUPAC Microsymposium on Optics and Dynamics of Polymers, Prague, July 1993.
[14] S.B. Smith and A.J. Bendich, Biopolymers, 29 (1990) 1167.
[15] B.M. Olivera, P. Baine and N. Davidson, Biopolymers, 2 (1964) 245.
[16] M.S. Hutson, G. Holzwarth, T. Duke and J.L. Viovy, Biopolymers, 35 (1995) 297.
[17] C. Bustamante, Annu. Rev. Biophys. Biophys. Chem., 20 (1991) 415.
[18] A.E. Barron, D.S. Soane and H.W. Blanch, J. Chromatogr. A, 652 (1993) 3.
[19] G.W. Slater, et al., in preparation.

ELSEVIER

Journal of Chromatography A, 710 (1995) 323–329

JOURNAL OF CHROMATOGRAPHY A

Separation of coumarins by micellar electrokinetic capillary chromatography

Cherng-Tsern Chen, Shuenn-Jyi Sheu*

Department of Chemistry, National Taiwan Normal University, 88, Sec. 4, Tingchow Road, Taipei, Taiwan

First received 13 February 1995; revised manuscript received 24 April 1995; accepted 24 April 1995

Abstract

Nine coumarins were successfully separated simultaneously using micellar electrokinetic capillary chromatography with 4-hydroxybenzoic acid as an internal standard. A carrier composed of buffer solution (20 m*M* sodium dodecyl sulfate–15 m*M* sodium borate–15 m*M* sodium dihydrogenphosphate)–acetonitrile (24:1) was found to be the most suitable electrolyte for this separation. The analysis time (22 min) was shorter than that using high-performance liquid chromatography (47 min). Contents of coumarins in the crude drug of Angelicae Tuhou Radix could be easily determined by the proposed method.

1. Introduction

Coumarins commonly exist in over 100 plant families, predominantly among the higher plants [1]. It is common to encounter species, especially the Guttiferae, Rutaceae and Umbelliferae, that contain 10, 20, or even more coumarins and of which four or five from the same species have often been reported. Angelicae Tuhou Radix is derived from the root of Umbelliferae plants, including *Angelica laxifora* Diels, *A. megaphylla* Diels and *A. pubescens* Maxim. [2]. Coumarins are their major components and about 20 kinds have been identified [3–15]. Several methods have been established to determine one or two coumarins contained in this crude drug, such as TLC–densitometry [16], high-performance liquid chromatography (HPLC) [17] and gas chromatography [18].

Micellar electrokinetic capillary chromatography (MEKC) was first reported by Terabe et al. [19] in 1984, and has been applied successfully to both charged and neutral compounds of some Chinese herbs [20,21]. Here we describe an application of MEKC to the separation of the coumarins most commonly contained in Angelicae Tuhou Radix, such as coumarin (**1**) umbelliferone (**2**), columbianetin (**3**), psoralen (**4**), xanthotoxin (**5**), bergapten (**6**), columbianetin acetate (**7**), osthol (**8**) and columbianadin (**9**) (Fig. 1). An HPLC method for simultaneous determination of these nine coumarins was also developed and compared.

2. Experimental

2.1. Reagents and materials

Columbianetin, columbianetin acetate, osthol and columbianadin were isolated from Angelicae Tuhou Radix [6,10]. Umbelliferone, coumarin,

* Corresponding author.

0021-9673/95/$09.50
SSDI 0021-9673(95)00509-9

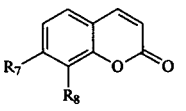

	R_7	R_8	
1	H	H	coumarin
2	OH	H	umbelliferone
8	OCH_3	CH_2-CH=$C(CH_3)_2$	osthol

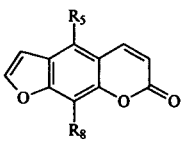

	R_5	R_8	
4	H	H	psoralen
5	H	OCH_3	xanthotoxin
6	OCH_3	H	bergapten

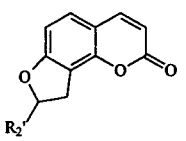

	$R_{2'}$	
3	$C(OH)(CH_3)_2$	columbianetin
7	$C(O\text{-}CO\text{-}CH_3)(CH_3)_2$	columbianetin acetate
9	$C(O\text{-}CO\text{-}C(CH_3)=CHCH_3)(CH_3)_2$	columbianadin

Fig. 1. Structures of the coumarins studied.

psoralen, xanthotoxin and bergapten were purchased from Aldrich (Milwaukee, WI, USA), 4-hydroxybenzoic acid from Merck (Darmstadt, Germany), sodium dodecyl sulfate (SDS) from Sigma (St. Louis, MO, USA), sodium borate from Nakarai Chemicals (Kyoto, Japan) and sodium dihydrogenphosphate from Kanto (Tokyo, Japan). Angelicae Tuhou Radix was obtained from the Chinese herbal market in Taipei (Taiwan). Acetonitrile and methanol of LC grade were obtained from Mallinckrodt (Paris, KY, USA). Deionized water was provided by a Milli-Q water-purification system (Millipore, Bedford, MA, USA).

2.2. Apparatus and conditions

MEKC analysis was carried out on a Spectra Phoresis 1000 capillary electrophoresis system (Spectra-Physics, San Jose, CA, USA) equipped with a UV detector set at 200 nm and a 67.5 cm × 50 μm I.D. fused-silica capillary tube (Polymicro Technologies, Phoenix, AZ, USA) with the detection window placed at 59.5 cm. The conditions were as follows: injection mode, hydrodynamic; injection time, 2 s; run time, 25 min; applied voltage, 20 kV (constant voltage, positive to negative polarity); cartridge temperature, 30°C. The electrolyte was buffer solution [20 m*M* sodium dodecyl sulfate (SDS)–15 m*M* sodium borate–15 m*M* sodium dihydrogenphosphate (pH 8.26)]–acetonitrile (24:1). The capillary was washed with 0.1 *M* NaOH for 3 min, deionized water for 3 min and buffer for 3 min before each run and washed with deionized water for 3 min after each run.

HPLC analysis was performed on a Waters (Milford, MA, USA) HPLC system consisting of two Model 510 pumps, a U6K injector, a Model 680 automated gradient controller and a Model 990 photodiode-array detector set at 322 nm. Satisfactory separation of the coumarins was achieved on a Cosmosil $5C_{18}$-AR column (250 mm × 4.6 mm I.D., particle size 5 μm) (Nacalai Tesque), which was eluted with a linear gradient of solvent A [H_2O–CH_3CN (8:2)] and solvent B [H_2O–CH_3CN–CH_3OH (2:9:9)] according to the following profile: 0–40 min, 100–0% A (0–100% B) and 40–50 min, 100% B. The flow-rate was maintained at 0.6 ml/min.

2.3. Preparation of Angelicae Tuhou Radix extract

A 1.00 g sample of powdered Angelicae Tuhou Radix was extracted with 70% methanol (5 ml) by refluxing for 10 min, then centrifuged at 1500 *g* for 5 min. Extraction was repeated three times. The extracts were combined and filtered through a No. 1 filter-paper. After the addition of 2.00 ml of internal standard solution (2 mg of 4-hydroxybenzoic acid in 1 ml of 70% methanol), the Angelicae Tuhou Radix extract was diluted to 25 ml with 70% methanol.

3. Results and discussion

3.1. HPLC method

It is very common to assay coumarins by HPLC. Thompson and Brown [22] used seven

solvent systems in sequence to separate a total of 67 coumarins [22] and Vande Casteele et al. [23] utilized a combination of isocratic and linear-gradient elution to separate 43 coumarins. However, the previous HPLC methods could not be easily applied to the simultaneously separation of the nine coumarins selected.

A preliminary experiment was first conducted with isocratic elution using 60% and 50% acetonitrile at a flow-rate of 0.6 ml/min. In both instances, the nine compounds gave only eight peaks, compounds **4** and **5** being completely overlapped. At 60% acetonitrile, the analysis could be accomplished within 20 min but the peaks of **2** and **3** were too close together. With 50% acetonitrile, a good separation of **1–3** and **6–9** could be obtained; the elution time was 42 min and peaks **8** and **9** were broad. After a series of experiments, it was found that linear-gradient elution with the profile given in Section 2.2 separated all the coumarins well. Fig. 2a shows the separation of the authentic coumarins with the following retention times: **2**, 17.8; **1**, 25.1; **3**, 25.7; **4**, 30.9; **5**, 31.5; **6**, 35.0; **7**, 37.5; **8**, 45.1 and **9**, 46.0 min. It is noticeable that a marked change in retention times was obtained with only slight variations of mobile phase composition. When the water–acetonitrile component of solvent B was changed to 1:9 and solvent A kept constant, the retention times of the coumarins were as follows: **2**, 16.8; **3**, 23.5; **1**, 23.7; **4**, 28.2; **5**, 28.6; **6**, 31.2; **7**, 33.4; **8**, 40.3; and **9**, 41.5 min. Thus not only was a much worse resolution of **4** and **5** obtained, but also a completely overlapped peak for **1** and **3** was found.

3.2. MEKC method

All nine coumarins and 4-hydroxybenzoic acid (internal standard) were successfully determined in a single run by MEKC under suitable conditions. The separation was achieved by optimizing the cartridge temperature, the applied voltage and the concentrations of SDS, organic modifier and buffer.

Cartridge temperatures of 20, 25, 28, 30, 35, 40 and 45°C and applied voltages of 15, 18, 20, 22, 25 and 28 kV were studied. Values of 30°C and 20 kV were chosen, because longer migration times and broader peak widths were ob-

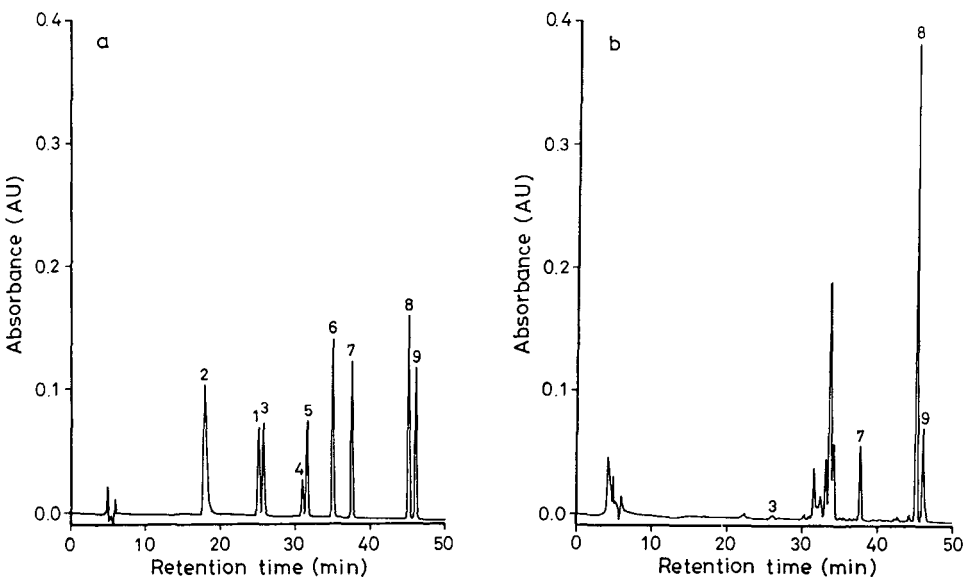

Fig. 2. HPLC of (a) a mixture of nine authentic coumarins and (b) an extract of Angelicae Tuhou Radix. Column: Cosmosil $5C_{18}$-AR (250 mm × 4.6 mm I.D., particle size 5 μm). Eluents: solvent A, H_2O–CH_3CN (8:2); solvent B, H_2O–CH_3CN–CH_3OH (2:9:9). Elution profile: 0–40 min, 100–0% A (0–100% B); 40–50 min, 100% B. Detection: UV at 322 nm. Peak numbers as in Fig. 1.

tained with lower values and a poorer resolution for the test solution was found with higher values.

Preliminary experiments were first carried out using 15 m*M* $Na_2B_4O_7$ and 15 m*M* NaH_2PO_4 without SDS in the electrophoretic medium. In this case, all courmarins except umbelliferone migrated with the electroosmotic flow (EOF), indicating that all the eight coumarins possess neutral and similar properties under such conditions. However, with SDS, the components in the mixture sample can be separated on the basis of their relative affinities for the micellar environment against the bulk aqueous phase. In order to study the effect of SDS concentration on the separability, seven electrolyte systems containing different SDS concentrations (0, 5, 10, 20, 30, 40 and 50 m*M*) were used. The results obtained are shown in Fig. 3. The migration times of all the compounds became longer as the SDS concentration increased. At 20 m*M* SDS, most peaks were separated very well except for **3** and **4**, which slightly overlapped. At lower concentrations (5 or 10 m*M*), **3** and **4** completely overlapped. At higher concentrations (30, 40 or 50 m*M*), the resolution between **8** and **9** became poorer. The resolution values (R_s) between **8** and **9** were 1.54, 0.67, 0.51 and 0.37 when 20, 30, 40 and 50 m*M* SDS were used, respectively.

It is known that the addition of organic modifier to the buffer solution can greatly improve

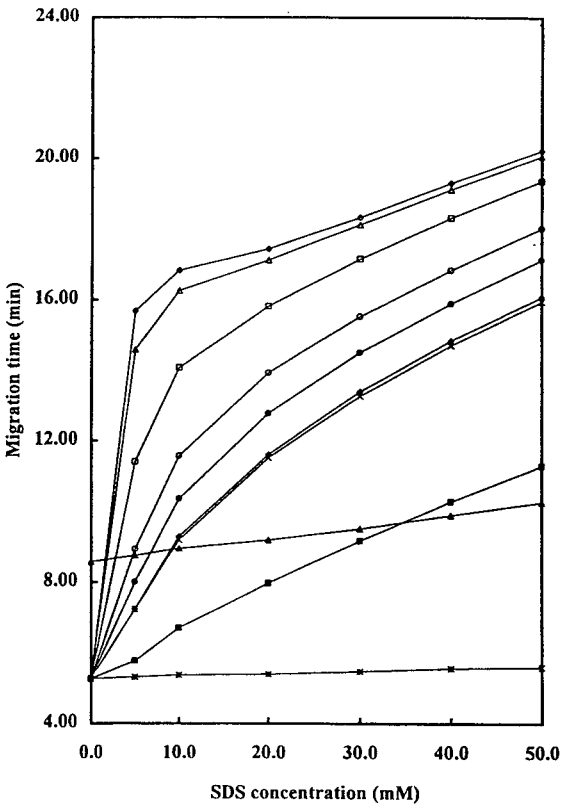

Fig. 3. Effect of SDS concentration on migration time. Electrophoretic medium: 0–50 m*M* SDS–15 m*M* $Na_2B_4O_7$–15 m*M* NaH_2PO_4. Capillary: 67.5 cm (59.5 cm to detector) × 50 μm I.D. Applied voltage: 20 kV. Cartridge temperature: 30°C. Detection: UV at 200 nm. * = EOF; ■ = **1**; ▲ = **2**; ◆ = **3**; × = **4**; ● = **5**; ○ = **6**; □ = **7**; △ = **8**; ◇ = **9**.

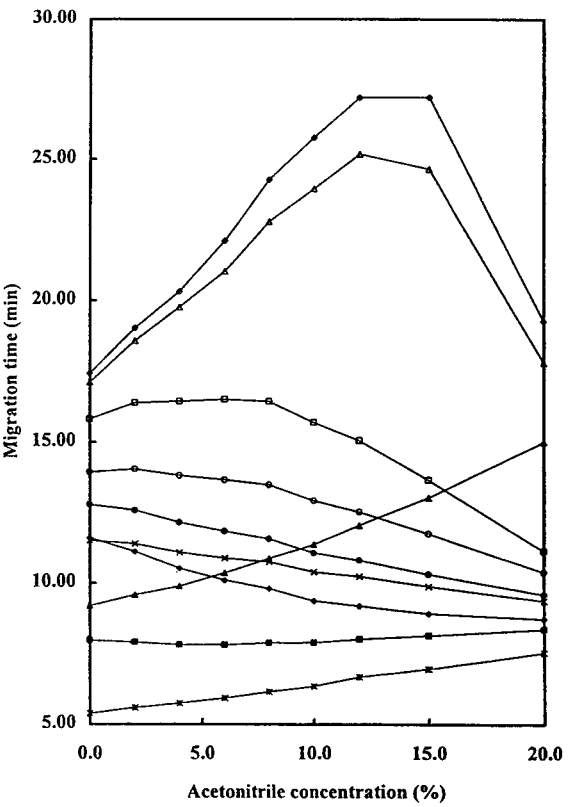

Fig. 4. Effect of CH_3CN concentration on migration time. Electrophoretic medium: mixture of 0–20% CH_3CN with a buffer of 20 m*M* SDS–15 m*M* $Na_2B_4O_7$–15 m*M* NaH_2PO_4. Other conditions and symbols as in Fig. 3.

the resolution of the solutes. Fig. 4 shows the effect of acetonitrile concentration (0–20%) on the selectivity of the separation. The electroosmotic flow decreases with increasing acetonitrile concentration. The migration times would be longer when the factor causing the decrease in electroosmotic flow was dominant. On the other hand, the migration times would become shorter if the factor lessening the interaction between solute and micelles was dominant. Fig. 4 indicates that the migration times of **2**, **8** and **9** became longer and those of **3**–**6** became shorter as the acetonitrile concentration was increased from 0 to 12%. At 20% acetonitrile, the migration times of most compounds became much shorter owing to the latter factor being completely dominant. In addition, the resolution between **3** and **4** was obviously improved when acetonitrile was added. The R_s values between **3** and **4** were 1.54, 2.10 and 3.42 when 0, 2 and 4% of acetonitrile were used, respectively. At 4% acetonitrile, **3** and **4** could be completely separated.

The buffer concentration and the pH of the electrophoretic medium are two other governing factors in separation. After a series of experiments, it was found that a solution consisting of 15 m*M* $Na_2B_4O_7$–15 m*M* NaH_2PO_4 (pH 8.26) was the optimum, and an electrolyte consisting of buffer solution (20 m*M* SDS–15 m*M* $Na_2B_4O_7$–15 m*M* NaH_2PO_4)–acetonitrile (24:1) was found to give the best resolution. Fig. 5a is an electropherogram showing the separation of the nine coumarins with the following migration times and plate numbers: **1**, 7.5 min, $3.04 \cdot 10^4$; **2**, 9.6 min, $2.76 \cdot 10^5$; **3**, 10.4 min, $1.10 \cdot 10^5$; **4**, 10.9 min, $9.96 \cdot 10^4$; I.S., 11.4 min, $8.61 \cdot 10^4$; **5**, 12.1 min, $1.08 \cdot 10^5$; **6**, 13.9 min, $9.52 \cdot 10^4$; **7**, 16.8 min, $1.10 \cdot 10^5$; **8**, 20.3 min, $4.42 \cdot 10^4$; and **9**, 21.0 min, $1.02 \cdot 10^5$.

3.3. Method validation

The λ_{max} of most coumarins is around 200 nm, which can be used as the detection wavelength for MEKC measurements but not for HPLC owing to a serious cut-off from the eluent in this region. A wavelength of 322 nm, another absorption maximum for **2**, **3**, **7**, **8** and **9** in UV

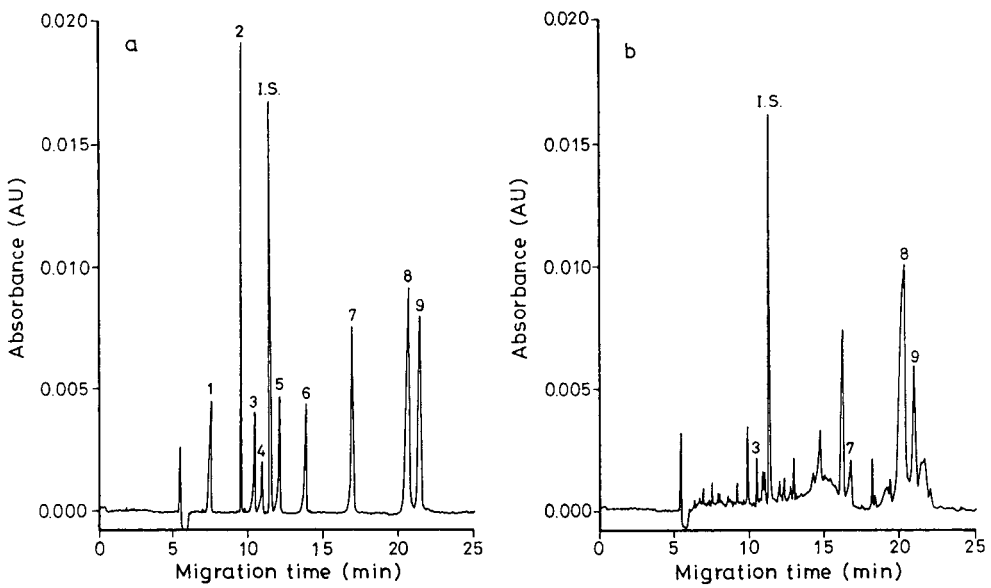

Fig. 5. Capillary electropherograms of (a) a mixture of nine authentic coumarins and (b) an extract of Angelicae Tuhou Radix. Electrophoretic medium: buffer (20 m*M* SDS–15 m*M* $Na_2B_4O_7$–15 m*M* NaH_2PO_4)–CH_3CN (96:4). Capillary: 67.5 cm (59.5 cm to detector) × 50 μm I.D. Applied voltage: 20 kV. Cartridge temperature: 30°C. Detection: UV at 200 nm. Peak numbers as in Fig. 1; I.S. (internal standard) = 4-hydroxybenzoic acid.

spectra, was therefore chosen for the HPLC assay. The sensitivities at 200 nm are about 1.16–3.57 times those of 322 nm. The detection limits (signal-to-noise ratio = 3) of these coumarins in HPLC varied from 0.20 to 0.38 μg/ml (flow cell length 10 mm) and those in MEKC are listed in Table 1.

Linearity

Calibration graphs (peak-area ratio, y, vs. concentration in mg/ml, x) were constructed in the range $9.28 \cdot 10^{-3}$–0.186 mg/ml for **3**, $5.60 \cdot 10^{-3}$–0.112 mg/ml for **4** and $1.60 \cdot 10^{-2}$–0.320 mg/ml for other seven compounds. Linear relationships were found with the correlation coefficients >0.999.

Precision

The reproducibility (R.S.D.) of the MEKC method, on the basis of peak-area ratios for six replicate injections, is shown in Table 1. The R.S.D.s of the migration time of each peak for six replicated injections were below 0.65% (intra-day) and 1.35% (inter-day). The R.S.D.s for the HPLC method, on the basis of peak area for six replicate injections, were 0.52–1.76% (intra-day) and 0.63–2.31% (inter-day) and the R.S.D.s of the retention time for six replicated injections were below 0.18% (intra-day) and 0.33% (inter-day).

Table 1
Detection limits and reproducibility of separation of coumarins.

Coumarin	Detection limit (μg/ml)	R.S.D. (%) ($n = 6$)	
		Intra-day	Inter-day
1	3.93	1.05	1.44
2	1.60	0.61	0.90
3	4.08	1.42	1.45
4	2.80	1.86	2.43
5	3.82	1.31	2.00
6	3.67	1.27	1.40
7	2.29	1.79	2.59
8	2.57	2.37	3.94
9	3.89	0.77	1.89

Accuracy

Suitable amounts of the nine coumarins were added to a standard solution with known concentrations of components and analysed using the proposed procedure. The recoveries of all coumarins determined were around 98–103%.

The asymmetry factor was 0.81 for **1**, 1.00 for **2**, 0.79 for **3**, 0.82 for **4**, 1.00 for I.S., 0.88 for **5**, 0.88 for **6**, 0.90 for **7**, 0.91 for **8** and 0.94 for **9**.

3.4. Separation of coumarins in Angelicae Tuhou Radix

When the test solution was analyzed by MEKC under the selected conditions, the electropherogram shown in Fig. 5b was obtained. The peaks were identified by comparison of the migration times and UV spectra with those obtained from authentic samples of the coumarins, and by spiking the mixture with a single coumarin in a subsequent run. It was found that only columbianetin, columbianetin acetate, osthol and columbianadin were present in the extract of Angelicae Tuhou Radix. By substituting the peak-area ratios of the individual peaks for y in the above equations, the contents of the individual coumarins in the test sample were obtained: **3**, 0.36 ± 0.03; **7**, 0.60 ± 0.03; **8**, 3.89 ± 0.20; and **9**, 1.88 ± 0.20 mg/g (mean ± S.D.; $n = 4$). Amounts of 0.25 mg of **3**, 0.24 mg of **7**, 0.97 mg of **8** and 0.56 mg of **9** were added to a sample of Angelicae Tuhou Radix with known concentrations of components and analysed using the proposed procedures. The recoveries of these coumarins determined were around 97–110%.

The test solution was also analysed by HPLC and the chromatogram is shown in Fig. 2b. A smoother baseline and much better resolution of **8** and **9** than those obtained by MEKC were obtained, but no separated peaks were observed in the 30–35-min region. Therefore, it is very difficult to ascertain whether or not **4** and **5** were present in the crude extract using the HPLC method.

In conclusion, the coumarins in crude drug extracts could be successfully determined either by MEKC or HPLC. The MEKC method gives a

shorter run time (MEKC, 22 min; HPLC, 47 min) and can provide better resolution for **4** and **5**, if present, but shows worse baseline noise and gives a lower resolution for **8** and **9**.

Acknowledgement

Financial support from the National Science Council, Republic of China, is gratefully acknowledged (NSC 83-0208-M003-001).

References

[1] R.D.H. Murray, J. Méndez and S.A. Brown, The Natural Coumarins, Wiley, Chichester, 1982.
[2] H.Y. Hsu, Y.P. Chen, S.J. Sheu, C.H. Hsu, C.C. Chen and H.C. Chang, Chinese Materia Medica—A Concise Guide, Modern Drug Press, Taipei, 1985, pp. 244–245.
[3] K. Hata and Y. Tanaka, Yakugaku Zasshi, 77 (1957) 937.
[4] Y. Tanaka, Kinki Daigaku Yakugakubu Kiyo, 4 (1963) 17; C.A., 59 (1963) 14354h.
[5] K. Hata and M. Kozawa, Tetrahedron Lett., 50 (1965) 4557.
[6] K. Hata, M. Kozawa, K. Baba and K.Y. Yen, Chem. Pharm. Bull., 19 (1971) 640.
[7] K. Hata and M. Kozawa, Yakugaku Zasshi, 87 (1967) 210.
[8] K. Hata and M. Kozawa, Yakugaku Zasshi, 88 (1968) 283.
[9] K. Hata and M. Kozawa, Yakugaku Zasshi, 88 (1968) 293.
[10] M. Kozawa, K. Baba, Y. Matsuyama and K. Hata, Chem. Pharm. Bull., 28 (1980) 1782.
[11] K. Hata, T. Nishino, Y. Hirai, Y. Wada and M. Kozawa, Yakugaku Zasshi, 101 (1981) 67.
[12] K. Baba, Y. Matsuyama and M. Kozawa, Chem. Pharm. Bull., 30 (1982) 2025.
[13] S. Chen, H. Zhang, C. Yuan, Y. Deng and G. Chen, Yaoxue Tongbao, 17 (1982) 120; C.A., 97 (1982) 20741y.
[14] S. Chen, H. Zhang, C. Yuan, Y. Deng and G. Chen, Yaoxue Tongbao, 17 (1982) 392; C.A., 97 (1982) 88731a.
[15] J. Pan, K. Lamy, B. Arison, J. Smith and G. Han, Yaoxue Tongbao, 22 (1987) 380; C.A., 107 (1987) 112685m.
[16] X. Li, W. Fang and R. Li, Zhongcaoyao, 21 (1990) 59; C.A., 112 (1990) 185907y.
[17] Z.F. Sha, W.J. Sun, H. Gao and M.L. Miao, Yaoxue Xuebao, 26 (1991) 798; C.A., 116 (1992) 136345n.
[18] H. Gao, W.J. Sun and Z.F. Sha, Yaowu Fenxi Zazhi, 12 (1992) 221; C.A., 117 (1992) 220206w.
[19] S. Terabe, K. Otsuka, K. Ichikawa, A. Tsuchiya and T. Ando, Anal. Chem., 56 (1984) 111.
[20] Y.M. Liu and S.J. Sheu, Anal. Chim. Acta, 288 (1994) 221.
[21] C.F. Lu and S.J. Sheu, Chin. Pharm. J., 45 (1993) 495.
[22] H.J. Thompson and S.A. Brown, J. Chromatogr., 314 (1984) 323.
[23] K. Vande Casteele, H. Geiger and C.F. Van Sumere, J. Chromatogr., 258 (1983) 111.

ELSEVIER

Journal of Chromatography A, 710 (1995) 331–337

JOURNAL OF CHROMATOGRAPHY A

Effect of urea addition on chiral separation of dansylamino acids by capillary zone electrophoresis with cyclodextrins

Masanobu Yoshinaga[a,*], Minoru Tanaka[b]

[a]*Kansai Technical Research Institute, Toppan Printing Co. Ltd., Ebie, Fukushima-ku, Osaka 553, Japan*
[b]*Research Center for Environmental Preservation, Osaka University, Yamada-oka, Suita, Osaka 565, Japan*

First received 6 February 1995; revised manuscript received 3 April 1995; accepted 21 April 1995

Abstract

The chiral separation ability of unmodified and di- and trimethylated α-, β- and γ-cyclodextrins (CDs) as chiral selectors in capillary zone electrophoresis was investigated in the presence of urea derivatives using twelve dansylamino acids as model solutes. The addition of these urea derivatives (unsubstituted, methyl-, ethyl- and 1,3-dimethylureas) produced dramatic enhancement in the enantioselectivity of unmodified β-CD but also reduced the enantioselectivities of the other CDs.

1. Introduction

Capillary zone electrophoresis (CZE) is a technique for the chiral separation of a wide range of ionic and ionizable compounds undergoing rapid development at the present time owing to its rapid run-times, extremely high separation efficiencies, low sample requirements, etc. [1,2]. In order to perform chiral separations, various chiral selectors are added to the CZE running buffers. Unmodified and chemically modified cyclodextrins (CDs) have been successfully utilized for these purposes. Among the various kinds of chemically modified CD derivatives, methylated ones have been widely used as chiral selectors for CZE [3–15].

In previous papers, we reported the chiral separation of dansylamino acids by CZE using unmodified α-, β- and γ-CDs or 2,6-di-methylated and 2,3,6-trimethylated α- and β-CDs [16] and selectively methylated β-CDs [17] as chiral selectors. The chemical modifications of α- and β-CDs produced remarkable changes in their enantioselectivities for the dansylamino acids. In these experiments, the chiral selector concentration was fixed at 10 m*M*, considering the low aqueous solubility of β-CD. The CD concentration is one of the very important factors which affect the CD enantioselectivity [18]. Urea has been utilized to increase the β-CD solution concentration further above its water solubility (ca. 14–16 m*M*) [19,20].

Recently, we found that the chiral separation of the dansylamino acid enantiomers is greatly enhanced by the addition of urea to a running-buffer solution containing unmodified β-CD as the chiral selector. In this paper, we describe the addition of unsubstituted, methylated or ethylated urea to running-buffer solutions for the chiral separation of dansylamino acids as model

* Corresponding author.

0021-9673/95/$09.50
SSDI 0021-9673(95)00501-3

solutes by CZE with unmodified and di- and trimethylated α-, β- and γ-CD derivatives.

2. Experimental

2.1. Apparatus

An Applied Biosystems (Foster City, CA, USA) Model 270A fully automated CZE system was used, with a 72 cm long (50 cm from inlet to detector) × 50 μm I.D. fused-silica capillary. On-column UV detection at 220 nm was performed at the cathodic end of the capillary. The temperature and applied voltage were held constant at 30°C and 20 kV, respectively, unless otherwise specified. Sample solutions (0.2 m*M*) were injected by a vacuum technique (12.7 cmHg pressure difference for 1.0 s) after introducing methanol as a neutral marker to estimate the osmotic flow. Before each run, the capillary was rinsed successively with 0.1 *M* NaOH and the running buffer. Electropherograms were recorded with a Hitachi (Hitachi, Japan) D-2500 Chromato-integrator. All experiments were run in duplicate to ensure reproducibility.

2.2. Reagents

Unmodified α-, β- and γ-CDs were purchased from Ensuiko Seito (Yokohama, Japan), and their 2,6-di-O-methylated and 2,3,6-tri-O-methylated derivatives were prepared by well-known methods [21,22]. After isolation, crude methylated CD derivatives were fractionated by silica-gel column chromatography, using chloroform–methanol as eluents. The methylated CD derivatives thus obtained were characterized by ^{1}H and ^{13}C NMR spectroscopy and fast atom bombardment mass spectrometry (FAB-MS). The di- and trimethylated CDs obtained are denoted by prefixing the unmodified CDs with DM- and TM-, respectively. The composition of the methylated CD derivatives used here for CZE was estimated by FAB-MS and is given in Table 1. Dansylamino acids were obtained from Sigma (St. Louis, MO, USA) and others from Wako (Osaka, Japan).

Table 1
Composition of methylated CD derivatives

CD derivative	Composition (%)[a]			
	$-CH_3$	O	$+CH_3$	$+2CH_3$
DM-γ-CD	0	60.6	30.9	8.5
TM-α-CD	7.5	92.5	0	0
TM-β-CD	8.2	91.8	0	0

[a] O = desired methylated CD; − = under-methylated CD derivative; + = over-methylated CD derivative.

Running buffers were prepared by dissolving each CD at 10 m*M* in 0.1 *M* sodium borate–0.05 *M* sodium phosphate buffer (ionic strength 0.143 *M*). Its pH was fixed at 9.0 in order to run the solutes in their fully ionized forms. The buffer solutions were filtered through a membrane filter after ultrasonication for 10 min prior to use.

3. Results and discussion

3.1. Addition of urea to unmodified β-CD-containing buffers

The extent of separation of the two peaks of a racemate is usually represented by the well-known factor of R_s. However, this R_s does not efficiently give the extent of separation for the poorly resolved peaks, because their width cannot be precisely measured. Therefore, the resolution was expressed as $R' = 100(H - H')/H$, where H and H' are the height of the first peak and that of the valley between the two peaks, respectively. In this definition, the greater the R' value, the better the resolution, and $R' = 100$ represents a baseline separation of the two peaks.

The separation of the enantiomers in this CZE method is based on their inclusion complex formation with CDs. Therefore, it is essential to examine the effect of CD concentration in the running buffer. Since the diameter of β-CD is similar to that of naphthalene, β-CD tightly encapsulates dansylamino acids [23]. Consequently, the effect of the β-CD concentration on

the chiral separation of the dansylamino acids was examined. β-CD could be dissolved even at 40 m*M* in the above-mentioned buffer at pH 9.0. Table 2 gives the chiral separation of the twelve pairs of dansylamino acid enantiomers in the presence of β-CD over a range of 0–40 m*M*. On the whole, the optimum β-CD concentration seems to be in the range of 10–15 m*M*, though dansyl-D,L-α-amino-*n*-butyric acid and -phenylalanine exhibit different behaviours.

The applied voltage is also considered to affect the chiral separation. Therefore, the *R'* values for the dansylamino acids were evaluated by increasing the applied voltage from 10 kV in steps of 5 kV. When 25 kV was applied to the buffer (pH 9.0) in the presence of 10 m*M* β-CD, the electrical current exceeded 80 μA. Based on the *R'* values, this is too high, and a current below ca. 60 μA is preferred. A linear decrease in current with an increase in urea concentration was reported in micellar electrokinetic chromatography [24]. The addition of urea (7 *M*) to the buffer containing 10 m*M* β-CD decreased the current to ca. 30 μA at 20 kV (about half of that observed in the absence of urea) and to ca. 56 μA even at 30 kV, as expected. Table 3 gives the effect of the applied voltage (15–30 kV) on the chiral separation of dansylamino acids in the presence of both 10 m*M* β-CD and 7 *M* urea.

Table 3
Effect of the applied voltage on the chiral separation (*R'* values) of dansylamino acids in the presence of 10 m*M* β-CD and 7 *M* urea (pH 9.0)

Dansylamino acid	Applied voltage (kV)			
	15	20	25	30
α-Amino-*n*-butyric acid	100	98.6	98.5	93.5
Aspartic acid	100	100	100	100
Glutamic acid	100	100	100	100
Leucine	91.3	97.8	99.0	70.9
Methionine	89.3	92.6	94.8	75.6
Norleucine	87.3	93.8	95.0	83.6
Norvaline	90.7	96.8	97.5	79.1
Phenylalanine	85.3	84.8	90.6	50.0
Serine	97.0	98.1	99.2	93.9
Threonine	98.6	100	100	96.5
Tryptophan	43.7	10.5	10.7	27.3
Valine	100	100	100	98.2

Except for dansyl-D,L-α-amino-*n*-butyric acid and -tryptophan, an applied voltage of 20 or 25 kV produced slightly larger *R'* values than those at 15 or 30 kV. Compared with the *R'* values for the buffer containing 10 m*M* β-CD in the absence of urea (Table 2), the addition of 7 *M* urea dramatically enhanced the enantioselectivity of β-CD for the dansylamino acids. Namely, their enantiomers could be completely or nearly

Table 2
Effect of β-CD concentration on the chiral separation (*R'* values) of dansylamino acids (pH 9.0)

Dansylamino acid	Concentration of β-CD (m*M*)						
	0	5	10	15	20	30	40
α-Amino-*n*-butyric acid	0	26.7	9.2	0	0	0	0
Aspartic acid	0	100	100	100	100	100	100
Glutamic acid	0	100	100	97.7	96.6	75.9	26.4
Leucine	0	41.8	52.7	79.3	66.2	53.0	48.7
Methionine	0	12.2	28.0	22.1	2.5	0	0
Norleucine	0	16.3	29.3	59.8	35.8	12.5	2.7
Norvaline	0	28.1	36.7	40.5	30.8	10.5	0
Phenylalanine	0	0	0	0	21.6	32.0	47.2
Serine	0	19.6	28.8	31.6	0	0	0
Threonine	0	80.2	88.1	86.6	79.4	61.6	26.0
Tryptophan	0	0	0	0	0	0	0
Valine	0	68.3	70.8	75.7	53.7	3.1	0

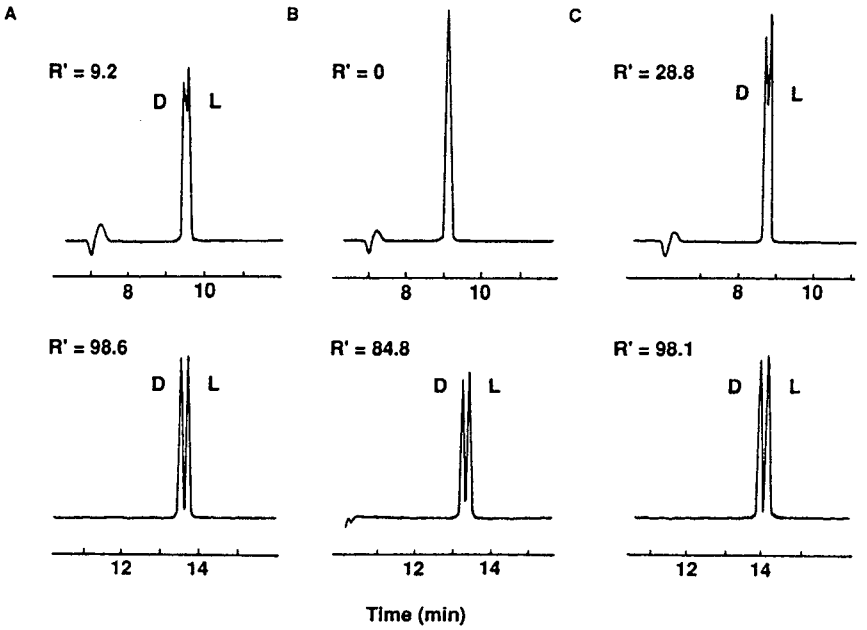

Fig. 1. Chiral separations of (A) dansyl-D,L-α-amino-*n*-butyric acid, (B) dansyl-D,L-phenylalanine and (C) dansyl-D,L-serine with 10 m*M* β-CD before (upper traces) and after (lower traces) the addition of 7 *M* urea.

baseline separated except for dansyl-D,L-tryptophan.

Fig. 1 shows typical electropherograms displaying the dramatic enhancement in the enantioselectivity of β-CD for dansyl-D,L-α-amino-*n*-butyric acid, -phenylalanine and -serine after the addition of 7 *M* urea. In the presence of unmodified β-CD, the D-enantiomer migrated faster than the corresponding L-enantiomer, regardless of the presence of urea. Under the CZE conditions described in the Experimental section, β-CD having no charge is transported toward the negative electrode by electroosmotic flow (V_{eo}). In the absence of β-CD, each negatively-charged dansylamino acid migrates toward the negative electrode with the difference between V_{eo} and its electrophoretic velocity (V_{ep}) being $V_{eo} > V_{ep}$. When included into a β-CD cavity, the solute is transported toward the negative electrode faster, because of the decrease in V_{ep}. This, therefore, indicates that a faster migrating enantiomer interacts more strongly with the β-CD cavity than a slower migrating one.

3.2. Effect of urea on the enantioselectivities of CDs other than β-CD

It is of great interest to investigate the effect of urea addition on the enantioselectivities of the CD derivatives other than the above-mentioned unmodified β-CD. The enhanced effect in the chiral separation with the already mentioned urea increased with an increase in the urea concentration (up to 7 *M* examined). Therefore, it was fixed at 7 *M*, while the CD concentration was fixed at 10 m*M* in further experiments. Table 4 gives the results for unmodified γ-CD, DM-γ-CD, TM-α-CD and TM-β-CD before and after the addition of 7 *M* urea, together with the results for unmodified β-CD already given. Except for dansyl-D,L-phenylalanine, the addition of urea reduced their enantioselectivities in the case of these CDs other than unmodified β-CD, in particular the methylated CD derivatives. The chiral separation of dansyl-D,L-phenylalanine was enormously enhanced by the addition of urea to the buffer solution containing γ-CD (*R'*, from 0 to 100) or DM-γ-CD (*R'*, from 37.3 to 98.0).

Table 4
Effect of urea addition on the chiral separation (R' values) of dansylamino acids (pH 9.0)

Dansylamino acid	Urea (M)									
	β-CD		γ-CD		DM-γ-CD[a]		TM-α-CD		TM-β-CD[a]	
	0	7	0	7	0	7	0	7	0	7
α-Amino-*n*-butyric acid	9.2	98.6	100	96.5	3.7	0	64.2	0	0	0
Aspartic acid	100	100	87.8	0	0	0	0	0	0	0
Glutamic acid	100	100	100	96.1	98.9	0	0	0	0	0
Leucine	52.7	97.8	100	100	0	0	99.2[a]	34.1[a]	100	90.7
Methionine	28.0	92.6	99.2	91.6	76.1	5.7	5.8	0	0	0
Norleucine	29.3	93.8	99.0	100	93.9	68.7	88.1	0	92.7	90.9
Norvaline	36.7	96.8	100	100	7.6	0	0	0	48.0	18.7
Phenylalanine	0	84.8	0	100	37.3	98.0	99.1[a]	20.6[a]	92.1	95.7
Serine	28.8	98.1	0	0	0	0	0	0	0	0
Threonine	88.1	100	100	76.1	16.1	0	0	0	0	0
Tryptophan	0	10.5	0	0	100	100	28.4[a]	0	76.6	0
Valine	70.8	100	99.4	98.6	0	0	43.9	0	38.7	0
Migration time of methanol (min)	7.05	9.79	7.63	10.22	7.35	10.00	7.88	10.67	7.67	10.61

[a] The L-enantiomer is the fast migrating enantiomer.

The dramatic enhancement in the enantioselectivity of unmodified β-CD induced by the addition of urea seems to be a unique behaviour. The reason for this enhanced effect in the chiral separation with urea is not clear at present. The resolution for a pair of enantiomers in CD-modified CZE varies with various parameters, such as the difference in apparent mobility between two enantiomers, their mobilities in the free and complexed forms and the electroosmotic flow. The electroosmotic flow is decreased by the addition of urea, as can be estimated from the migration times of methanol in Table 4. This decreased electroosmotic flow may result in the enhanced enantioselectivity. In the case of unmodified β-CD, the migration-time difference between the D- and L-enantiomers of each solute is larger after the addition of urea. However, this is not necessarily true for the other CDs listed in Table 4. Moreover, the larger time difference does not always bring about a higher enantioselectivity. The R' value for dansyl-D,L-phenylalanine increased from 0 to 84.8 by the addition of urea to the β-CD-containing buffer and also from 0 to 100 by the addition of urea to the γ-CD-containing buffer. It seems to be unlikely that these abrupt increases can be ascribed to only the decreased electroosmotic flow. The urea addition is also considered to affect the complex formation of the enantiomers with CDs. Consequently, in order to convincingly explain the enhanced effect in the chiral separation with urea, further quantitative work is needed.

Neither α-CD nor TM-γ-CD exhibited any enantioselectivity for the dansylamino acids, regardless of the presence of urea. This is ascribed to the weak and/or scarce interaction between the dansylamino acids and α-CD or TM-γ-CD. Both DM-α- and -β-CDs could separate only two dansylamino acid enantiomers.

3.3. Addition of substituted ureas to β-CD

The additional effect of three alkylated ureas (methyl-, ethyl- and 1,3-dimethylurea) on the enantioselectivity of β-CD was also examined. Methylurea at 1, 4 or 7 M was added to the running buffer containing 10 mM β-CD in order to investigate the effect of the methylurea concentration on the enantioselectivity. Fig. 2 shows

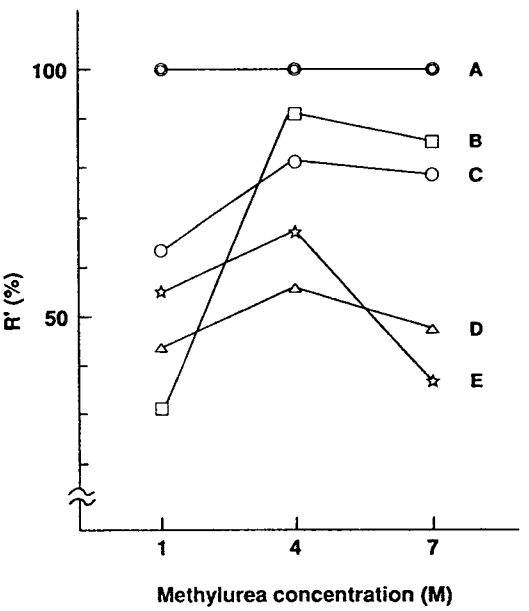

Fig. 2. Effect of methylurea concentration on enantioselectivity of β-CD (10 m*M*). Solutes: A = dansyl-D,L-aspartic acid, B = dansyl-D,L-leucine, C = dansyl-D,L-α-amino-*n*-butyric acid, D = dansyl-D,L-norleucine, E = dansyl-D,L-phenylalanine.

the results for five pairs of the dansylamino acid enantiomers. In the presence of 7 *M* methylurea, the migration time of each solute was more than 40 min and those of dansyl-D,L-aspartic and -glutamic acids exceeded 2 h. Therefore, the concentration of methylurea was fixed at 4 *M*. Table 5 gives the *R'* values for the dansylamino acids after the addition of 4 *M* methyl-, ethyl- or 1,3-dimethylurea to the 10 m*M* β-CD buffer solution. Compared with unsubstituted urea, these alkylated ones produced larger migration times for methanol and the solutes, which means smaller electroosmotic flows. Dansyl-D,L-aspartic and -glutamic acids were not eluted in the presence of 4 *M* ethyl- or 1,3-dimethylurea. Apparently, the addition of these alkylated ureas also enhanced the enantioselectivity of β-CD, as well as the addition of unsubstituted urea.

Fig. 3 shows typical electropherograms for the separations of the dansyl-D,L-leucine and -D,L-threonine enantiomers with 10 m*M* β-CD before and after the addition of 4 *M* 1,3-dimethylurea.

In conclusion, the addition of urea or the alkylated ureas produced a dramatic enhancement in the enantioselectivity of β-CD for dansylamino acid enantiomers. Further detailed work is needed to convincingly explain this increased enantioselectivity of β-CD and the decreased enantioselectivities of the other CDs. The proposed method can separate the dansylamino acid enantiomers but not the racemic dansylamino acids from each other.

Table 5
Effect of the addition of substituted ureas (4 *M*) on the chiral separation (*R'* values) of dansylamino acids in the presence of 10 m*M* β-CD (pH 9.0)

Dansylamino acid	Methylurea	Ethylurea	1,3-Dimethylurea[a]
α-Amino-*n*-butyric acid	81.6	78.0	94.7
Aspartic acid	100	–[b]	–[b]
Glutamic acid	100	–[b]	–[b]
Leucine	91.1	94.1	100
Methionine	45.6	31.0	80.4
Norleucine	56.7	37.1	91.2
Norvaline	59.7	56.1	85.0
Phenylalanine	68.5	55.7	85.3
Serine	74.0	70.2	93.1
Threonine	95.1	94.6	100
Tryptophan	0	0	0
Valine	93.3	94.7	98.3

[a] Applied voltage = 30 kV.
[b] Not eluted.

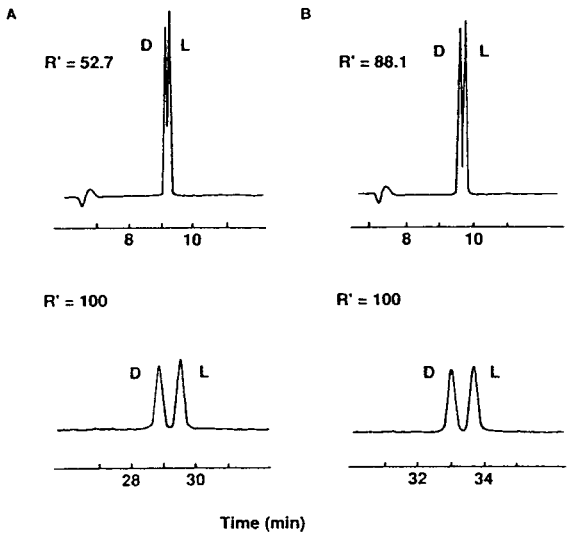

Fig. 3. Chiral separations of (A) dansyl-D,L-leucine and (B) dansyl-D,L-threonine with 10 m*M* β-CD before (upper traces) and after (lower traces) the addition of 4 *M* 1,3-dimethylurea.

More than twenty racemic dansylamino acids have been successfully separated by micellar electrokinetic chromatography using sodium dodecyl sulphate [25,26]. Thus the introduction of sodium dodecyl sulphate to the described β-CD method is of great interest in chiral separation of racemic dansylamino acid mixtures.

References

[1] S.F.Y. Li, Capillary Electrophoresis, Elsevier, Amsterdam, 1992.
[2] P.D. Grossman and J.C. Colburn, Capillary Electrophoresis, Academic, San Diego, CA, 1992.
[3] S. Fanali, J. Chromatogr., 474 (1989) 441–446.
[4] J. Snopek, H. Soini, M. Novotny, E. Smolkova-Keulemansova and I. Jelinek, J. Chromatogr., 559 (1991) 215–222.
[5] T.E. Peterson and D. Trowbridge, J. Chromatogr., 603 (1992) 298–301.
[6] S. Fanali, M. Flieger, N. Steinerova and A. Nardi, Electrophoresis, 13 (1992) 39–43.
[7] P. Gareil, J.P. Gramond and F. Guyon, J. Chromatogr., 615 (1993) 317–325.
[8] T.E. Peterson, J. Chromatogr., 630 (1993) 353–361.
[9] M.W.F. Nielen, Anal. Chem., 65 (1993) 885–893.
[10] S.A.C. Wren and R.C. Rowe, J. Chromatogr., 635 (1993) 113–118.
[11] M. Heuermann and G. Blaschke, J. Chromatogr., 648 (1993) 267–274.
[12] C. Quang and M.G. Khaledi, J. High Resolut. Chromatogr., 17 (1994) 99–101.
[13] S.G. Penn, E.T. Bergström, D.M. Goodall and J.S. Loran, Anal. Chem., 66 (1994) 2866–2873.
[14] I.S. Lurie, R.F.X. Klein, T.A.D. Cason, M.J. LeBelle, R. Brenneisen and R.E. Weinberger, Anal. Chem., 66 (1994) 4019–4026.
[15] H. Nishi, Y. Kokusenya, T. Miyamoto and T. Sato, J. Chromatogr. A, 659 (1994) 449–457.
[16] M. Tanaka, M. Yoshinaga, S. Asano, Y. Yamashoji and Y. Kawaguchi, Fresenius J. Anal. Chem., 343 (1992) 896–900.
[17] M. Yoshinaga and M. Tanaka, J. Chromatogr. A, 679 (1994) 359–365.
[18] S.A.C. Wren and R.C. Rowe, J. Chromatogr., 603 (1992) 235–241.
[19] D.Y. Pharr, Z.-S. Fu, T.K. Smith and W.L. Hinze, Anal. Chem., 61 (1989) 275–279.
[20] R.P. Frankewich, K.N. Thimmaiah and W.L. Hinze, Anal. Chem., 63 (1991) 2924–2933.
[21] J. Boger, R.J. Corcoran and J.-M. Lehn, Helv. Chim. Acta, 61 (1978) 2190–2218.
[22] J. Szejtli, A. Lipták, I. Jodá, P. Fügedi, P. Nanási and A. Neszmélyi, Starch/Stärke, 32 (1980) 165–169.
[23] D.W. Armstrong, T.J. Ward, R.D. Armstrong and T.E. Beesley, Science, 232 (1986) 1132–1135.
[24] S. Terabe, Y. Ishihama, H. Nishi, T. Fukuyama and K. Otsuka, J. Chromatogr., 545 (1991) 359–368.
[25] E. Skočir, J. Vindevogel and P. Sandra, Chromatographia, 39 (1994) 7–10.
[26] S. Michaelsen, P. Møller and H. Sørensen, J. Chromatogr. A, 680 (1994) 299–310.

ELSEVIER

Journal of Chromatography A, 710 (1995) 339–345

JOURNAL OF CHROMATOGRAPHY A

Enantiomeric separation of amphetamine related drugs by capillary zone electrophoresis using native and derivatized β-cyclodextrin as chiral additives

Sabine Cladrowa-Runge[a], Robert Hirz[b], Ernst Kenndler[a], Andreas Rizzi[a,*]

[a]*Institute of Analytical Chemistry, University of Vienna,Währingerstraße 38, A-1090 Vienna, Austria*

[b]*Department of Forensic Sciences, Federal Ministry of Interior, Liechtenwerderplatz, A-1090 Vienna, Austria*

First received 20 February 1995; revised manuscript received 20 April 1995; accepted 21 April 1995

Abstract

Amphetamine, methamphetamine and several ring-substituted analogs which are under governmental regulations have been separated by capillary zone electrophoresis employing native and various substituted β-cyclodextrins as additives to the background electrolyte. The following chiral selectors were used: native β-cyclodextrin, heptakis-(2,6-di-O-methyl)-β-cyclodextrin, heptakis-(2,3,6-tri-O-methyl)-β-cyclodextrin, (2-hydroxy)propyl-β-cyclodextrin and carboxymethyl-β-cyclodextrin. The amphetamines were separated without derivatization. Separations are reported with respect to the kind of chiral selector. Native β-cyclodextrin and carboxymethyl-β-cyclodextrin turned out to give optimal resolutions within only a few minutes. This direct method is compared with the indirect method separating the diastereomeric Marfey's derivatized amphetamines by means of non-chiral sodium dodecylsulfate micelles.

1. Introduction

Because of the increasing popularity of amphetamine, methamphetamine and various ring-substituted amphetamines as drugs which act as central nervous stimulants, these compounds are receiving more and more attention in clinical, pharmacological and toxicological science [1]. As the enantiomers of amphetamine have different pharmacological and toxicological potential [2,3]–and a similar situation can be expected for their derivatives–separation and quantitation of the single enantiomers are required. The enantiomeric composition is also of interest in forensic analysis, as in some countries the controlling regulations for the optical isomers are different. The enantiomer pattern is further supposed to lead to information about the origin and the way of preparation of the administered drug samples [4].

Recently enantioseparation has been reported for nine amphetamine related drugs using HPLC [5]. Direct separation by means of a chiral stationary phase consisting of immobilized β-cyclodextrin (β-CD) was obtained within analysis times of ca. 20 to 30 min. Some of the compounds could be separated without derivatization, for some others derivatization prior to enantiomeric separation was required. Alterna-

* Corresponding author.

0021-9673/95/$09.50
SSDI 0021-9673(95)00497-1

tively, most of the analytes could be separated also by simple non-chiral reversed-phase chromatography after derivatization of the analytes with optical pure Marfey's reagent to form diastereomeric compounds.

Beside the HPLC methods, capillary zone electrophoresis (CZE) has become a powerful tool for enantiomer separation, particularly because of the shorter analysis times which often can be achieved [6]. Direct methods of enantioseparation can be performed by simply adding a chiral selector to the background electrolyte (BGE). Cyclic oligosaccharides, especially cyclodextrins, are widely used as chiral selectors [7–11]. The present paper deals with the direct enantioseparation of nine different amphetamines (see Fig. 1), covering amphetamine, methamphetamine and ring-substituted derivatives of both, by using native β-CD or several derivatized β-cyclodextrins as additives to the BGE. The use of modified chiral selectors allows to achieve different enantioselectivity coefficients due to differences in the host–guest complexation constants caused by differences in the cavity size and shape, differences in the hydrophobicity and introduction of additional interaction sites. The amphetamines are analyzed without any derivatization using their native UV absorbance. The method thus becomes even more simple, cheap and fast, especially concerning sample preparation. The aim of the present work is to specify conditions where all of the amphetamines can be enantioseparated and to study the influence of different selector substituents and analyte structure on the enantioseparation.

The results obtained with the proposed method are finally compared with the results of an alternative electrophoretic method proposed previously [12], i.e. the indirect enantioseparation of the amphetamines after derivatizing the enantiomers to diastereomers by optically pure Marfey's reagent. These uncharged derivatives are separated by use of micellar electrokinetic chromatography (MEKC) employing non-chiral SDS micelles in alkaline solutions.

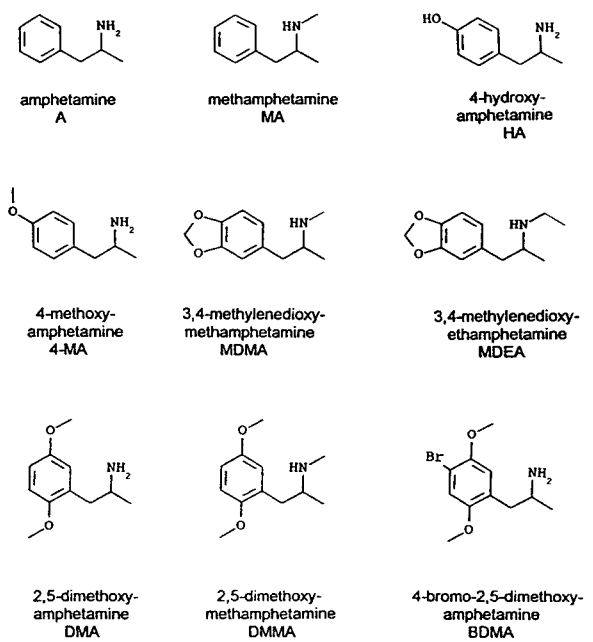

Fig. 1. Structure of amphetamines and abbreviations used.

2. Experimental

2.1. Chemicals

Sodium hydroxide, sodium dihydrogenphosphate and phosphoric acid were purchased from E. Merck (Darmstadt, Germany). Amphetamine standards were gifts from the UNIDO laboratories (Vienna, Austria). Native β-cyclodextrin (β-CD) was a gift from the Department of Chemistry of the Polish Academy of Sciences (Warsaw, Poland). Heptakis-(2,6-di-O-methyl)-β-cyclodextrin (DM-β-CD) containing about 14 methoxy-groups per β-CD molecule), heptakis-(2,3,6-tri-O-methyl)-β-cyclodextrin (TM-β-CD) containing 21 methoxy-groups per β-CD molecule, (2-hydroxy)propyl-β-cyclodextrin (HP-β-CD) containing about 6.3 hydroxypropyl-groups per β-CD ring, and carboxymethyl-β-cyclodextrin (CM-β-CD) containing 2.5–3 carboxymethyl groups per β-CD ring) were purchased from

Cyclolab R&D Laboratory (Budapest, Hungary).

Sodium dodecylsulfate (SDS) was purchased from Fluka (Buchs, Switzerland), and Marfey's reagent from Sigma (Deisenhofen, Germany).

2.2. Apparatus and electrophoretic conditions

All experiments were carried out using an HP-3D capillary electrophoretic instrument (Hewlett-Packard, Waldbronn, Germany), equipped with a diode-array detector monitoring a wavelength of 214 nm. A non-coated fused-silica capillary (Hewlett-Packard; 48.5 cm total length, 40 cm effective length, 50 μm I.D.) was kept at a constant temperature of 20 ± 0.1°C and the applied voltage was 20 kV, unless stated otherwise.

The background electrolyte (BGE) consisted of an aqueous solution of 50 m*M* sodium dihydrogenphosphate at pH 2.5 (adjusted with phosphoric acid) and 10 m*M* selector (β-CD or derivatives).

3. Results and discussion

3.1. Enantioseparation with different substituted β-cyclodextrins

Enantioselectivity coefficients, r, for the amphetamines listed in Fig. 1 obtained by using different β-CD based selectors are given in Table 1. Enantioselectivity coefficients (separation factors) are calculated as the ratios of the effective mobilities of the enantiomers. The migration order of the amphetamines has not been determined in this paper. The pH of 2.5 chosen for all analyses reported allowed to keep the electroosmotic flow completely suppressed and all of the analytes protonated.

Native β-CD

With native, nonderivatized β-CD all of the amphetamines investigated could, at least partially, be resolved. Baseline resolution was not achieved for all compounds, although in all instances the separation was sufficient to provide

Table 1
Migration times and enantioselectivity coefficients (r) measured for amphetamines employing different chiral selectors

Amphetamine	Chiral selector									
	β-CD		DM-β-CD		TM-β-CD		HP-β-CD		CM-β-CD[a]	
	t (min)	r	t (min)	r	t (min)	r	t (min)	r	t (min)	r
A	8.50	1.015	9.39	1.007	6.07	<1.003	6.48	1.011	13.07	1.028
MA	8.29	1.015	8.56	1.010	6.42	1.003	6.82	1.011	13.00	1.027
HA	10.09	1.017	6.36	1.008	6.61	1.011	6.06	1.011	19.03	1.043
4-MA	9.85	1.011	11.22	1.000	7.02	<1.003	7.60	1.011	17.55	1.027
MDMA	10.90	1.021	12.42	1.010	6.84	1.016	9.15	1.026	16.96	1.028
MDEA	12.01	1.017	13.32	1.007	7.38	1.020	10.31	1.025	30.76	1.026
DMA	8.30	1.013	10.24	1.020	6.96	1.015	8.61	1.004	12.50	1.016
DMMA	8.92	1.013	10.75	1.021	7.60	1.027	8.19	1.007	14.72	1.017
BDMA	8.32	1.005	9.19	1.004	7.83	1.000	7.54	1.000	11.94	1.000

Enantioselectivity coefficients are obtained by dividing the effective mobility of the faster migrating enantiomer, μ_1, by that of the slower one, μ_2. Experimental conditions as specified in the Experimental section. BGE: aqueous solution of 50 m*M* sodium dihydrogenphosphate, pH 2.5; selector concentration, 10 m*M*; temperature, 20°C; applied voltage, 20 kV.
Abbreviations: β-CD = nonderivatized (native) β-cyclodextrin; DM-β-CD = heptakis-(2,6-di-O-methyl)-β-CD; TM-β-CD = heptakis-(2,3,6-tri-O-methyl)-β-CD; HP-β-CD = (2-hydroxy)propyl-β-CD; CM-β-CD = carboxymethylated β-CD.
[a] Applied voltage: 15 kV.

information whether racemic or non-racemic samples are investigated. Fairly well resolution is achieved for all compounds exhibiting enantioselectivity coefficients larger than 1.014 (cf. Fig. 2).

Methylated β-CDs

Both methylated cyclodextrins, i.e. DM-β-CD and TM-β-CD, gave only low enantioselectivity coefficients for most of the amphetamines. The large and bulky di-substituted analytes DMA and DMMA are the two exceptions. Both of them are baseline separated with DM-β-CD and best selectivity coefficients could be achieved for DMA in this system, whereas for DMMA TM-β-CD showed the highest selectivity. It is a matter of efficiency that DMMA was separated to the baseline only with DM-β-CD.

From the mechanistic point of view it is obvious that methylation of two (DM-β-CD) or three (TM-β-CD) hydroxyl groups per glucose unit in the CD ring leads to increased hydrophobicity in the CD ring which simply enlarges the size and width of the host molecule. It is likely that the good resolution achievable with methylated β-CDs, particularly for the bulky dimethyl-substituted amphetamines which are supposed not to be able to completely penetrate the hydrophobic interior of the cavity of native β-CD [5], can mainly be attributed to the reduced polarity of the rims of the cavity and the enlargement of the host molecule.

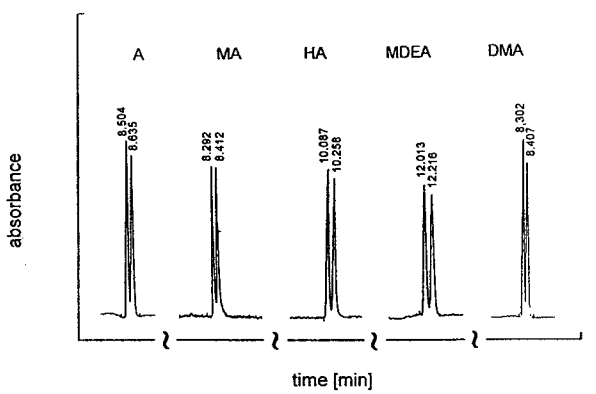

Fig. 2. Electropherograms of five well separated amphetamines using native β-CD as selector. Abbreviations as in Fig. 1. Experimental conditions: Non-coated fused-silica capillary with 50 μm I.D., total length of 48.5 cm and effective length of 40 cm. Detection wavelength, 214 nm. BGE: aqueous solution of 50 m*M* sodium dihydrogenphosphate at pH 2.5, 10 m*M* β-CD; temperature, 20°C, applied voltage, 20 kV.

Hydroxypropyl-β-CD

This selector molecule is used with a substitution degree of about 6.3. This means that on the average each glucose unit in the β-CD molecule carries one substituent. The use of the hydroxypropylated selector gave good results for the bicyclic amphetamines. For all other analytes no improvement in resolution was observed compared to the nonderivatized selector. Especially for the bulky amphetamines DMA, DMMA and BDMA–which are not able to penetrate the cavity–the resolving power was low.

Carboxymethylated β-CD

The degree of substitution of the carboxymethyl-β-CDs was ca. 2.5–3 carboxymethyl groups per CD ring. The application of carboxymethyl-β-CD gave very good selectivities. Particularly compared to native β-CD, the separation factors were higher with CM-β-CD in all cases except for BDMA. This compound and the other two bulky dimethoxy amphetamines were the only exceptions; they are better separated by a different selector, e.g. DM-β-CD and to some extent TM-β-CD. However, even for two of these analytes baseline resolution (DMMA) or near-baseline resolution (DMA) was achieved with the carboxymethylated selector. However, some improvement in resolution can be expected when improving the efficiency by increasing the voltage. Best separation of all amphetamines was found for the hydroxyl-substituted amphetamine HA.

The particularly high selectivity coefficients achieved with this selector can be considered as follows: First, the carboxy group serves as an additional type of site allowing for strong interactions with basic and acidic groups in the analytes, depending on the degree of dissociation. Ion-pairing might be included. Strong interactions like these, particularly when occurring near the chiral centers, very often enhance the

selectivity of the system. Furthermore, at the used pH of 2.5 the carboxymethyl groups of the host are at least partially dissociated as can be concluded from the increased current compared to the other selectors. In contrast to the positively charged analytes the partially charged selector molecule thus migrates to the anode. This causes an additional increase of the separation factor independent of the selectivity of the host–guest complexation itself.

When regarding not only the selectivity but also the efficiency it becomes obvious that it is often the latter which determines the achievable resolution. This is illustrated in Fig. 3 which shows the electropherograms of the two bicyclic amphetamines MDMA and MDEA. They are very similar in structure and only differ in the substituent at the amino group (methyl- vs. ethyl-). However, in all systems better efficiency due to better peak symmetry is found for MDEA. As a consequence, MDEA is better resolved in all cases, although the systems with β-CD, HP-β-CD and CM-β-CD selectors are more selective for MDMA. The higher noise in the electropherograms with modified CDs corresponds to the lower analyte concentrations chosen to reduce peak tailing and formation of triangular peaks.

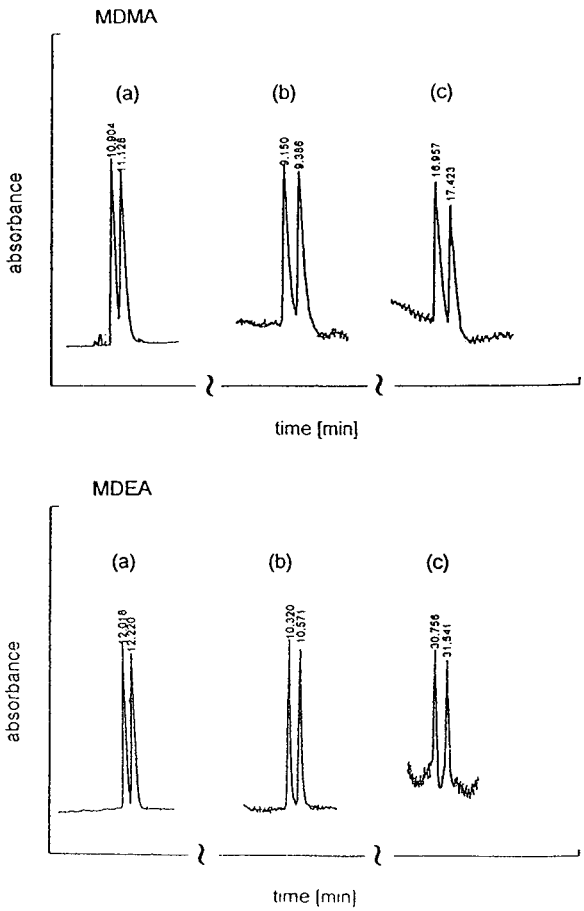

Fig. 3. Electropherograms of 3,4-methylenedioxymethamphetamine (MDMA) and 3,4-methylenedioxyethamphetamine (MDEA) employing different selectors. (a) 10 mM β-CD, (b) 10 mM HP-β-CD, (c) 10 mM CM-β-CD. For other experimental conditions see Fig. 2.

Remarks on the experimental conditions

Selectivity coefficients are known to be dependent on the selector concentration in the BGE [13]. The concentration at which optimum separation is achieved depends on the magnitude of the host–guest complexation constant. All experiments reported in Table 1 were carried out at a selector concentration of 10 mM. Without using buffer additives like urea to enhance the solubility this is about the highest concentration which can be used for β-CD. Reducing the β-CD concentration from 10 mM to 5 mM resulted in a decrease in selectivity in all instances, e.g. the selectivity coefficient of MA dropped from 1.015 to below 1.003. In spite of the increased water solubility of all the derivatized cyclodextrins all selector concentrations were kept at 10 mM.

For all measurements employing uncharged selectors a voltage of 20 kV was chosen. Typical currents observed at this voltage were ca. 30 μA. Increasing the voltage to 30 kV leads to improved efficiencies as expected from fundamental relationships but at the same time to a loss in selectivity which probably results from Joule heating generated in the capillary which cannot be controlled by the thermostating device. With the chosen electrolyte solution and the equipment described, a voltage of 20 kV should thus not be exceeded.

4. Conclusion

Various methods are presented that allow the enantioseparation of nine different amphetamine-related compounds of clinical and forensic interest employing different β-CD based chiral selectors as BGE additives. Native β-CD was the only selector which was able to resolve all the amphetamines investigated at least partially. The methyl-substituted cyclodextrins, DM-β-CD and TM-β-CD, gave improved selectivity only for the bulky disubstituted amphetamines DMA and DMMA. HP-β-CD gave no advantage compared to the native selector except for a slight improvement of the separation of the two bicyclic analytes MDMA and MDEA. However, the carboxymethylated β-CD was superior to β-CDs for all amphetamines, except for BDMA where no separation could be achieved. Native β-CD and CM-β-CD are thus the selectors of choice for routine screening of amphetamine samples. The analysis times are in most instances below 12 min and thus significantly shorter than those of the HPLC methods described previously [5], where up to 40 min were required in some instances. As for the CZE separation no derivatization is needed prior to the analysis, the speed of analysis is unsurpassed by the HPLC methods. The chiral selector additives used are significantly cheaper than chiral stationary HPLC phases.

The results obtained by the method based on β-CD selectors is unmatched also by the alternative CZE method based on indirect enantioseparation [12]. This alternative method yields separation of the diastereomeric derivatives of the amphetamines after derivatization with Marfey's reagent and employing SDS micelles. Electropherograms of successful separations are shown in Fig. 4. Especially the bicyclic amphetamines MDMA and MDEA could be separated with excellent selectivity coefficients (1.073 and 1.117) and baseline separation could also be achieved for MA and HA. However, all of the baseline resolutions could also be achieved by at least one of the direct methods described above. The time required for the micellar separations is about the same as that needed for the direct methods with β-CD. However, the derivatization step is rather time-consuming. Thus, no advantage can be seen for this alternative method, especially as the separations achieved for the two bulky dimethoxy amphetamines, DMA and DMMA, as well as for 4-MA were insufficient, and BDMA was not separated at all.

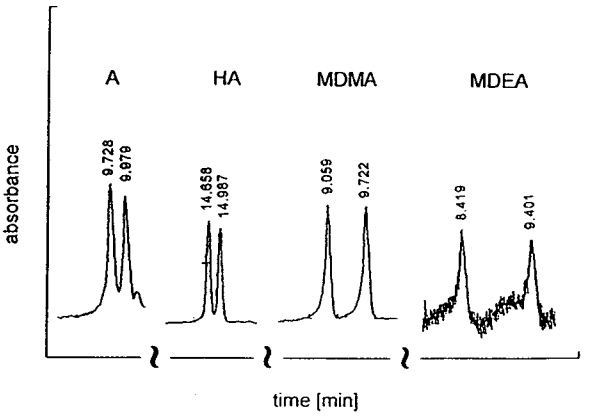

Fig. 4. Electropherograms of selected Marfey's reagent derivatized amphetamines applying nonchiral SDS micelles. Experimental conditions: Non-coated fused-silica capillary with 50 μm I.D., total length of 48.5 cm and effective length of 40 cm. Detection wavelength, 340 nm. BGE: 80% (v/v) aqueous solution of 5 m*M* sodium borate at pH 9.0, 100 m*M* SDS, 20% (v/v) methanol; temperature, 40°C; applied voltage, 30 kV.

Acknowledgement

This study was made possible by a grant from the Austrian Science Foundation (Fond zur Förderung der Wissenschaftlichen Forschung, FWF), Project number P09814-CHE. The authors appreciate this support.

References

[1] C.J. Schmidt, J. Pharmacol. Exp. Ther., 240 (1987) 1.
[2] I.W. Wainer and T.D. Doyle, J. Chromatogr., 259 (1983) 465.
[3] R.A. Glennon and R. Young, Pharmacol. Biochem. Behav., 20 (1984) 501.
[4] F.T. Noggle, Jr., J. DeRuiter and C.R. Clark, J. Chromatogr. Sci., 28 (1990) 529.

[5] A.M. Rizzi, R. Hirz, S. Cladrowa-Runge and H. Jonsson, Chromatographia, 39 (1994) 131.
[6] S. Terabe, K. Otsuka and H. Nishi, J. Chromatogr. A, 666 (1994) 295.
[7] S. Fanali, J. Chromatogr., 474 (1989) 441.
[8] S. Fanali, J. Chromatogr., 545 (1991) 437.
[9] M.J. Sepaniak, R.O. Cole and B.K. Clark, J. Liq. Chromatogr., 15 (1992) 1023.
[10] H. Nishi, T. Fukuyama and S. Terabe, J. Chromatogr., 553 (1991) 503.
[11] H. Nishi, Y. Kokusenya, T. Miyamoto and T. Sato, J. Chromatogr. A, 659 (1994) 449.
[12] S. Cladrowa-Runge, R. Hirz, A. Rizzi and E. Kenndler, Poster presented at the 6th International Symposium on High Performance Capillary Electrophoresis, San Diego, CA, Feb. 1994, Poster No. 216.
[13] S.A.C. Wren and R.C. Rowe, J. Chromatogr., 603 (1992) 235.

ELSEVIER

Journal of Chromatography A, 710 (1995) 347–350

JOURNAL OF CHROMATOGRAPHY A

Short communication

Direct determination of 4-nitrobenzoyl chloride by high-performance liquid chromatography based on silanophilic interaction

Hongyan Li[a,*], Qizhi Hu[b], Xuequen Yang[a], Zhiren Zhou[a]

[a]*Central Laboratory, Xiangtan University, Hunan 411105, China*

[b]*Department of Chemistry of Xiangtan University, Hunan 411105, China*

First received 24 January 1995; revised manuscript received 19 April 1995; accepted 20 April 1995

Abstract

A high-performance liquid chromatographic method without prederivatization was investigated for the direct determination of 4-nitrobenzoyl chloride and 4-nitrobenzoic acid. The separation was carried out on C_3, C_8 and C_{18} alkyl-bonded silica columns with cyclohexane–tetrahydrofuran as the eluent. The retention behaviour observed was obviously caused by the silanophilic interaction between the solute and stationary phase. Optimum separation of 4-nitrobenzoyl chloride and 4-nitrobenzoic acid was obtained on the C_3 column and the calibration graph showed a significant linear relationship. The method was found to be quantitative, reproducible and rapid.

1. Introduction

The most widely employed methods for the determination of acid chlorides are titrimetric [1,2]. Hasegawa et al. [3], Colgan and Krull [4] and Bissinger et al. [5] reported RP-HPLC methods for the determination of acid chlorides using their ester and amide derivatives. Acid chlorides cannot be determined directly by RP-HPLC with an aqueous–organic eluent as they can react with water, so a non-aqueous solvent system must be adopted.

The aim of this work was to develop an HPLC method without prederivatization for the simultaneous determination of 4-nitrobenzoyl chloride and 4-nitrobenzoic acid. Conventional liquid–solid chromatography (LSC) with a silica column is assumed to be suitable for the separation of these compounds because, based on their molecular structures, 4-nitrobenzoic acid and 4-nitrobenzoyl chloride have different abilities to forming hydrogen bonds with silanol groups on the silica surface. However, these polar compounds interact very strongly with the adsorbent surface and result in peaks of poor symmetry and poor efficiency.

A non-polar alkyl-bonded silica stationary phase is usually used in the RP-HPLC mode with the use of a polar mobile phase. The use of an alkylsilica column with a pure non-polar organic eluent or a non-polar solvent-rich organic eluent would be classified as LSC owing to the polar residual silanol groups on the surface of the alkyl-bonded silica phase. We indeed found in

* Corresponding author.

0021-9673/95/$09.50
SSDI 0021-9673(95)00495-5

this work that LSC could be carried out by using an alkylsilica gel as the stationary phase. The weaker interaction between the solutes and the residual silanol groups on the surface of the alkylsilica gel results in peaks with good symmetry and high efficiency.

Optimum analytical conditions were determined to ensure complete separation, quantification and reproducibility. The applicability of this method to the determination of 4-nitrobenzoyl chloride which was synthesized from 4-nitrobenzoic acid with PCl_3 as a chlorinating agent was demonstrated. It is also suggested that this method can be extended to the determination of other acid chlorides.

2. Experimental

2.1. Chemicals and equipment

Cyclohexane, tetrahydrofuran (THF) and 4-nitrobenzoic acid of analytical-reagent grade were obtained from Shanghai Chemical Supply (Shanghai, China). THF was redistilled before use. 4-Nitrobenzoyl chloride (purity 99.8%) was obtained from Professor Y.-B. Lin (Department of Chemistry, Xiangtan University, China). Chromatography was performed on a Shimadzu LC-6A chromatgraph equipped with an SPD-6AV variable-wavelength detector (190–900 nm) and a CR-3A data processor. The columns used were Shim-Pack CLC-C_3, CLC-C_8 and CLC-C_{18} (150 × 4.6 mm I.D.).

2.2. Procedures

Cyclohexane–THF was used as the eluent on the C_3, C_8, C_{18} columns at a flow-rate of 1.0 ml/min. The detector wavelength setting was 300 nm and the sensitivity was 0.04 AUFS. Capacity factors (k') were evaluated from the retention times of the test substances and that of an unretarded component, tetrachloroethylene (detection wavelength 254 nm). The eluent compositions were varied and the k' values of these compounds in each system were determined. The amount of 4-nitrobenzoyl chloride was calculated by a five-point external standard method under optimized conditions. The standards for analysis were prepared by dissolution of known amounts of 4-nitrobenzoyl chloride in cyclohexane–THF (70:30, v/v) solvent; the theoretical concentration of the solute was in the range 45.36–226.8 μg/ml. Aliquots (5 μl) of the standard solutions were injected on to the chromatographic column. Sample analyses were carried out under the same conditions. The amount of acid chloride was calculated by comparing the peak area in the reference chromatogram with that of the appropriate component in the sample chromatogram.

3. Results and discussion

3.1. Dependence of retention on composition of mobile phase

As illustrated in Table 1, changes in the capacity factors of 4-nitrobenzoyl chloride and 4-nitrobenzoic acid with the volume fraction of THF in binary cyclohexane–THF eluent were obtained on the C_3, C_8, C_{18} columns. The retention behaviours shown by 4-nitrobenzoyl chloride and 4-nitrobenzoic acid could be interpreted in terms of the LSC mode; the active adsorption sites were the residual silanol groups on the surface of the alkyl-bonded phase and the separation was carried out based on the silanophilic interaction between solutes and active sites. 4-Nitrobenzoic acid has a greater ability than 4-nitrobenzoyl chloride to form hydrogen bonds with silanols, which should result in a greater retention, and this was borne out by the experimental results.

Fig. 1 show the plots of k' versus eluent composition on the three columns. A common feature is an increase in retention with decrease in THF concentration, which is consistent with the interpretation that the retention was due to silanophilic interactions at low THF concentration whereas THF masked the silanol sites at higher concentration.

Table 1
Experimental values of k' for 4-nitrobenzoic acid (k_1') and 4-nitrobenzoyl chloride (k_2') with cyclohexane–THF from 40:60 to 98:2 (v/v)

Column	k'	Volume fraction of THF (v/v)													
		0.6	0.5	0.45	0.40	0.35	0.30	0.25	0.20	0.15	0.10	0.08	0.06	0.04	0.02
C_3	k_1'	0.103	0.162	0.201	0.260	0.331	0.414	0.534	0.738	1.100	1.992	–	–	–	–
	k_2'	0.027	0.046	0.056	0.070	0.090	0.111	0.137	0.177	0.243	0.337	–	–	–	–
C_8	k_1'	–	–	–	–	–	0.007	0.013	0.026	0.056	0.124	0.180	0.275	0.469	0.998
	k_2'	–	–	–	–	–	0.002	0.005	0.009	0.018	0.033	0.043	0.054	0.067	0.079
C_{18}	k_1'	–	–	0.048	0.055	0.064	0.067	–	0.108	–	0.202	0.253	0.326	0.571	1.358
	k_2'	–	–	0.065	0.067	0.071	0.081	–	0.105	–	0.139	0.147	0.163	0.186	0.212

Columns, Shim-Pack CLC-C_3, CLC-C_8 and CLC-C_{18} (150 × 4.6 mm I.D.); eluent, cyclohexane–THF; flow-rate, 1.0 ml/min.

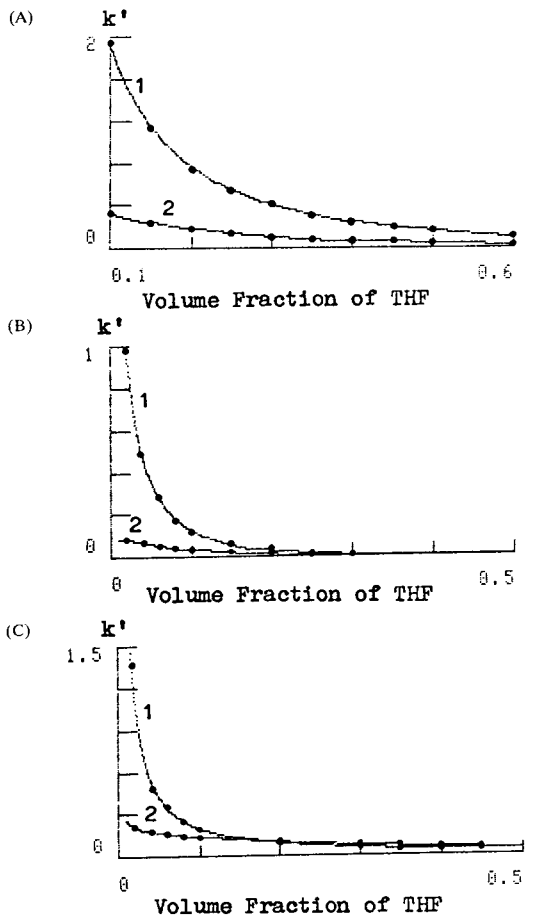

Fig. 1. Change in capacity factors of 4-nitrobenzoic acid (1) and 4-nitrobenzoyl chloride (2) with variation of the volume fraction of THF in eluent of the three Shim-Pack CLC columns: (a) C_3; (b) C_8; (c) C_{18}.

3.2. Quantitative analysis

Fig. 1 also provided a visual approach to the optimization of the chromatographic conditions for quantitative analysis. The change in the k' of two components with the volume fraction of THF in the eluent (V_{THF}) on the three columns indicated that the C_3 column showed the widest variation in V_{THF} and the greatest difference between k_1' and k_2' for the complete separation of the two compounds, hence this column was selected as the optimum. Considering the solubility of the solutes in the eluent, the separation of the two components and the speed of analysis, the proportion of THF in the eluent was selected as at 30% (v/v), i.e., the optimum eluent was cyclohexane–THF (70:30, v/v). Under the optimized conditions, rapid ($k' < 1$) elution of the two components was obtained, as shown in Fig. 2. The first component eluted was 4-nitrobenzoyl chloride, followed by 4-nitrobenzoic acid.

The calibration graph for the determination of 4-nitrobenzoyl chloride was constructed by analysing a series of standards of known concentration. A significant linear relationship between peak area and solute concentration was found, as shown in Fig. 3; the correlation coefficient (r) was 0.9998.

The results obtained for sample analysis for 4-nitrobenzoyl chloride with six replicate determinations were 81.67, 81.51, 80.89, 81.34, 81.87 and 82.10%, mean 81.56, R.S.D. 0.52% and average recovery 99.1%. The relative standard

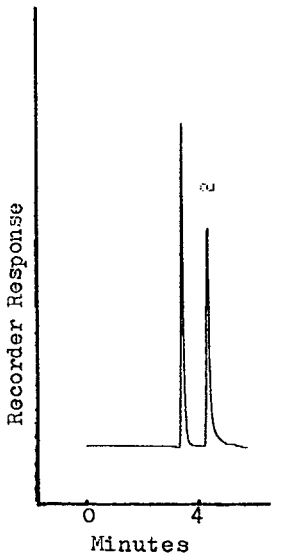

Fig. 2. Chromatogram of a mixture containing (1) 4-nitrobenzoyl chloride and (2) 4-nitrobenzoic acid. Column, Shim-Pack CLC-C_3 (150 × 4.6 mm I.D.); eluent, cyclohexane–THF (70/30, v/v); flow-rate, 1.0 ml/min; injection volume, 5 μl; detection, UV at 300 nm.

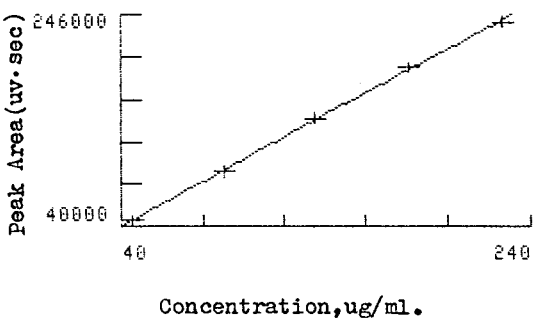

Fig. 3. Calibration graph for 4-nitrobenzoyl chloride. Column, Shim-Pack CLC-C_3 (150 × 4.6 mm I.D.); eluent, cyclohexane–THF (70/30, v/v); flow-rate, 1.0 ml/min; detection, UV at 300 nm.

deviation and average recovery were satisfactory.

4. Conclusion

The method described is very useful for the reproducible, rapid and easy determination of 4-nitrobenzoyl chloride. The separation is based on silanophilic interactions between the solutes and the residual silanol groups in the surface of the alkyl-bonded silica phase. This work also demonstrated that beyond its traditional use, a non-polar alkyl-bonded silica phase can be used in normal-phase HPLC for special separation purposes.

References

[1] W. Selig, Microchem. J., 16 (1971) 385.
[2] E.A. Griboya, Zavod. Lab., 45 (1979) 212.
[3] K. Hasegawa, T. Matsuno, S. Ikagawa and H. Hoshida, Yakugaku Zasshi, 101 (1981) 1059.
[4] S.T. Colgan and I.S. Krull, J. Chromatogr. Sci., 26 (1988) 501.
[5] J.M. Bissinger, K.J. Rullo, J.T. Stoklosa, C.M. Shearer and N.J. Deangdis, J. Chromatogr., 268 (1983) 102.

ELSEVIER

Journal of Chromatography A, 710 (1995) 351–356

JOURNAL OF CHROMATOGRAPHY A

Short communication

Reversed-phase high-performance liquid chromatographic method for the quantitative determination of alkylbis(2-benzothiazolylsulfen)amides

Magdalena Štolcová[a,*], Alexander Kaszonyi[a], Milan Hronec[a], Tibor Liptaj[b]

[a]*Department of Organic Technology, Slovak Technical University, Radlinského 9, 812 37 Bratislava, Slovak Republic*

[b]*Central Laboratories of the Chemical Faculty, Slovak Technical University, Radlinského 9, 812 37 Bratislava, Slovak Republic*

First received 10 January 1995; revised manuscript received 26 April 1995; accepted 26 April 1995

Abstract

An isocratic, reversed-phase HPLC procedure was developed for the simultaneous determination of isopropyl-, *tert.*-butyl-, *tert.*-amyl-, cyclohexylbis(2-benzothiazolylsulfen)amides. Quantitation is performed on a C_{18} bonded-phase column (Separon SGX C_{18}, 5 μm) using N-dicyclohexyl-2-benzothiazolesulfenamide as internal standard followed by UV photodiode-array detection. The precision ($n = 7$) for all derivatives of alkylbis(2-benzothiazolylsulfen)amides is within 1.5%. Identification of the compounds also in the mixtures was done by NMR spectroscopy.

1. Introduction

Alkylbis(2-benzothiazolylsulfen)amides (alkylbisBS) are used in the rubber industry as vulcanisation accelerators. Like the N-alkyl-2-benzothiazolesulfenamides (alkylBS), these compounds are thermolabile. Therefore, HPLC methods can not be used in the analysis of these compounds.

Šmejkal et al. [1] applied a reversed-phase HPLC method with a macroporous gel, Separon SE, for the determination of some compounds in rubber, one of them being N-morpholinyl-2-sulfenamide.

Various LC–MS techniques were studied for their ability to detect and identify minor components in benzothiazole derived compounds [2].

CyclohexylBS, cyclohexylbisBS and 2,2′-dithiobisbenzothiazole alone and in their mixtures were analyzed by Isaeva et al. [3] using coulometric titration in acetic acid with electrically generated bromine and by Borisova et al. [4] using oxidative bromination in acetic acid with amperometric detection.

In this paper, a simple, isocratic reversed-phase HPLC procedure is described for the simultaneous determination of isopropyl-, *tert.*-butyl-, *tert.*-amyl-, and cyclo-hexylbis(2-benzothiazolylsulfen)amides. Quantitation is performed on a C_{18} bonded-phase column using N-dicyclohexyl-2-benzothiazolesulfenamide as internal standard. Identification of the com-

* Corresponding author.

0021-9673/95/$09.50
SSDI 0021-9673(95)00513-7

pounds also in the mixtures is done by NMR spectroscopy.

2. Experimental

2.1. Materials

Acetonitrile was of HPLC quality (Labscan, Ireland). Water was purified with an osmometric system made by Wilhelm Werner (Germany). Other chemicals were of analytical reagent grade.

The derivatives of alkylbisBS (Fig. 1) were prepared by the method described in Ref. [5] and recrystallized from diethyl ether. Purity was checked by NMR spectroscopy. Melting points of isopropylbisBS, *tert.*-butylbisBS, *tert.*-amylbisBS and cyclohexylbisBS were 106–107°C, 144–146°C, 125–126°C and 133–134°C, respectively. N-Dicyclohexyl-2-benzothiazolesulfenamide was a commercial product recrystallized from ethanol. Samples containing about 15 μg of the component in 1 cm^3 of acetone were prepared freshly before use. A longer than 4-h contact of the alkylbisBS derivatives with acetone causes a decrease of the precision. Solvents such as heptane, hexane and others used to prepare the real samples containing these compounds were removed by vacuum distillation. The mobile phases and the liquid samples were filtered and degassed under vacuum before use. The mobile phases were prepared volumetrically from various amounts of methanol, acetonitrile, tetrahydrofuran and water.

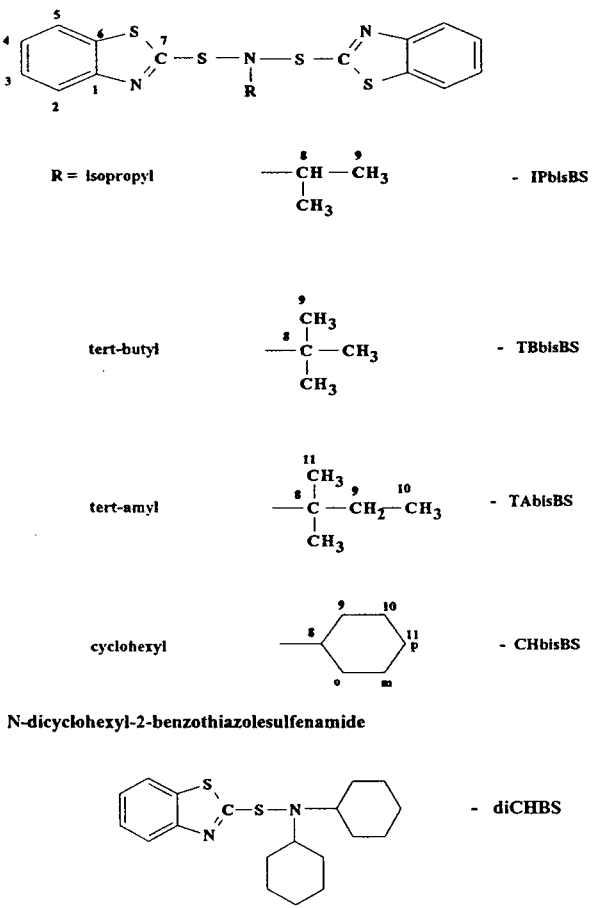

Fig. 1. Derivatives of alkylbis(2-benzothiazolylsulfen)amides and dicyclohexyl-2-benzothiazolesulfenamide.

2.2. NMR spectroscopy

Measurements were performed at 30°C using a Varian VXR-300 spectrometer with an operating frequency of 300 MHz for protons and 75 MHz for carbons. Standard [^{1}H]-, [^{13}C]- and [^{13}C]-ATP spectra were measured. For the same samples, additional H,H and one-bond or long-range H,C correlation NMR experiments were performed. The samples were dissolved in $CHCl_3$ (ca. 50 mg/cm^3).

2.3. High-performance liquid chromatography

Elution was performed using a Rheodyne injection valve fitted with a 4-μl injection loop (Shimadzu, Kyoto, Japan), an LC 10AD solvent delivery system, a 150 × 3.0 mm I.D. Separon SGX C_{18} column filled with 7 or 5 μm particle diameter ODS silica (Tessek, Czech Republic), and a Shimadzu SPD M6A photodiode-array detector operating in the range 195–670 nm, equipped with a Syntron computer and Class LC 10 software for control of the system and data acquisition and integration. Another column tested was packed with Nucleosil 120-3C_{18} 7 μm particle diameter (150 × 3.0 mm I.D.). All analy-

sis were carried out at ambient temperature. The measurements were performed in triplicate. The precision of the determination for all derivatives was calculated from seven replicated injections. The dead time was determined by using water as the non-retained compound. The capacity factor was calculated as $k' = (t_R - t_o)/t_o$, where t_R is the retention time, t_o is the dead time and the resolution was given by the equation $R_s = (t_{R,j} - t_{R,i})/2(\sigma_i + \sigma_j)$, where $t_{R,j}$ and $t_{R,i}$ are the retention times of compounds i and j, and σ_i and σ_j are the standard deviations of the peak for the compounds i and j, respectively.

3. Results and discussion

3.1. NMR spectroscopy

The number of spectral lines, their relative intensity, the position in the spectra and comparison with the known spectra of N-alkyl-2-benzothiazolesulfenamide derivatives unambiguously proved the expected structure of the alkylbisBS compounds presented in Fig. 1. Assignment of the ^{13}C NMR chemical shifts was done by comparison with spectra of N-alkyl-2-benzothiazolesulfenamide derivatives. In the case of possible ambiguousity of the results, H,H and H,C correlation experiments were exploited. The starting points in the assignment were the well-defined resonances of the quaternary carbons C_1 and $C_{6'}$. Based on the long-range 3-bond H,C correlations with these carbon protons, H_3 and H_4 could be unambiguously discriminated. ^1H multiplet resonances are severely overlapping. Using H,H–COSY and one-bond H,C–COSY all other proton and carbon resonances of the aromatic ring were identified. Whereas ^1H resonances of alkylbis(2-benzothiazolylsulfen)amides are severely overlapping, their ^{13}C resonances are clearly distinguishable. Carbon spectra proved to be useful for the reliable and quick identification of alkylbisBS compounds in the mixtures, also in the presence of other benzothiazole derivatives such as N-alkyl-2-benzothiazole-sulfenamides, 2,2′-dithiobisbenzothiazole and benzothiazole. Data are shown in Table 1.

3.2. RP-HPLC

A reversed-phase HPLC technique was chosen for the simultaneous determination of isopropyl-, *tert.*-butyl-, *tert.*-amyl-, and cyclohexylbis(2-benzothiazolesulfen)amides. Two types of C_{18} bonded-phase columns were used for the separation, i.e. Nucleosil 120-3C_{18} with 7 μm particle diameter and Separon SGX C_{18} with 7 or 5 μm particle diameter .

Though all alkylbisBS derivatives are very well soluble in diethyl ether and tetrahydrofuran, these solvents are not suitable in our case. In the presence of these solvents, the elution curves of

Table 1
^{13}C NMR chemical shifts (δ/ppm) of alkylbis(2-benzothiazolylsulfen)amides

C_i/alkyl	Isopropyl	*tert.*-Butyl	*tert.*-Amyl	Cyclohexyl
C-1	154.1	154.0	153.8	154.2
C-2	121.2	121.2	121.2	121.1
C-3	124.4	124.4	124.5	124.3
C-4	126.5	126.2	126.2	126.2
C-5	122.3	122.3	122.4	122.2
C-6	135.4	135.5	135.6	135.3
C-7	172.6	173.2	173.0	173.0
C-8	67.3(C-q)	69.3(C-q)	72.3(C-q)	74.3(CH)
C-9	22.5(CH_3)	29.5(CH_3)	34.0(CH_2)	32.9(CH_2,o)
C-10	–	–	29.8(CH_3-1)	25.6(CH_2,m)
C-11	–	–	26.4(CH_3-2)	25.0(CH_2,p)

all derivatives on the columns described above and eluted with acetonitrile–methanol–water or acetonitrile–water were asymmetric and peak widths were doubled. The same phenomenon was found when tetrahydrofuran was only a part of the mobile phase. NMR analysis showed that in diethyl ether and tetrahydrofuran no isomers or other compounds occurred. Finally, acetone proved to be a suitable solvent for our analysis.

The mobile phase composition used for the simultaneous determination of all derivatives of akylbisBS and the calculated capacity factors are summarized in Tables 2 and 3. Retention times and capacity factors were measured at a flow-rate of 0.8 cm^3 min^{-1}. All alkylbisBS derivatives had two absorption maxima, at ca. 230 and 280 nm.

On the chosen columns elution with methanol–water did not result in the separation of the alkylbisBS derivatives.

On the Nucleosil 120 $3C_{18}$ (7 μm) and Separon SGX C_{18} (7 μm) columns eluted with acetonitrile–water (7–8:3–2, v/v) we were able to separate all alkylbisBS derivatives, but resolution of isopropylbisBS from *tert.*-butylbisBS ($R_s = 0.9$) was not sufficient for quantitative analysis. Resolution of these two derivatives was improved by using a ternary mobile phase, acetonitrile–methanol–water (5:3.5:1.5, v/v). However, as shown in Table 4, the resolution for this problematic couple of derivatives was only 1.2, still not sufficient enough for quantitative determination. Under the conditions used the resolution for this couple of alkylbisBS derivatives could not been improved by changing the flow-rate of the mobile phase, as shown in Table 4.

Substantially better results were achieved on a Separon SGX C_{18} 5 μm column. As shown in Table 3, using acetonitrile–water (7–8:2–3, v/v) as the mobile phase, the capacity factors were

Table 3
Capacity factors of alkylbis(2-benzothiazolylsulfen)amides at various composition of the mobile phase at a flow-rate of 0.8 cm^3 min^{-1} and λ_{max} 233 nm on the Separon SGX C_{18} column with particle diameter 5 μm

Mobile phases							
Water	30	20	9	13	15	18	21
MeOH	0	0	21	17	15	12	9
MeCN	70	80	70	70	70	70	70
AlkylbisBS							
IPbisBS	19.3	13.1	3.9	6.0	7.1	9.9	10.7
TBbisBS	22.6	15.2	4.3	6.5	8.1	11.3	12.4
TAbisBS	30.3	19.4	5.4	9.1	10.4	14.8	16.3
CHbisBS	45.0	25.8	7.5	11.7	14.9	21.7	23.8
diCHBS	55.8	34.9	9.1	15.1	18.3	26.7	29.4

Table 2
Capacity factors of alkylbis(2-benzothiazolylsulfen)amides at various compositions of the mobile phase at a flow-rate of 0.8 cm^3 min^{-1} and λ_{max} 230 nm on the Separon SGX C_{18} column with particle diameter 7 μm

Mobile phases									
Water	30	30	20	30	15	21	21	15	15[a]
MeOH	70	0	0	0	35	49	49	35	35[a]
MeCN	0	70	80	0	0	0	30	50	50[a]
THF	0	0	0	70	50	30	0	0	0
AlkylbisBS									
IPbisBS	NA	6.6	5.5	–[b]	–[b]	–[b]	4.1	5.5	4.0
TBbisBS	NA	7.3	6.2	–[b]	0.6	2.0	4.6	6.3	4.3
TAbisBS	NA	9.6	8.3	–[b]	1.0	–[b]	6.0	8.1	5.7
CHbisBS	NA	14.1	13.6	0.4	–[b]	3.6	8.6	11.6	9.1
diCHBS	–[b]	17.9	–[b]	–[b]	–[b]	–[b]	11.0	–[b]	10.5

NA: not achieved.
[a] Nucleosil 120-$3C_{18}$, 7 μm column.
[b] Not present in the samples.

Table 4
Resolution of alkylbis(2-benzothiazolylsulfen)amides at various flow-rates of the mobile phase MeCN–MeOH–H_2O (50:35:15, v/v) at λ_{max} 230 nm on the Separon SGX C_{18} column with particle diameter 7 μm

	Flow-rate (cm^3 min^{-1})				
	0.6	0.7	0.8	0.9	1.0
alkylbisBS					
IPbisBS	1.1	1.1	1.2	1.0	0.8
TBbisBS	2.8	2.8	2.9	2.5	1.8
TAbisBS	4.9	5.1	5.4	4.2	3.1
CHbisBS					

high. The capacity factor can be lowered by gradient elution of acetonitrile and water or, as shown below, by a ternary mobile phase of acetonitrile–methanol–water under isocratic condition. Because of the smaller and simpler equipment needed, we chose the isocratic procedure for the determination. A suitable combination of acetonitrile–water with methanol allows to separate all alkylbisBS derivatives quickly and effectively with excellent resolution of isopropylbisBS from *tert.*-butylbisBS, as the problematic couple of derivatives. We found (see Table 3) that replacing part of the water (up to 15 vol.%) in the acetonitrile–water (7:3, v/v) mobile phase by methanol, decreased the capacity factors of the alkylbisBS derivatives. However, the resolution for the couple of IPbisBS and TBbisBS derivatives was not decreased below the limit value $R_s = 1.5$. By changing the flow-rate of the mobile phase acetonitrile–methanol–water (7:1.5:1.5, v/v), as shown in Table 5, we were also able to shorten the elution times of the alkylbisBS derivatives. The time of analysis is similar or shorter compared with that of the gradient method.

Table 5
Resolution of alkylbis(2-benzothiazolylsulfen)amides at various flow-rates of the mobile phase MeCN–MeOH–H_2O (70:15:15, v/v) at λ_{max} 233 nm on the Separon SGX C_{18} column with particle diameter 5 μm

	Flow-rate (cm^3 min^{-1})				
	0.8	1.0	1.2	1.4	1.6
alkylbisBS					
IPbisBS	1.9	1.7	1.6	1.5	1.4
TBbisBS	4.5	4.0	3.9	3.7	3.5
TAbisBS	7.1	6.8	6.0	6.0	6.0
CHbisBS	4.3	4.2	3.7	3.7	3.7
diCHBS					

N-Dicyclohexyl-2-benzothiazolesulfenamide proved to be a suitable internal standard for our analysis. In Fig. 2 a chromatogram of all alkylbisBS derivatives is shown with the internal standard using acetonitrile–methanol–water (7:1.5:1.5, v/v) as the mobile phase at the flow-rate of 1.4 cm^3 min^{-1} and detection at λ_{max} 233 nm.

The detection limit using acetonitrile–methanol–water at a flow-rate of 1.4 cm^3 min^{-1} and detection at $\lambda_{max} = 233$ nm, is $1.1 \cdot 10^{-4}$ AU. The determined limits of quantitation for IPbisBS, TBbisBS, TAbisBS, CHbisBS and diCHBS are 127, 118, 128, 151 and 166 ng cm^{-3}, respectively.

The precision of the internal standard method for all alkylbisBS derivatives was determined with freshly prepared samples using acetonitrile–methanol–water (7:1.5:1.5, v/v) as the mobile phase at a flow-rate of 1.4 cm^3 min^{-1} and detection at $\lambda_{max} = 233$ nm. Samples were in contact with acetone no longer than 4 h at ambient temperature. NMR analysis confirmed that after this time a slow decomposition of these compounds occurred. The precision was estimated from the analysis of a sample containing

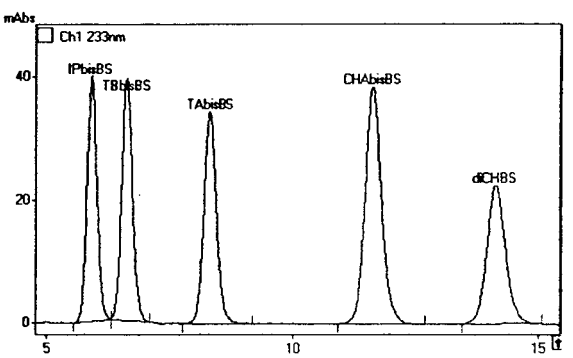

Fig. 2. Chromatogram of alkylbis(2-benzothiazolylsulfen)amides with N-dicyclohexyl-2-benzothiazolesulfenamide as internal standard using acetonitrile–methanol–water (7:1.5:1.5, v/v) as mobile phase at the flow-rate of 1.4 cm^3 min^{-1} and λ_{max} 233 nm.

Table 6
Determined amounts of separated alkylbis(2-benzothiazolylsulfen)amides on the Separon SGX C_{18} column with particle diameter 5 μm eluted with mobile phase AcCN–MeOH–H_2O (7:1.5:1.5, v/v) at a flow-rate of 1.4 cm^3 min^{-1} and λ_{max} 233 nm

n	Component				
	IPbisBS (wt.%)	TBbisBS (wt.%)	TAbisBS (wt.%)	CHbisBS (wt.%)	Grade (wt.%)
1	22.81	21.05	23.21	32.56	99.63
2	22.20	21.40	23.59	32.82	100.01
3	22.58	21.08	23.51	32.43	99.60
4	22.03	21.25	23.50	32.39	99.17
5	22.72	20.99	23.64	32.74	100.09
6	23.05	21.20	23.71	32.48	100.44
7	22.52	21.16	23.39	32.77	99.84
Mean (wt.%)	22.55	21.16	23.50	32.59	99.82
S.D.	0.35	0.14	0.16	0.17	–
R.S.D. (%)	1.55	0.66	0.68	0.52	–
Real value (μg cm^{-3})	11.7	11.0	12.2	16.9	51.8
Real value (wt.%)	22.59	21.24	23.55	32.62	100.00

about 12 μg cm^{-3}, i.e. approximately 25 wt.% of each alkylbisBS derivative. The determined areas were recalculated to the content (wt.%) of the component in the samples by the software used. The R.S.D. of 7 replicate injections for all alkylbisBS derivatives was within 1.5% (Table 6).

The method presented here has been found to be suitable for the analysis of alkylbisBS derivatives in waste water and other solvents used in their manufacture. The analyses are not interfered with raw material or by-products, such as N-alkyl-2-benzothiazolesulfenamides, 2,2′-dithiobisbenzothiazole and benzothiazole, that may be present in samples.

References

[1] F. Šmejkal, M. Popl and A. Čihová, J. Polym. Sci. Polym. Symp., 68 (1980) 145.
[2] W.M.A. Niessen, C.C. McCarney, P.E.G. Moult, V.R. Tjaden and J. van der Greef, J. Chromatogr., 647 (1993) 107.
[3] B.I. Isaeva, M.I. Lebedeva and L.B. Oganesyan, Tr. Mosk. Khim. Tekhnol. Inst., 71 (1972) 290.
[4] R.V. Borisova, M.I. Lebedeva, B.I. Isaeva and A.N. Dubovitskaya, Tr. Tambov. Inst. Khim. Mashinostr., 7 (1971) 124.
[5] J.M. Maison, GB pat. 1 288 701 (1971).

ELSEVIER

Journal of Chromatography A, 710 (1995) 357–360

JOURNAL OF CHROMATOGRAPHY A

Short communication

Measurement of desmosine and isodesmosine by capillary zone electrophoresis

Philippe Giummelly[a], Bernard Botton[b], Raphaëlle Friot[a], Deddi Prima-Putra[b], Jeffrey Atkinson[a,*]

[a]*Laboratoire de Pharmacologie Cardio-vasculaire, Faculté de Pharmacie, Université Henri Poincaré Nancy 1, 5 rue Albert Lebrun, BP 403, F-54001 Nancy, France*

[b]*Laboratoire de Biologie Forestière associé INRA, Faculté des Sciences, Université Henri Poincaré Nancy 1, F-54506 Vandoeuvre-les-Nancy, France*

Received 22 March 1995; accepted 19 April 1995

Abstract

Desmosine (DES) and isodesmosine (IDE) were separated and quantitated by a simple and sensitive capillary zone electrophoretic (CZE) method, using hydrostatic injection and direct UV detection at 254 or 185 nm. Two different electrophoretic mobilities for the two isoforms were observed in 90 m*M* phosphoric acid pH 2.2. The presence of a mixture of amino acids in the sample did not affect the separation of DES and IDE. The method was successfully used to quantitate the amounts of DES and IDE in elastin hydrolysates.

1. Introduction

Desmosine (DES) and isodesmosine (IDE) are cross-linking amino acids of elastin, a fibrous protein of vertebrate connective tissue; their determination is used as an indicator of the presence or alteration of elastin, and also to measure elastase activity [1].

A radioimmunoassay method [2] has been used to detect DES and IDE in urine samples, whilst high-performance liquid chromatography has been applied to tissue hydrolysates [3,4], or purified elastin hydrolysates [5]. This latter technique usually requires preliminary extraction of the two amino acids on a cellulose mini-column [3,4] (according to the method described by Skinner [6]), and in some cases an additional precolumn derivatization [4,5,7] in order to increase the sensitivity of the detection.

Current HPLC techniques meet most of the demands of amino acid analysis but the determination of minute amounts, when, for example, sample size is limited, requires the use of capillary zone electrophoretic (CZE) techniques. Femtomole-scale amino acid analysis by CZE generally requires laser-induced fluorescence detection, implying a derivatization reaction. In this work CZE was applied to the separation and quantitation of DES and IDE. As both DES and IDE have a pyridinium ring in their structure, direct UV detection was employed, without any

* Corresponding author.

0021-9673/95/$09.50
SSDI 0021-9673(95)00487-4

prior chemical modification of the molecules. Standard filters of 185 or 254 nm were used.

2. Experimental

2.1. Chemicals

Bovine ligamentum nuchae elastin, 2,4-dinitrofluorobenzene and borax were obtained from Sigma (St. Louis, MO, USA), DES and IDE from ICN Biomedicals (Costa Mesa, CA, USA), phosphoric acid and hydrochloric acid (analytical) were from Prolabo (Paris, France).

2.2. Apparatus

Electrophoresis was carried out on a Quanta 4000 capillary electrophoresis system (Waters, Milford, MA, USA) using a 60 cm (53 cm to the detector) × 75 μm I.D. fused-silica capillary (Supelco, Gland, Switzerland). The system was equipped with a UV detector set at 185 or 254 nm with filters. Separation was performed by applying a positive voltage (10–20 kV) to the capillary. Hydrostatic introduction of the sample was used rather than electromigration, to avoid discrimination between faster and slower ions [8].

In order to obtain high resolution and avoid peak distortion, the injection/capillary volume ratio was 1:100. With an injection time of 30 s, the injection volume was ca. 30 nl (capillary volume: 3 μl).

The capillary was pretreated for 10 min with 0.5 *M* potassium hydroxide and 10 min with deionized water before analysis. The capillary was washed with degassed, filtered (0.45 μm) buffer until equilibrium was reached.

2.3. Sample

Elastin powder was suspended in 6 *M* hydrochloric acid and hydrolysed for 24 h, in sealed tubes, under vacuum, at 105°C. The hydrolysate was dried under vacuum, dissolved in water, filtered on 0.45-μm pore size filters and frozen. Standards of DES and IDE were dissolved in water, filtered and frozen.

2.4. Titration of free–NH_2 groups

The total amino acid content of the hydrolysates was estimated by measuring the free–NH_2 groups using Sanger's reagent, as described by Ghyusen et al. [9].

3. Results and discussion

3.1. Separation of DES and IDE

The structure and size of these amino acids are close to those of an oligopeptide so the choice of the electrophoretic buffer was based on those used for oligopeptide separation. Diluted phosphoric acid used for the separation of peptides by CZE [10], was successfully employed for the separation of DES and IDE. Optimization of the separation was performed by first modifying the molarity of the phosphoric acid solution. A linear relationship was observed between the square root of the molarity and the migration time (slope ± S.D. = −0.147 ± 0.009; intercept ± S.D. = 12.2 ± 0.2; S.D.y = 0.2; n = 12; r = 0.97). Optimal separation of DES and IDE was obtained with 90 m*M* phosphoric acid. Secondly, the influence of pH was estimated by gradual addition of sodium hydroxide to the phosphoric acid solution over a pH range of 1.9 to 2.5. Complete separation was obtained at pH 2.2. As the migration time increased with pH the voltage applied was modified in order to reduce the migration time, without changing the resolution. An optimal value of 15 kV gave complete separation in 13 ± 1 min. A typical electrophoregram obtained with a 1:1 mixture of DES and IDE, is presented in Fig. 1.

All attempts to further separate the two peaks, by addition of agents to complex –NH_2 groups (i.e. trifluoroacetic acid) or by cationic complexation (i.e. Cu, Ca, Cs), were unsuccessful. This presumably reflects the fact that the primary chemical structures of the two amino acids are identical.

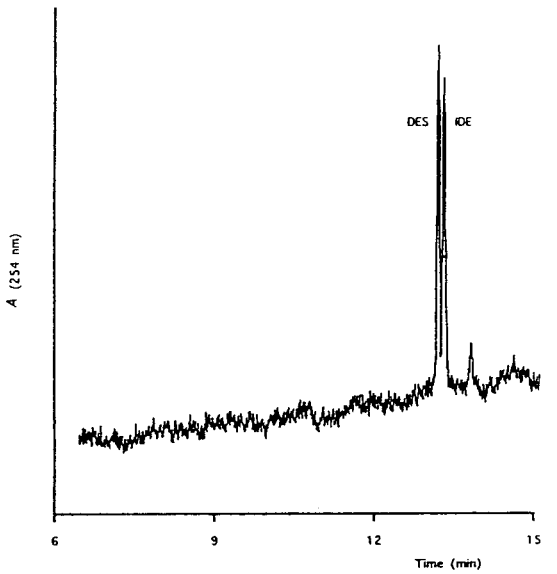

Fig. 1. Electrophoregram of a standard mixture of DES and IDE (1:1) with detection at 254 nm.

3.2. Quantitation of DES and IDE

A linear relationship between the DES and IDE peak areas and the amounts injected was obtained over the range 1–500 pmoles with detection at 185 or 254 nm (Table 1). These two wavelengths were used because they correspond to the standard filters of the Quanta 4000 apparatus. They are not specific for DES, the absorbtion of which shows maxima at 234 and 268 nm in 0.1 *M* hydrochloric acid [11]. Under the conditions used the minimal amount detected was 2 pmole at 254 nm, with a signal-to-noise ratio of 5, and 0.2 pmoles at 185 nm, with a signal-to-noise ratio of 4. These limits can be compared with that of 100 pmoles obtained with direct UV detection at 275 nm, using the HPLC technique reported by Lunte et al. [5].

Table 1
Linearity of the calibration curves of DES and IDE at 254 and 185 nm

	Slope ± S.D.	Intercept ± S.D.	S.D.*y*	*n*	*r*
DES 254 nm	38 ± 3	222 ± 114	177	8	0.96
IDE 254 nm	22 ± 2	96 ± 63	161	8	0.96
DES 185 nm	430 ± 19	1243 ± 680	1076	9	0.99
IDE 185 nm	654 ± 26	2102 ± 940	1489	9	0.99

3.3. Analysis of elastin

Elastin was hydrolysed and the resulting solution was injected into the capillary without any preliminary extraction or chemical modification. Using detection at 254 nm only two peaks of DES and IDE appear on the electrophoregram (Fig. 2). DES and IDE were identified by adding excess standards. Unidentified peaks are present in the electrophoregram using detection at 185 nm, however they do not interfere with the resolution of DES and IDE (Fig. 3).

Amounts of DES and IDE in elastin were 17 μg/mg and 3 μg/mg respectively. These values are in accordance with values obtained by Lunte et al. using HPLC [5]. The number of DES + IDE residues compared to the total of amino acid residues (estimated by Sanger's method) was 3 DES + IDE for 1000 amino acids of

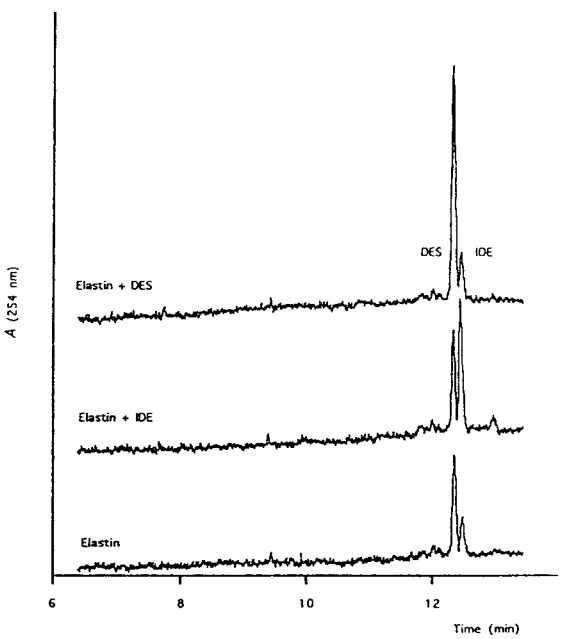

Fig. 2. Electrophoregram of elastin hydrolysate with detection at 254 nm. Identification of DES and IDE by addition of excess standards.

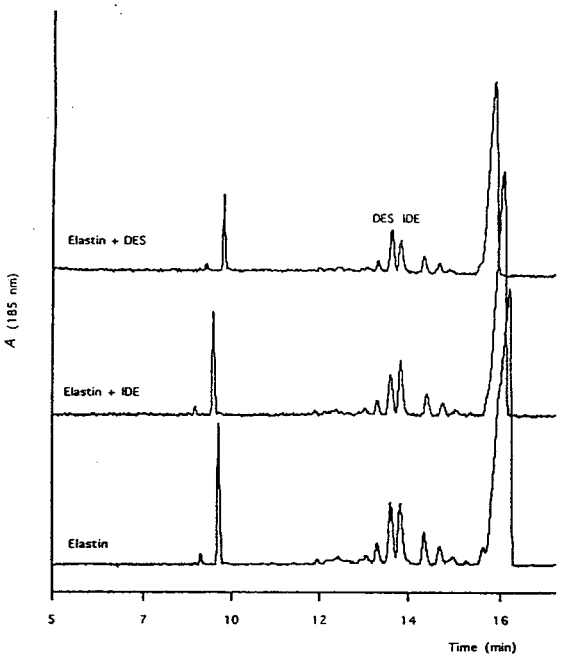

Fig. 3. Electrophoregram of elastin hydrolysate with detection at 185 nm. Identification of DES and IDE by addition of excess standards.

elastin. This is in agreement with published data [12].

4. Conclusion

A sensitive method for the separation and quantitation of DES and IDE by CZE was developed. This method allows the detection of DES and IDE without preliminary purification or chemical modification of the amino acids. We are now investigating the application of this method to the analysis of tissue hydrolysates.

References

[1] I. Pasquali-Ronchetti, M. Baccarani-Contri, C. Fornieri, G. Mori and D. Quaglino, Micron, 24 (1993) 75.
[2] G.S. King, V.S. Mohan and B.C. Starcher, Conn. Tissue Res., 7 (1980) 263.
[3] Y. Yamaguchi, J. Haginaka, M. Kunitomo, H. Yasuda and Y. Bando, J. Chromatogr., 422 (1987) 53.
[4] E. Guida, M. Codini, C.A. Palmerini, C. Fini, C. Lucarelli and A. Floridi, J. Chromatogr., 507 (1990) 51.
[5] S.M. Lunte, T. Mohabbat, O.S. Wong and T. Kuwana, Anal. Biochem., 178 (1989) 202.
[6] S.J.M. Skinner, J. Chromatogr., 229 (1982) 200.
[7] M. Salomoni, M. Muda, E. Zuccato and E. Mussini, J. Chromatogr., 572 (1991) 312.
[8] O. Devêvre, D. Prima Putra, B. Botton and J. Garbaye, J. Chromatogr. A, 679 (1994) 349.
[9] J.M. Ghyusen, D.J. Tipper, C.H. Birge and M. Strominger, Biochem. J., 4 (1965) 2245.
[10] Z. Deyl and R. Struzinsky, J. Chromatogr., 569 (1991) 63.
[11] K. Suyama and F. Nakamura, Biochem. Biophys. Res. Commun., 170 (1990) 713.
[12] T. Hanis, Z. Deyl, R. Struzinsky and I. Miksik, J. Chromatogr., 553 (1991) 93.

Author Index Vol. 710

Carbohydrate Analysis

High Performance Liquid Chromatography and Capillary Electrophoresis

Edited by **Z. El Rassi**

Journal of Chromatography Library, Volume 58

The objective of the present book is to provide a comprehensive review of carbohydrate analysis by HPLC and HPCE by covering analytical and preparative separation techniques for all classes of carbohydrates including mono- and disaccharides; linear and cyclic oligosaccharides; branched heterooligosaccharides (e.g., glycans, plant-derived oligosaccharides); glycoconjugates (e.g., glycolipids, glycoproteins); carbohydrates in food and beverage; compositional carbohydrates of polysaccharides; carbohydrates in biomass degradation; etc.

The book will be of interest to a wide audience, including analytical chemists and biochemists, carbohydrate, glycoprotein and glycolipid chemists, molecular biologists, biotechnologists, etc. It will also be a useful reference work for both the experienced analyst and the newcomer as well as for users of HPLC and HPCE, graduates and postdoctoral students.

Contents: Part I. The Solute.
1. Preparation of carbohydrates for analysis by HPLC and HPCE (A.J. Mort, M.L. Pierce).
Part II. Analytical and Preparative Separations.
2. Reversed-phase and hydrophobic interaction chromatography of carbohydrates and glycoconjugates (Z. El Rassi). 3. High performance hydrophilic interaction chromatography of carbohydrates with polar solvents (S.C. Churms). 4. HPLC of carbohydrates with cation- and anion-exchange silica and resin-based stationary phases (C.G. Huber, G.K. Bonn). 5. Analysis of glycoconjugates using high-pH anion-exchange chromatography (R.R. Townsend). 6. Basic studies on carbohydrate - protein interaction by high performance affinity chromatography and high performance capillary affinity electrophoresis using lectins as protein models (S. Honda). 7. Modern size exclusion chromatography of carbohydrates and glycoconjugates (S.C. Churms). 8. High performance capillary electrophoresis of carbohydrates and glycoconjugates (Z. El Rassi, W. Nashabeh). 9. Preparative HPLC of carbohydrates (K.B. Hicks).
Part III. The Detection.
10. Pulsed electrochemical detection of carbohydrates at gold electrodes following liquid chromatographic separation (D.C. Johnson, W.R. LaCourse). 11. On-column refractive index detection of carbohydrates separated by HPLC and CE (A.E. Bruno, B. Krattiger). 12. Mass spectrometry of carbohydrates and glycoconjugates (C.A. Settineri, A.L. Burlingame). 13. Evaporative light scattering detection of carbohydrates in HPLC (M. Dreux, M. Lafosse). 14. Chiroptical detectors for HPLC of carbohydrates (N. Purdie). 15. Pre- and post-column detection-oriented derivatization techniques in HPLC of carbohydrates (S. Hase). 16. Post-column enzyme reactors for the HPLC determination of carbohydrates (L.J. Nagels, P.C. Maes). 17. Other direct and indirect detection methods of carbohydrates in HPLC and HPCE (Z. El Rassi, J.T. Smith). Subject index.

©1995 692 pages Hardbound
Price: Dfl. 425.00 (US$250.00)
ISBN 0-444-89981-2

ELSEVIER
An imprint of Elsevier Science

ORDER INFORMATION

ELSEVIER SCIENCE
Customer Service Department
P.O. Box 211
1000 AE Amsterdam
The Netherlands
Fax: +31 (20) 485 3432

For USA and Canada:
ELSEVIER SCIENCE
Customer Service Department
P.O. Box 945, New York
NY 10159-0945
Fax: +1 (212) 633 3764

US$ prices are valid only for the USA & Canada and are subject to exchange rate fluctuations; in all other countries the Dutch guilder price (Dfl.) is definitive. Customers in the European Union should add the appropriate VAT rate applicable in their country to the price(s). Books are sent postfree if prepaid.

THE DATA ANALYSIS HANDBOOK

By **I.E. Frank** and **R. Todeschini**

Data Handling in Science and Technology Volume 14

Analyzing observed or measured data is an important step in applied sciences. The recent increase in computer capacity has resulted in a revolution both in data collection and data analysis. An increasing number of scientists, researchers and students are venturing into statistical data analysis; hence the need for more guidance in this field, which was previously dominated mainly by statisticians.

This handbook fills the gap in the range of textbooks on data analysis. Written in a dictionary format, it will serve as a comprehensive reference book in a rapidly growing field. However, this book is more structured than an ordinary dictionary, where each entry is a separate, self-contained entity. The authors provide not only definitions and short descriptions, but also offer an overview of the different topics. Therefore, the handbook can also be used as a companion to textbooks for undergraduate or graduate courses.

Approximately 1700 entries are given in alphabetical order grouped into 20 topics and each topic is organized in a hierarchical fashion. Additional specific entries on a topic can be easily found by following the cross-references in a top-down manner. Several figures and tables are provided to enhance the comprehension of the topics and a list of acronyms helps to locate the full terminologies. The bibliography offers suggestions for further reading.

ELSEVIER
An imprint of Elsevier Science

©1994 386 pages Hardbound
Price: Dfl. 325.00
US$ 185.50
ISBN 0-444-81659-3

ORDER INFORMATION

ELSEVIER SCIENCE
Customer Service Department
P.O. Box 211
1000 AE Amsterdam
The Netherlands
Fax: +31 (20) 485 3432

For USA and Canada:
ELSEVIER SCIENCE
Customer Service Department
P.O. Box 945, New York
NY 10159-0945
Fax: +1 (212) 633 3764

US$ prices are valid only for the USA & Canada and are subject to exchange rate fluctuations; in all other countries the Dutch guilder price (Dfl.) is definitive. Customers in the European Union should add the appropriate VAT rate applicable in their country to the price(s). Books are sent postfree if prepaid.

PUBLICATION SCHEDULE FOR THE 1995 SUBSCRIPTION

Journal of Chromatography A and *Journal of Chromatography B: Biomedical Applications*

MONTH	1994	J–J[a]	A	S	O	
Journal of Chromatography A	Vols. 683–688	689–708/1	708/2 709/1 709/2 710/1	710/2 711/1 711/2 712/1	712/2	The publication schedule for further issues will be published later.
Bibliography Section		713		714/1		
Journal of Chromatography B: Biomedical Applications		663–669	670/1 670/2	671/1 + 2	672/1 672/2	

[a] Vol. 701 (Cumulative Indexes Vols. 652–700) expected in October.

INFORMATION FOR AUTHORS

(Detailed *Instructions to Authors* were published in *J. Chromatogr. A*, Vol. 657, pp. 463–469. A free reprint can be obtained by application to the publisher, Elsevier Science B.V., P.O. Box 330, 1000 AH Amsterdam, Netherlands.)

Types of Contributions. The following types of papers are published: Regular research papers (full-length papers), Review articles, Short Communications and Discussions. Short Communications are usually descriptions of short investigations, or they can report minor technical improvements of previously published procedures; they reflect the same quality of research as full-length papers, but should preferably not exceed five printed pages. Discussions (one or two pages) should explain, amplify, correct or otherwise comment substantively upon an article recently published in the journal. For Review articles, see inside front cover under Submission of Papers.

Submission. Every paper must be accompanied by a letter from the senior author, stating that he/she is submitting the paper for publication in the *Journal of Chromatography A* or *B*.

Manuscripts. Manuscripts should be typed in **double spacing** on consecutively numbered pages of uniform size. The manuscript should be preceded by a sheet of manuscript paper carrying the title of the paper and the name and full postal address of the person to whom the proofs are to be sent. As a rule, papers should be divided into sections, headed by a caption (*e.g.*, Abstract, Introduction, Experimental, Results, Discussion, etc.). All illustrations, photographs, tables, etc., should be on separate sheets.

Abstract. All articles should have an abstract of 50–100 words which clearly and briefly indicates what is new, different and significant. No references should be given.

Introduction. Every paper must have a concise introduction mentioning what has been done before on the topic described, and stating clearly what is new in the paper now submitted.

Experimental conditions should preferably be given on a *separate* sheet, headed "Conditions". These conditions will, if appropriate, be printed in a block, directly following the heading "Experimental".

Illustrations. The figures should be submitted in a form suitable for reproduction, drawn in Indian ink on drawing or tracing paper. Each illustration should have a caption, all the *captions* being typed (with double spacing) together on a *separate sheet*. If structures are given in the text, the original drawings should be provided. Coloured illustrations are reproduced at the author's expense, the cost being determined by the number of pages and by the number of colours needed. The written permission of the author and publisher must be obtained for the use of any figure already published. Its source must be indicated in the legend.

References. References should be numbered in the order in which they are cited in the text, and listed in numerical sequence on a separate sheet at the end of the article. Please check a recent issue for the layout of the reference list. Abbreviations for the titles of journals should follow the system used by *Chemical Abstracts*. Articles not yet published should be given as "in press" (journal should be specified), "submitted for publication" (journal should be specified), "in preparation" or "personal communication".

Vols. 1–651 of the *Journal of Chromatography*; *Journal of Chromatography, Biomedical Applications* and *Journal of Chromatography, Symposium Volumes* should be cited as *J. Chromatogr.* From Vol. 652 on, *Journal of Chromatography A* (incl. Symposium Volumes) should be cited as *J. Chromatogr. A* and *Journal of Chromatography B: Biomedical Applications* as *J. Chromatogr. B.*

Dispatch. Before sending the manuscript to the Editor please check that the envelope contains four copies of the paper complete with references, captions and figures. One of the sets of figures must be the originals suitable for direct reproduction. Please also ensure that permission to publish has been obtained from your institute.

Proofs. One set of proofs will be sent to the author to be carefully checked for printer's errors. Corrections must be restricted to instances in which the proof is at variance with the manuscript.

Reprints. Fifty reprints will be supplied free of charge. Additional reprints can be ordered by the authors. An order form containing price quotations will be sent to the authors together with the proofs of their article.

Advertisements. The Editors of the journal accept no responsibility for the contents of the advertisements. Advertisement rates are available on request. Advertising orders and enquiries can be sent to the Advertising Manager, Elsevier Science B.V., Advertising Department, P.O. Box 211, 1000 AE Amsterdam, Netherlands; Tel: 31 (20) 485 3796; Fax: 31 (20) 485 3810. Courier shipments to street address: Molenwerf 1, 1014 AG Amsterdam, Netherlands. *UK*: T.G. Scott & Son Ltd., Venessa Bird, Portland House, 21 Narborough Road, Cosby, Leics. LE9 5TA, UK; Tel: (0116) 2750 521/2753 333; Fax: (0116) 2750 522. *USA and Canada*: Weston Media Associates, Daniel S. Lipner, P.O. Box 1110, Greens Farms, CT 06436-1110, USA; Tel: (203) 261 2500; Fax: (203) 261 0101.

Chromatography in the Petroleum Industry

Edited by **E.R. Adlard**

Journal of Chromatography Library, Volume 56

Petroleum mixtures consist primarily of relatively unreactive complex hydrocarbons covering a wide boiling range. Such mixtures are difficult to separate by most analytical techniques. Therefore, the petroleum industry has for many years played a leading role in the development of chromatographic methods of analysis. Since the last book specifically concerned with chromatographic analysis of petroleum appeared 15 years ago, numerous advances have been made including developments in liquid and supercritical fluid chromatography, the advent of silica capillary columns with bonded stationary phases and the commercial availability of new selective detectors.

The current book contains chapters written by experts concerning the analysis of mixtures ranging from low boiling gases to waxes and crude oils.

Although the volume is specifically aimed at the petroleum analyst, there is much information of general interest which should be of benefit to a very wide readership.

Contents:

©1995 452 pages Hardbound
Price: Dfl. 435.00 (US$ 255.75)
ISBN 0-444-89776-3

ELSEVIER
An imprint of Elsevier Science

ORDER INFORMATION

ELSEVIER SCIENCE
Customer Service Department
P.O. Box 211
1000 AE Amsterdam
The Netherlands
Fax: +31 (20) 485 3432

For USA and Canada:
ELSEVIER SCIENCE
Customer Service Department
P.O. Box 945, New York
NY 10159-0945
Fax: +1 (212) 633 3764

US$ prices are valid only for the USA & Canada and are subject to exchange rate fluctuations; in all other countries the Dutch guilder price (Dfl.) is definitive. Customers in the European Union should add the appropriate VAT rate applicable in their country to the price(s). Books are sent postfree if prepaid.